# Translational cancer research: from the bench to the bedside - and back again

Torsten Holm Nielsen

Segal Cancer Centre

Lady Davis Institute for Medical Research

Jewish General Hospital

Division of Experimental Medicine

McGill University, Montreal

April 2013

A thesis submitted to McGill University in partial fulfillment of the requirements of the degree of Doctor of Philosophy.

# Table of Contents

**Abstract:** Translational research, as defined by the National Institutes of Health, "includes two areas of translation. One is the process of applying discoveries generated during research in the laboratory, and in preclinical studies, to the development of trials and studies in humans. The second area of translation concerns research aimed at enhancing the adoption of best practices in the community". This thesis will present examples from my PhD work to illustrate both types of translation.

One project describes work in preclinical models of diffuse large B-cell lymphoma treated with histone deacetylase inhibitors, alone and in combination with rituximab, which has been translated into a phase II clinical trial. Included in this work is a methods project, which aims to evaluate, and publish, our experiences with isolating biomaterials from lymph node biopsies in the setting of a clinical trial. This knowledge will, hopefully, contribute to enhancing "best practices" in the lymphoma community. A second project describes data from a clinical case study where a patient with acute myeloid leukemia was treated with an organic arsenical. This work has, in turn, prompted the initiation of preclinical projects in the lab and thus represents an example of translation from the clinic to the bench.

Overall, the work presented here illustrates the full spectrum of translational research "from bench to bedside and back again".

**Résumé:** La recherche translationnelle, telle que définie par le National Institutes of Health, comprend deux domaines de translation. D'une

part, il s'agit du processus d'application des découvertes générées lors de la recherche, dans le laboratoire et dans les études précliniques, au développement d'essais et d'études chez les humains. D'autre part, il s'agit de la recherche ayant pour objectif d'améliorer l'adoption de bonnes pratiques dans la communauté. Cette thèse a pour but de vous présenter des exemples issus de mon travail de Ph.D afin d'illustrer ces deux domaines de translation.

Le premier projet concerne l'étude de modèles précliniques de traitements de lymphomes diffus à grandes cellules B avec des inhibiteurs de déacétylases d'histones, seuls ou en combinaison avec rituximab, qui conduisit à un essai clinique de phase II. Est inclus dans cette partie un projet de méthode, ayant pour but d'évaluer et de publier notre expérience dans l'isolation de matériel biologique à partir de biopsies de ganglions lymphatiques dans le cadre d'un essai clinique. Nous espérons que ces informations contribueront à améliorer les bonnes pratiques dans le domaine du lymphome.

Le second projet décrit des données provenant d'une étude de cas clinique où un patient ayant une leucémie myéloïde aigüe fut traité avec un composé organique à base d'arsenic. Cela, à son tour, conduisit à la naissance de projets précliniques dans le laboratoire et représente ainsi un exemple de translation des soins vers le laboratoire.

Dans l'ensemble, le travail ici décrit illustre tous les aspects de la recherche translationnelle, « du laboratoire au chevet du patient, allers et retours ».

# Preface

The data presented in this thesis include representative examples of translational medicine, intended to illustrate the full spectrum of translational research "from bench to bedside and back again". Chapter one serves as an introduction to the main body of my PhD research, the investigation of the effect of histone deacetylase inhibitors (HDACi), alone and in combination with rituximab, in diffuse large B-cell lymphoma (DLBCL). Chapter two describes my results of combination treatment with HDACi and rituximab in preclinical models of DLBCL while chapter three illustrates our efforts to translate results from preclinical models into patients in the form of a phase II clinical trial. Chapters two and three together illustrate the classical process of translational research where interesting results from the laboratory are investigated in the clinical setting. Chapter four recounts a case study in which a patient with a specific type of acute myeloid leukemia was treated with experimental therapy. Our efforts to monitor clinical response/resistance and our efforts in the lab to understand these results are described as an example of "reverse" translational medicine where knowledge gained in the clinical setting is used to generate hypotheses that can be tested in preclinical models. Information specific to chapter four will be introduced separately in this chapter. Finally, chapter five will briefly present a few overarching thoughts and conclusions on the topic of translational medicine and what has been learned from the work presented in this thesis.

In compliance with the guidelines from McGill University, the following sections state the contributions of all parties involved in the research described in this thesis.

**Contributions to work presented in chapter two:**

Torsten Holm Nielsen performed all "wet" lab work, including analysis and graphical representation of the results. Performed Ingenuity Pathway Analysis (IPA) of gene lists provided by Koren K. Mann.

Koren K. Mann provided guidance, encouragement and oversight of the project. Extracted gene lists from microarray experiments. Co-authored the IRB protocol under which patient samples were collected.

Wilson H. Miller, Jr. provided guidance, encouragement and oversight of the project. Co-authored the Institutional Review Board (IRB) protocol under which patient samples were collected. Provided financial support.

Sarit Assouline provided guidance, encouragement and oversight of the project.

Tina Haliotis provided guidance, encouragement and oversight of the project, particularly the work with primary patient samples.

Sonia del Rincon provided guidance, encouragement and oversight of the project.

Monica C. Dobocan and Luca A. Petruccelli each processed one patient sample.

**Contributions to work presented in chapter three:**

Torsten Holm Nielsen co-authored the investigator initiated trial "sales pitch" to the drug companies and the trial protocol. Performed the optimization assays to evaluate different ways of handling biomaterials. Developed and wrote the SOPs outlining the processing of blood and biopsy material. Processed and archived the majority of patient samples collected to date. Organized the receipt of samples arriving from other hospitals and sent samples to collaborators. Prepared samples for sequencing and microarray analysis. Co-organized collaborations with the many different experts involved in this project.

Koren K. Mann provided guidance and oversight of the project, particularly the isolation and processing of patient samples. She is chiefly responsible for the lab aspects of the trial. Co-authored the investigator initiated trial "sales pitch" to the drug companies and the trial protocol. Co-organized collaborations with the many different experts involved in this project.

Sarit Assouline provided guidance and oversight of the project. Is the principal investigator of the trial and has been in charge of everything from the initial idea, to negotiations with Novartis and Roche and opening the trial at multiple sites. She is chiefly responsible for the clinical aspects of the trial including accrual of patients. Co-authored the investigator initiated trial "sales pitch" to the drug companies and the trial protocol. Co-organized collaborations with the many different experts involved in this project.

Wilson H. Miller, Jr. provided guidance and oversight of the project, especially with experience with multi-center clinical trials, trial design and negotiation with pharmaceutical companies.

Nathalie Johnson provided guidance and oversight of the project, particularly with regard to our sequencing efforts, and has enrolled several patients on the trial.

Tina Haliotis provided guidance and oversight of the project, specifically with questions of hemato-pathology.

The study is part of the Quebec Clinical Research Organization in Cancer (QCROC) umbrella organization for clinical research in cancer. Zuanel Diaz, Samia Qureshi and Caroline Rousseau from QCROC have all contributed greatly to the development of regulatory documents and protocols for handling of biological materials, as well as management of trial logistics.

Naciba Benlimame has been responsible for performing and optimizing immunohistochemistry assays.

Lu Yao, Cynthia Guilbert and Monica C. Dobocan have been very helpful with the processing of several patient samples.

Michael Crump at Princess Margaret Hospital in Toronto, is not only the largest contributor of patients to the trial, but has also been very helpful during the planning and design phase.

David MacDonald, Queen Elizabeth II Health Sciences Centre, and Axel Tosikyan, Sacré-Coeur Hospital, have enrolled patients on the trial.

The clinical research units of the Jewish General Hospital (in

particular Rosa Christodoulopoulos), Princess Margaret Hospital, Queen Elizabeth II Health Sciences Centre and Sacré-Coeur Hospital have been superbly helpful with the coordination and acquisition of patient samples.

Erol Camlioglu provided expert assistance with the initial development of the biopsy protocol.

Éric Paquet is in charge of analysis of microarray data analysis.

Ryan Morin is in charge of analysis of sequencing data analysis.

Ozmosis Research manages the trial and collects data on clinical endpoints and adverse events.

Division of Hematology, Jewish General Hospital sponsored exome sequencing of 11 patients.

Novartis sponsors the trial including enrollment, data management, biopsies and microarray analysis for the trial. They also provide panobinostat.

Roche provides rituximab free of charge in provinces where experimental treatment is not covered by the provincial health care system.

**Contributions to work presented in chapter four:**

Torsten Holm Nielsen performed the *ex vivo* experiments with different arsenicals, processed patient samples, performed the immunoblots on patient samples, performed the cytokine assay, ran the IPA analyses of microarray data provided by Éric Paquet and wrote the manuscript with Koren K. Mann.

Nathalie Johnson had the initial idea to test arsenicals in this patient.

She was the primary treating physician for the patient and took care of obtaining regulatory approval for compassionate use of experimental therapy. Provided the micrograph of an apoptotic cell, temperature recordings and white blood cell counts for the duration of the study. Co-authored the manuscript.

Nicolas Garnier processed samples for inductively coupled plasma mass spectrometry, helped with processing of several patient samples and with the cytokine assay. Co-authored the manuscript and prepared most of the figures.

Stanley Kwan helped perform the *ex vivo* experiments and helped with qPCR analysis. Co-authored the manuscript.

Lu Yao performed the PTEN, BIRC3, NFKB2 and TNFSF1B qPCRs, performed the cell death and immunoblot assays on cell line samples and has performed the EVI1 flow cytometry assay and related cell death assays. Co-authored the manuscript.

Eftihia Cocolakis oversaw treatment with experimental therapy in the clinical research unit and coordinated delivery of patient samples to the lab. Co-authored the manuscript.

Josée Hébert provided karyotype and FISH analyses. She also provided background information on the patient history prior to when the patient was seen at the Jewish General Hospital. Co-authored the manuscript.

Robert A. Morgan provided darinaparsin for both patient and *in vitro* treatment. Co-authored the manuscript.

Éric Paquet analyzed microarray data and co-authored the manuscript.

Kevin P. Callahan and Craig T. Jordan performed leukemia initiating cell assays in mice using primary patient cells. Co-authored the manuscript.

Sarit Assouline treated the patient with darinaparsin and co-authored the manuscript.

Wilson H. Miller, Jr. provided ideas and guidance for the project including the idea to investigate leukemia initiating cell numbers before and after treatment. Co-authored the manuscript.

Koren K. Mann had the idea to include darinaparsin in the initial *ex vivo* arsenical screen, oversaw lab work on the project and wrote the manuscript with Torsten Holm Nielsen. In addition, she has developed the EVI1 flow cytometry assay and is in charge of the lab projects the patient case report has led to.

**Original scholarship and distinct contributions to knowledge:**

**Chapter two:** Combination treatment of preclinical models of DLBCL with HDACi plus rituximab has been described previously, however, our investigations add to this knowledge in several ways: Results of HDACi treatment in activated B-cell (ABC) type DLBCL, either alone or in combination with rituximab, have not been described previously. Our findings suggest that synergy between panobinostat and rituximab may occur more commonly in germinal center B-cell (GCB) type than in ABC-type DLBCL. We do not find evidence of increased CD20 expression as a

mechanism of synergy. This is in contrast to some published results. We also do not find evidence of decreased expression of Bcl-2 as a mechanism of synergy. Again, this is counter to some published reports. We do have some evidence to support previous reports implicating the p38 MAPK family in the mechanism of synergy. In addition, we are investigating preliminary evidence linking B-cell receptor signaling to the mechanism of synergy of panobinostat and rituximab.

**Chapter three:** The QCROC-02 trial of panobinostat, alone or in combination with rituximab in relapsed DLBCL was the first trial of its kind. Since its initiation, two other trials investigating panobinostat in DLBCL have been launched, however, none of these have reported results yet. We believe the QCROC-02 trial is the first trial in DLBCL to incorporate pre- and post-treatment biopsies in the trial design. We have developed novel protocols for the isolation of biomaterials from lymph node biopsies and peripheral blood samples. The development and validation of these form the basis of the work presented in chapter three.

**Chapter four:** The results presented in this chapter have been published. They describe the first use of the organic arsenical darinaparsin in the treatment of acute myeloid leukemia (AML) with inversion of chromosome three (inv(3)). Through longitudinal sampling of peripheral blood from the patient, we were able to profile the initial response to treatment and the eventual development of resistance. Our findings implicate the alternative NF-κB pathway and suggest that expression of IL-8 may be a

useful marker response. In contrast to previously published work on arsenic treatment of AML with inv(3), we were unable to detect modulation of EVI1 expression or function.

**Acknowledgements:**

Wilson H. Miller, Jr.: Thank you very much for the support and guidance. I feel that I've learned a lot during my time in your lab: Not just how to do good science but also a bit about how to provide the requisite environment to allow people to do good science (I suspect there's more to it than bagels and cream cheese, but it's a good start).

Koren K. Mann, my science-godmother: I'm very grateful for all the guidance and inspiration you've given me (not to mention shelter). I could not have completed this PhD without your help.

Sarit Assouline: You too have been a great source of support and inspiration. I am very happy with the project(s) that we have come up with. Thank you.

Chantal Autexier and Sylvie Mader: Thank you for all your help and good ideas. I very much appreciate the time you have spent on my projects.

The Miller and Mann Lab Members (past and present), colleagues and collaborators: Thank you all for your help, support and friendship.

Last, but not least, a heartfelt thank you to my family for the love and support.

# List of Abbreviations

| | |
|---|---|
| ABC | Activated B-Cell subtype of DLBCL |
| ADCC | Antibody-dependent cell-mediated cytotoxicity |
| AID | Activation-induced cytidine deaminase |
| AML | Acute myeloid leukemia |
| APL | Acute promyelocytic leukemia |
| ATO | Arsenic trioxide |
| B-NHL | B-cell Non-Hodgkin lymphoma |
| Bcl-2 | B-cell CLL/lymphoma 2 |
| BCL6 | B-cell CLL/lymphoma 6 |
| BIRC3 | Baculoviral IAP repeat containing 3 |
| Blimp-1 | B-lymphocyte-induced maturation protein 1 |
| CARD11 | Caspase recruitment domain family, member 11 |
| CD20 | Cluster of Differentiation 20 |
| CDC | Complement-dependent cytotoxicity |
| CHOP | Cyclophosphamide, Hydroxydaunorubicin (doxorubicin), Oncovin (vincristine) and Prednisone |
| CI | Combination Index |
| CLL | Chronic lymphocytic leukemia |
| CNS | Central nervous system |
| CREBBP | CREB binding protein |
| CT | X-ray computed tomography |
| CTCL | Cutaneous T-cell lymphoma |

| | |
|---|---|
| Dar | Darinaparsin |
| DLBCL | Diffuse large B-cell lymphoma |
| DMSO | Dimethyl sulfoxide |
| DNA | Deoxyribonucleic acid |
| ECOG | Eastern Cooperative Oncology Group |
| EDTA | Ethylenediaminetetraacetic acid |
| EP300 | E1A binding protein p300 |
| EVI1 | Ecotropic viral integration site 1 |
| EZH2 | Enhancer of zeste homolog 2 |
| FACS | Fluorescence-activated cell sorting |
| FBS | Fetal bovine serum |
| FISH | Fluorescence In Situ Hybridization |
| FITC | Fluorescein isothiocyanate |
| FK228 | Romidepsin |
| GAPDH | Glyceraldehyde-3-phosphate dehydrogenase |
| GCB | Germinal CenterB-cell subtype of DLBCL |
| H3K27me3 | Tri-methylation of histone H3 at lysine K27 |
| HAT | Histone acetyltransferase |
| HDAC | Histone deacetylase |
| HDACi | Histone deacetylase inhibitor |
| HSP-27 | Heat shock 27kDa protein 1 |
| ICP-MS | Inductively coupled plasma mass spectrometry |
| Ig | Immunoglobulin |

| | |
|---|---|
| IHC | Immunohistochemistry |
| IL | Interleukin |
| inv(3) | Inversion of chromosome 3 |
| IPA | Ingenuity pathway analysis |
| IRB | Institutional review board |
| IRF4 | Interferon regulatory factor 4 |
| JGH | Jewish General Hospital, Montreal |
| LBH589 | Panobinostat |
| LD50 | Lethal dose, 50% or median lethal dose |
| MAPK | Mitogen activated protein kinase |
| MCL | Mantle cell lymphoma |
| MDS | Myelodysplastic syndrome |
| MEF2B | Myocyte enhancer factor 2B |
| MGCD0103 | Mocetinostat |
| MLL2 | Myeloid/lymphoid or mixed-lineage leukemia 2 |
| MS4A1 | Membrane-spanning 4-domains, subfamily A, member 1 |
| MYC | Myelocytomatosis viral oncogene homolog |
| MYD88 | Myeloid differentiation primary response gene (88) |
| n.s. | Not significant |
| NAD | Nicotinamide adenine dinucleotide |
| NF-κB | Nuclear factor kappa-light-chain-enhancer of activated B cells |
| NFKB2 | Nuclear factor of kappa light polypeptide gene enhancer in B-cells 2 |

| | |
|---|---|
| NHL | Non-Hodgkin lymphoma |
| NIH | National Institutes of Health |
| NK | Natural Killer |
| PARP | Poly (ADP-ribose) polymerase |
| PBMC | Peripheral blood mononuclear cell |
| PI | Propidium iodide |
| PMH | Princess Margaret Hospital, Toronto |
| PMSF | Phenylmethylsulfonyl fluoride |
| PRDM1 | PR domain containing 1, with ZNF domain |
| PTEN | Phosphatase and tensin homolog |
| QCROC | Quebec Clinical Research Organization in Cancer |
| QEII | Queen Elizabeth II Health Sciences Centre, Halifax |
| qPCR | quantitative polymerase chain reaction |
| R-CHOP | Rituximab plus CHOP |
| RBLB | Red blood cell lysis buffer |
| RIN | RNA integrity number |
| Rit | Rituximab |
| RNA | Ribonucleic acid |
| ROS | Reactive oxygen species |
| RPN1 | Ribophorin I |
| SAHA | Suberoylanilide hydroxamic acid |
| SCH | Sacré-Coeur Hospital, Montreal |
| SEM | Standard error of the mean |

| | |
|---|---|
| shRNA | Short hairpin RNA |
| SLL | Small lymphocytic lymphoma |
| SOP | Standard operating procedure |
| SP1 | Sp1 transcription factor |
| TNFSF1B | Tumor necrosis factor receptor superfamily, member 1B |
| WBC | White blood cell |
| WHO | World Health Organization |

# Chapter 1

# Introduction

**1.1 Personalized medicine and translational research:** Cancer ranks among the leading causes of death in many parts of the Western world[1,2], yet despite great expenditure of both time and money, the treatment of most cancers remains unsatisfactory. One reason for this may be that the heterogeneity of cancer has been underestimated. Anatomically similar, and later histologically similar tumors have been considered as homogeneous biological categories and have therefore, traditionally been treated the same way. This approach has been due both to a lack of knowledge of distinct molecular sub-groups of histological cancer diagnoses, as well as a lack of drugs targeting molecular differences among recognized sub-groups. Increasingly, the impact of molecular differences, not discernable through the microscope, is being recognized as an important aspect of the differential response of tumors to treatment and "targeted" therapies are being developed to selectively attack cancer-specific aberrations.

The ability to analyze distinguishing features of individual tumors and their host environment at an ever-increasing molecular resolution has given rise to the field of personalized cancer therapy which aims to use "molecular characteristics of the tumour and microenvironment, as well as characteristics of the patient, in order to tailor therapies delivered, and treat cancer more effectively and with less toxicity"[3]. In order for a personalized

medicine approach to be able to effectively predict whether a patient with specific tumor characteristics will benefit from a given treatment, a thorough knowledge of the mechanism of action of anti-cancer agents is required. A wealth of data on the mechanistic details of anti-cancer agents exist in preclinical models of malignancy however, the transition from model systems to actual patient treatment is often slow and may not always reproduce preclinical results. In order to accelerate the diffusion of knowledge from basic research efforts to clinical use, the idea of translational research has been proposed. According to the National Institutes of Health (NIH), translational research is defined as follows: "Translational research includes two areas of translation. One is the process of applying discoveries generated during research in the laboratory, and in preclinical studies, to the development of trials and studies in humans. The second area of translation concerns research aimed at enhancing the adoption of best practices in the community"[4]. Thus, the first area of translation deals with the challenge of testing insights learned in the lab in a clinical setting, a process that is often referred to as "from bench to bedside". It is increasingly recognized that this is a bi-directional process as insights learned in the clinic can equally be used to guide laboratory investigations as vice-versa. The second area of translation involves disseminating novel research findings to the community. This can either be the community of health care professionals, which needs to act on new findings or the greater community of laypersons who need to be made aware of novel results.

The work presented in this thesis relates to both areas of translational research described in the NIH definition: Results obtained in preclinical models of diffuse large B-cell lymphoma (DLBCL), described in chapter two, have been "translated" into a phase II clinical trial in relapsed DLBCL, described in chapter three. In chapter four, we present a case study of a patient with a molecularly defined sub-type of acute myeloid leukemia (AML), treated with experimental therapy, which has led to investigations in preclinical models in the lab. These examples serve to illustrate how work in the lab can be used to develop hypotheses that can be tested clinically, and vice-versa. In addition, the protocols described in chapter three will allow others to investigate lymphoma biology in the context of a clinical trial, thereby helping the lymphoma community to obtain a more detailed picture of the molecular intricacies involved in tumor responses to experimental treatment.

**1.2 Insights into the characteristics of cancer:** A wealth of knowledge on the characteristics of cancer has been amassed over the past several years, with practical implications for both the study and treatment of this disease (figure 1.1). Hanahan and Weinberg have enumerated six hallmarks of cancer, which represent acquired capabilities shared by most, if not all, human tumors. These cancer hallmarks include: self-sufficiency in growth stimulatory signaling, insensitivity to growth inhibitory signals, limitless replicative potential, resistance to cell death, induction of

angiogenesis and invasion and metastasis. In addition, evasion of immune surveillance and reprogramming of cellular energy metabolism have been suggested as emerging hallmarks of cancer[5,6]. These acquired characteristics allow malignant cells to by-pass the normal checks and balances governing multicellular organization into tissues and organs. There are a multitude of ways in which aberrations in cancer cells may lead to dysregulated signaling and the emergence of a particular hallmark. The point made in the cited articles is that, although a virtually limitless number of aberrations are possible, the end result in terms of cancer cell behavior can be categorized into a smaller, and conceptually more manageable, number of overarching hallmarks. This greatly facilitates the way one thinks about the consequences of a particular aberration or group of aberrations in an individual cancer. One other important point to emerge over the past several years, and alluded to in the abovementioned hallmarks, is the role of the tumor-host interaction. Tumors cannot be viewed as isolated clumps of cells independent from the organism within which they are proliferating. The tumor microenvironment and the systemic interactions between tumor and host tissues play a key role in cancer proliferation and progression and are now *bona fide* targets for therapeutic approaches in many different ways. Therapies with an effect on the microenvironment include anti-angiogenic and immunomodulatory treatments.

One characteristic of cancer, which facilitates the development of malignancy, is genomic instability[5,6]. Changes in the expression and/or

function of proteins due to mutation of their corresponding gene is a well established underlying factor of each of the acquired characteristics of cancer outlined above. The acquisition of the changes necessary for uncontrolled growth and invasion is greatly accelerated by genomic instability, either through increased tolerance towards DNA damage or through compromised DNA repair mechanisms. Genes implicated in the development of cancer can be broadly divided into two groups: oncogenes and tumor suppressor genes. Oncogenes are mutated forms of genes that contribute to cancer formation. They are typically mutated versions of normal genes, proto-oncogenes, involved in cellular proliferation. A common theme in cancer is that mutation renders the oncogene protein product insensitive to inhibitory signals, thereby allowing for continuous pro-proliferative signaling. Tumor suppressor genes, on the other hand, are genes involved in normal control of cell growth. They often act by inhibiting the activity of (proto-) oncogenes. Loss of tumor suppressor genes, through mutation or other mechanisms, tips the balance towards uncontrolled growth and thus predisposes to malignant transformation.

**1.3 Tumor heterogeneity:** As outlined above, cancers arise through the acquisition of aberrant characteristics through mutation or epigenetic changes (see below). Given the large number of aberrations that increase the likelihood of malignant transformation and the fact that several aberrations are predicted to be necessary to develop malignancy, the particular

constellation of aberrations in an individual cancer will almost certainly be unique to that tumor. A look at any of the recent large-scale sequencing efforts in several different cancers reveals very varied mutational profiles between individual tumors[7-11]. Due to the genomic instability associated with malignant transformation, mutations continue to accumulate after transformation has occurred. Therefore, some of the mutations found in a tumor sample will play an important role in the malignant phenotype while other mutations will be without impact on the ability of cancer cells to proliferate and survive. The former are sometimes referred to as driver mutations, while the latter are called passenger mutations. Some aberrations occur more frequently in cancer, regardless of tissue of origin, and these, particularly the driver mutations, make attractive targets for anticancer treatment. Intertumoral heterogeneity is a major challenge from the point of view of anti-cancer treatment and the personalized medicine approach outlined above has been put forward as a strategy to better manage such heterogeneity.

A second type of tumor heterogeneity, for which evidence is accumulating, is intratumoral heterogeneity. It is becoming increasingly apparent that there is not just variation between individual tumors but also variation within a single tumor. Cancer is thought to arise from a single cell that via its progeny acquires increasing numbers of aberrations, thereby gaining the hallmark characteristics described above. The acquisition of random mutations in one cell and its progeny will introduce heterogeneity

into the cell population. Deep sequencing or lesion-specific PCR analysis in several types of cancer, including B-cell malignancies, has detected direct evidence of intratumoral heterogeneity. Analysis of shared and unique mutations between cell populations from the same tumor will often allow for mapping of the evolutionary relationship of different sub-clones of a tumor[12-17]. Evidence of intratumoral heterogeneity has also lent some support to the idea of cancer stem cells. The hypothesis here being that a sub-set of cells within the tumor possess the ability to give rise to all the other cells within a tumor population. The concept of intratumoral heterogeneity presents a serious challenge for personalized medicine and cancer diagnostics more broadly because 1) it greatly increases the number of different cancer clones that must be targeted by therapy and, 2) there is no way to ensure that the material that you biopsy will contain representative tissue of all clones that need to be eliminated.

Insights into tumor heterogeneity have led to increasing interest in the use of biomarkers to identify tumors with a particular susceptibility to targeted treatment. A biomarker, as defined by the NIH, is "a characteristic that is objectively measured and evaluated as an indicator of normal biological processes, pathogenic processes, or pharmacologic responses to a therapeutic intervention"[18]. Biomarkers are often used as surrogate markers for more meaningful endpoints such as clinical response or survival and their correlation with such clinical endpoints can be used to help determine the

mechanism of action of a given drug and/or to help predict which patients will benefit from a given treatment.

**1.4.1 Hematological malignancies:** Hematological cancers include neoplastic diseases derived from the hematopoietic tissues. Based on the lineage of the malignant cells, they are classified into either myeloid or lymphoid neoplasms and each of these can be further subdivided based on cellular morphology, intra- and extra-cellular markers, genetic, and clinical features. Often, it is possible to determine the normal hematopoietic counterpart of the malignant cell and this "cell of origin" information is incorporated into the World Health Organization (WHO) classification[19]. Two different malignancies will be discussed in this thesis, one lymphoid cancer: diffuse large B-cell lymphoma (DLBCL), and one myeloid cancer: acute myeloid leukemia (AML) with inv(3)(q21q26.2) or t(3;3)(q21;q26.2). The latter will be introduced in chapter four.

**1.4.2 Normal B-cell differentiation:** Before getting into the finer details of current lymphoma classifications, a brief overview of some of the stages of normal B-cell development is in order. A major function of B-cells is to produce high-affinity antibodies targeting specific epitopes that are foreign to the host organism and B-cell differentiation follows development from a pluripotent hematopoietic stem cell to a fully differentiated, antibody secreting plasma cell. There is evidence that particular hematological cancers

arise in a progenitor cell at a specific stage of development. Given this, many hematological malignancies share attributes with their normal counterparts. Several types of lymphoma, including DLBCL, probably originate from B-cells at the germinal center stage of development[20-22]. The germinal center is where mature B-cells initially develop after first encountering antigen. In the germinal center, two major events, which reshape the B-cell receptor, take place. These are somatic hypermutation and class-switch recombination. Once mature B-cells encounter their antigen in conjunction with appropriate T-cell stimulation in the secondary lymphoid tissues, they develop into rapidly proliferating centroblasts that undergo somatic hypermutation. Somatic hypermutation is the process whereby the variable regions of the immunoglobulin genes are mutated to increase (or sometimes decrease) affinity for the antigen that triggered the germinal center reaction[23,24]. Centroblasts differentiate to centrocytes, which are subjected to a "quality control" of their newly mutated immunoglobulin chains. Cells with strong affinity for antigen are allowed to proliferate, while those with poor antigen recognition are targeted for apoptosis[25]. Centrocytes also undergo class-switch recombination. This describes the change of the immunoglobulin heavy chain from IgM to IgG, IgE or IgA. Class-switch recombination confers different properties on the antibodies produced and thus allows for greater versatility in the immune response. Both somatic hypermutation and class-switch recombination require the activity of activation-induced cytidine deaminase (AID)[26,27]. This enzyme causes double stranded breaks and

mutation of DNA in order to modify the immunoglobulin genes to produce high-affinity antibodies. However, such genotoxic activity comes at the cost of increasing the risk of malignant transformation and evidence of both AID-induced mutation and translocation can be found in DLBCL[28,29]. In order to tolerate the DNA-damaging effects of AID activity, germinal center B-cells express the transcriptional repressor BCL6, which functions to dampen the DNA-damage response by inhibiting expression of a number of DNA-damage sensing proteins (see below). BCL6 also potently represses the expression of transcription factors that allow differentiation into plasma cells (mainly Blimp-1/PRDM1)[30]. However, once centrocytes have successfully rearranged their immunoglobulin class and produced a B-cell receptor with high affinity for antigen, BCL6 expression is diminished while NF-κB, IRF4 and Blimp-1 signaling is induced, allowing the centrocyte to mature into a plasmablast and finally into an antibody secreting plasma cell. Alternatively, some germinal center B-cells become memory B-cells after having undergone immunoglobulin class-switching and hypermutation[31,32].

**1.4.3 Diffuse large B-cell lymphoma (DLBCL):** Non-Hodgkin lymphoma (NHL) accounts for the fifth highest number of new cases of cancer and the sixth highest number of cancer deaths per year in Canada[2]. DLBCL is the most common type of lymphoma, accounting for 30-40% of NHL[19,31]. This translates into an estimated 2700 patients who will be diagnosed with DLBCL in 2012 in Canada[2]. DLBCL is an aggressive lymphoma

type with a median survival of less than a year in untreated cases[33]. Current standard therapy for DLBCL consists of combination chemotherapy (cyclophosphamide, doxorubicin, vincristine and prednisolone (CHOP)) plus immunotherapy in the form of the anti-CD20 antibody rituximab (together called R-CHOP). This regimen achieves 50-80% overall survival after three years depending on the patient population treated[34-36]. However, for those patients who progress or relapse on first-line treatment, the prognosis is extremely poor with a median survival of 6 months or less[37]. Patients who fail first-line treatment will typically be evaluated for tolerability of high dose chemotherapy followed by autologous stem cell transplant[33]. However, many patients are not candidates for this treatment. As such, well-tolerated second-line treatment regimens are sorely needed for the relapsed DLBCL patient population and these patients are currently encouraged to participate in clinical trials.

DLBCL is a heterogeneous disease category. This is evident from the plethora of lymphoma classification systems that have been suggested, including the latest WHO classification of DLBCL, which lists no less than 15 sub-types[19]. The heterogeneous nature of this disease is also highlighted by treatment response rates. As mentioned above, approximately two thirds of patients treated with R-CHOP will be cured while the remainder has a very poor prognosis. These response rates suggest some kind of, as yet unidentified, biological difference between those who respond well to R-CHOP and those who do not.

Recurrent aberrations are frequently found in DLBCL. These commonly involve chromosomal translocations, placing an oncogene under the regulatory control of a new promoter (often from an immunoglobulin gene) and resulting in aberrant over-expression. Translocations involving the *BCL6* locus at band 3q27 are the most common, seen in about 30% of DLBCL[38]. BCL6 is a transcriptional repressor normally expressed in germinal center centroblasts. It is a transcription factor which functions to negatively regulate the expression of more than a thousand genes, many of which are involved in the DNA damage response and cell death[39]. In the normal centroblast, this temporary attenuation of the DNA damage machinery is essential to permit somatic hypermutation and class switch recombination to proceed without triggering apoptosis. However, in malignant cells, BCL6 over-expression increases the threshold of genotoxic stress necessary to trigger cell death and so allows cancer cells to survive under increased levels of stress and tolerate increased levels of genomic instability[31]. Translocations resulting in over-expression of Bcl-2 occur in approximately 20% of DLBCL[40]. Bcl-2 protein is a powerful inhibitor of apoptosis and cells with high levels of Bcl-2 exhibit a survival advantage. Normal centroblasts do not express Bcl-2[Ref 31]. Rearrangement of *MYC* is seen in approximately 5-15% of DLBCL and patients with translocation of *MYC* have a significantly worse outcome than those without *MYC* rearrangement[36,41].

Efforts to account for the observed heterogeneity of DLBCL have led to several classification schemes based on gene expression profiles[20,42]. In

particular, the classification scheme developed by Staudt *et al.* has proved popular with the lymphoma community and will be employed in this thesis[20,43,44]. This classification splits DLBCL into so-called "cell of origin" categories: activated B-cell (ABC) type, germinal center B-cell (GCB) type and others/unclassified. Lymphomas in these categories cluster with samples of normal B-cells at either the GCB- or ABC stage of development, when ranked using gene expression data[20], suggesting that tumors of each subtype arise from B-cells at these stages of development[31]. Cell of origin classification has been shown to have prognostic value with approximately 50% of ABC type and 80% of GCB type patients surviving five years on R-CHOP[43]. Encouragingly, gene expression profiles from different tumors from the same patient clustered next to each other when assessed for cell of origin subtype, perhaps suggesting that intertumoral heterogeneity (of tumors from the same patient) is not a major issue in this setting[20].

ABC-type DLBCL was so named because this type of DLBCL clustered with normal B-cells that had been activated by cross-linking of their B-cell receptor[20] and, indeed, a proportion of ABC-type DLBCL show constitutive activation of B-cell receptor signaling due to mutations in *CD79A* or *CD79B*[45]. Another signaling pathway shared by activated normal B-cells and ABC-type DLBCL is the NF-κB pathway. Constitutive activation of this pathway either through chronic B-cell receptor activation or mutation of down-stream pathway members such as *CARD11*, *A20* or *MYD88* is frequently found in ABC-type DLBCL[45-50]. NF-κB inhibition is selectively toxic to ABC-type DLBCL,

confirming that this pathway plays a decisive role in this type of lymphoma[51-53]. *BCL6* translocation is more commonly seen in ABC-type DLBCL than GCB-type[54]. The cell of origin of ABC-type DLBCL is not known with certainty however, it appears to be a plasmablast, whose terminal differentiation has been blocked by mutation of the transcription factor *Blimp-1*[Ref 49,55-57]. Since most ABC-type DLBCLs have not undergone class-switch recombination, it is also possible that the cell of origin is a pre-germinal center, extrafollicular B-cell, which expresses AID or a post-germinal center memory B-cell[31,58,59].

The cell of origin of GCB-type DLBCL is generally agreed to be a germinal center B-cell[20,60] and evidence of both somatic hypermutation and class switch recombination can be demonstrated in this subtype[29,61]. GCB-type DLBCL is characterized by BCL6 expression, as well as *Bcl-2* translocation or other genetic aberrations resulting in increased Bcl-2 expression, *PTEN* deletion, *MYC* activation and *p53* mutation[20,31,54,62-64]. As will be described in more detail below, it also appears that mutations of certain epigenetic regulatory proteins are more common in GCB-type DLBCL.

In addition to commonly occurring translocations and gene expression based classification schemes, recent large-scale sequencing efforts have revealed a wealth of recurring mutations in DLBCL, some of which have been mentioned above. Of particular interest for the topic of this thesis is the fact that many of these mutations affect enzymes that play a role in chromatin modification and epigenetic regulatory mechanisms (see below for examples). Also of interest, some mutations correlate with cell of origin

subtype and may contribute to the subtype-specific differences in gene expression patterns. A few of the mutations that can be related to the research presented in this thesis will be described in more detail.

Mutations of the histone acetyl transferases *CREBBP* and *EP300* are commonly found in DLBCL. Twenty-nine percent of all DLBCL have mono-allelic mutation of *CREBBP* and this is significantly more common in GCB type DLBCL than in ABC type. Mutation of *EP300* is seen in 10% of DLBCL and only rarely coincides with concurrent *CREBBP* mutation. *In vitro* investigation of the detected mutations revealed that they result in decreased acetyl transferase activity[65,66].

Heterozygous mutation of the histone methyltransferase *EZH2* occurs in 22% of GCB type DLBCL but only rarely in ABC-DLBCL[67,68]. *EZH2* mutation appears to be highly specific in DLBCL, most commonly occurring at tyrosine 641, and less commonly alanine 677[Ref 67,69]. The specific pattern of mutations suggests that they may confer a functional change of EZH2 activity and this has, indeed, been found to be the case by several independent groups. EZH2 is responsible for trimethylation of histone H3 at lysine 27 (H3K27me3). The wild type enzyme is highly efficient at adding the first two methyl groups while the mutated form of EZH2 catalyzes addition of the third methyl group with high efficiency. Since EZH2 mutations always occur as mono-allelic mutations, both the wild type and the mutant enzyme would be expected to be present in cancer cells and therefore, all activities required for the efficient mono-, di- and tri-methylation of H3K27 should be present[70-73].

H3K27me3 is a repressive histone mark (see below) and as such, EZH2 mutated cells would be expected to epigenetically repress certain target genes. The down-stream implications of EZH2 mutation are an area of fertile investigation that is already being translated into the clinic[74,75].

Inactivating mutations of the histone methyltransferase *MLL2* are seen in about 30% of DLBCL with no apparent predilection for a particular subtype[66]. Mutation of *MEF2B*, a transcription factor that recruits histone-modifying enzymes to target genes in a calcium dependent manner was found in 10% of DLBCL[66].

Based on the above, DLBCL is a heterogeneous disease with a significant proportion of patients in need of improved second-line therapies. A wealth of information is forthcoming on many of the aberrations that make up the combined (epi-)genetic landscape of DLBCL. The translational medicine challenge now becomes to use this new knowledge to try to target new treatments to patient populations defined by specific recurring aberrations.

**1.5.1 Epigenetics in cancer:** Epigenetics, defined as somatically heritable changes in gene function that do not alter the primary DNA sequence, plays an important role in the regulation of both normal development, as well as malignant transformation[76,77]. Epigenetic control of gene expression is achieved through a variety of mechanisms such as: histone modifications (including acetylation and methylation), DNA methylation,

nucleosome positioning, nucleosome variant composition and microRNA regulation. The effect of these epigenetic marks can either be to repress or activate transcription of genes located nearby.

The evidence linking epigenetics and cancer is based on two different mechanisms: First, epigenetic silencing in the form of DNA methylation can lead directly to increased genomic instability through either an increased mutation rate of methylated cytosines to thymidines[78] or through the silencing of DNA repair genes (reviewed in ref [79]). Second, a number of recurrent, cancer-specific mutations have been described in several epigenetic enzymes involved in histone acetylation[65], histone methylation[66-68,80] and DNA methylation[81,82]. So, rather than being isolated processes, genetics and epigenetics appear to be intimately linked in the emergence of malignant transformation. It is important to bear in mind that there is extensive cross-talk between different epigenetic regulatory mechanisms, therefore, an aberration affecting one type of epigenetic regulation may well perturb other mechanisms of epigenetic control[83,84].

The importance of epigenetic dysregulation in malignancy is underscored by the development of drugs targeting the epigenetic machinery in several hematological cancers. Inhibitors of DNA methyltranserases and histone deacetylases are now approved for use in myelodysplastic syndrome and cutaneous T-cell lymphoma (CTCL) respectively and modulation of many other epigenetic regulators is being investigated for multiple indications.

**1.5.2 Introduction to histone deacetylase inhibitors (HDACi):** In order to fit the entire eukaryotic genome into the limited space in the nucleus, DNA is wound around histone proteins, thereby compacting it. One hundred forty-seven base pairs of DNA wound around an octamer of histones makes up a nucleosome, the basic unit of chromatin. Rather than only serving "space-conserving" purposes, compaction of DNA into chromatin has also been found to serve as a means of regulating which genes are turned on and off. Acetylation of the N-terminal tail of histones was first demonstrated to play a role in transcriptional regulation by Allfrey *et al.* in the 1960's[85-87]. This group also proposed a mechanism that could explain how acetylation of histones impacts transcription: "As a charge neutralization mechanism, acetylation of the histones would be expected to modify DNA-histone interactions, and this may offer a molecular basis for the pronounced changes in histone acetylation and RNA synthesis during the course of gene activation in many cell types"[87]. The hypothesis is that addition of acetyl-groups to histone tails cancels out some of the positive charge of histones, thereby reducing their binding to the negatively charged DNA backbone. The looser interaction between DNA and histones results in the DNA being more accessible to the transcriptional machinery, thereby favoring transcriptional activation. Histone tails are also targets of other covalent modifications, besides acetylation. Additional post-translational modifications include phosphorylation, methylation, ubiquitination and sumoylation[88]. The myriad possible combinations of different covalent marks at different sites led to the

hypothesis that there exists a "histone code" where different combinations of histone marks provide binding sites for different chromatin binding proteins and transcription factors[89]. The addition of reversible histone marks thus can impact both the accessibility of chromatin to the transcriptional machinery and can dictate which transcriptional regulators are present at a given location of the genome.

The description of both the first mammalian histone acetyl-transferase (HAT) and histone deacetylase (HDAC) in 1996 provided the starting point for research into the effects of reversible acetylation[90,91]. Acetylation levels are the result of a balance between the activity of HATs, which add acetyl-groups, and HDACs, which remove acetyl-groups. HATs add acetyl groups to lysine residues on histones and other protein targets, using Acetyl coenzyme A as an acetyl donor. As described above, loss-of-function mutations of HATs are very common in DLBCL, suggesting that proper acetylation levels are critical in this disease[65,66].

Since the initial discovery of the first HDAC in 1996, a total of 18 mammalian HDACs have been described. These are arranged into four classes based on sequence similarity to yeast HDACs and their co-factor requirements[92]. Class I HDACs include: HDAC1, HDAC2, HDAC3 and HDAC8. Class II: HDAC4, HDAC5, HDAC6, HDAC7, HDAC9 and HDAC10. Class III is composed of the sirtuins, a group of HDACs that require nicotinamide adenine dinucleotide (NAD) as a co-factor instead of zinc, which is used by all other HDACs. Class IV currently only includes HDAC11. In general, class I

HDACs are located in the nucleus while class II HDACs can shuttle between the nucleus and cytoplasm. HDACs are overexpressed in certain cancers compared with normal tissue[93].

Histone deacetylase inhibitors (HDACi) are also called protein or lysine deacetylase inhibitors in acknowledgement of the fact that histones are not the only targets of acetylation. Choudhary *et al.* detected acetylation of 1750 different proteins using a mass spectrometry approach[94]. Interestingly, the list of non-histone targets of acetylation includes BCL6[Ref 95], c-Myc[96-98] and the NF-κB subunits p50[Ref 99] and p65[Ref 100].

Aberrant epigenetic control of cell behavior makes an attractive target for pharmacological modulation because of the reversible nature of epigenetic regulatory mechanisms and, to date, numerous inhibitors of histone deacetylases have been developed. The HDACi investigated in this thesis exert their inhibitory effects through interference with the zinc binding pocket of HDACs from classes I, II and IV[101]. As such, the HDACi described in this thesis have very limited inhibitory effect on the sirtuins.

Preclinical investigations of HDACi have revealed anti-cancer effects in many types of malignancy. Not surprisingly, given the pleiotropic targets of acetylation, the mechanisms of action of HDACi that have been described are legion. As expected, treatment of cells with HDACi does change gene expression, however, generally, less than 10% of the genes investigated change more than two-fold and of these, approximately equal numbers increase and decrease expression[102,103]. Therefore, it is likely that the

mechanism of anti-cancer activity of HDACi is not exclusively dependent on the derepression of transcription that would be expected from drugs that increase global acetylation of histones. Other mechanisms of anti-cancer activity, which may or may not depend on changes in gene expression, include: induction of apoptosis[104,105], induction of autophagy[106,107], induction of reactive oxygen species and DNA damage[108,109] and induction of cell cycle arrest[110] among others. Currently, many questions concerning how HDACi induce their pleiotropic effects and which effects are important for the anti-cancer mechanism(s) remain unanswered.

Since 2001, HDACi have been extensively tested as anti-cancer agents in patients suffering from a variety of malignancies[111,112]. Two HDACi, namely vorinostat (also known as zolinza or SAHA) and romidepsin (also known as istodax or FK228), have received regulatory approval for the indication cutaneous T-cell lymphoma (CTCL). Both drugs achieve overall response rates of approximately 30% in CTCL and share similar side effect profiles, with thrombocytopenia, granulocytopenia, fatigue and gastro-intestinal disturbances as the most common untoward effects[113-116].

Results from HDACi trials in DLBCL have been somewhat less impressive than in CTCL, with overall response rates of 5.5% and 25% reported for vorinostat[117,118] and 23.5% for mocetinostat (MGCD0103)[119]. However, these numbers, based on a total of 47 DLBCL patients treated with vorinostat or mocetinostat, suggest that HDACi treatment does have activity

in a subset of DLBCL patients. The side effects observed in these trials include thrombocytopenia and gastro-intestinal disturbances as observed for CTCL.

The work presented in this thesis mostly concerns the HDACi panobinostat (LBH589), developed by Novartis. This HDACi has not yet been extensively tested in the setting of DLBCL, however, it appears to be relatively well tolerated by patients suffering from hematological malignancies (with a similar side effect profile as seen for other HDACi) after both oral and intravenous administration[120-122].

**1.6 Introduction to rituximab:** Rituximab (Rituxan/MabThera) is a chimeric (part-mouse, part-human), monoclonal antibody targeting an extracellular epitope of the membrane spanning protein CD20. Expression of CD20 can be detected on B-cells at all stages of maturation except the very early stages in the bone marrow and the fully differentiated plasma cell[123,124]. Malignancies derived from different stages of B-cells often express CD20 and are thus, amenable to treatment with rituximab. The addition of rituximab to chemotherapy containing regimens has significantly improved survival in DLBCL and standard treatment for this disease is now composed of rituximab plus CHOP[34,35].

Rituximab is generally very well tolerated with an infusion reaction including fever and chills reported as the most common side effect. Of import for the combination with HDACi, rituximab has been associated with thrombocytopenia[125].

The proposed mechanisms whereby rituximab exerts its anti-tumor activity are three-fold: antibody dependent cytotoxicity (ADCC), complement dependent cytotoxicity (CDC) and direct signaling events triggered by rituximab binding to CD20 at the cell surface. The relative importance of each of these effector mechanisms in the anti-cancer effect of rituximab is controversial and newer CD20-targeting antibodies designed to optimize either ADCC or CDC are being developed to further investigate this.

Binding of rituximab to CD20 serves to "tag" the target B-cell for destruction by several different immune effector cells. Binding of the Fc part of rituximab to the Fc receptor of cytotoxic immune cells triggers ADCC. Cytotoxic cells that have been demonstrated to participate in ADCC include natural killer (NK) cells[126], macrophages[127] and neutrophil granulocytes[128]. Importantly, different polymorphisms of FcγRIIIa (CD16), the Fc receptor on NK cells, predict for different responses to rituximab mono-therapy in several types of B-cell malignancy[129-132]. The polymorphism of FcγRIIIa with higher affinity for rituximab predicts for a better outcome. This suggests that ADCC is an important determinant of rituximab effect in the clinic.

Opsonization of malignant B-cells by rituximab leads to CDC, with activation of the complement cascade on the surface of the targeted B-cells and subsequent cell death. Expression of the complement inhibiting protein CD59 has been linked with resistance to rituximab, suggesting that CDC plays a role in the *in vivo* mechanism of rituximab induced cytotoxicity[133].

Rituximab also has been reported to exert direct signaling effects in *in vitro* models where no immune effector cells or complement was added. Such direct effects are difficult to distinguish from the rituximab effects described above *in vivo*, however, some evidence exists that direct signaling of rituximab has anti-cancer effects *in vivo*: Intrathecal injection of rituximab directly into the cerebrospinal fluid of patients with lymphoma of the central nervous system (CNS) can elicit responses[134]. The CNS is an immune-privileged area where limited immune surveillance takes place under normal circumstances. This suggests that the effects of rituximab in the CNS happen in the absence of auxiliary factors.

Of import to the results discussed in this thesis, rituximab direct signaling has been demonstrated to inhibit a number of pathways implicated in the survival and proliferation of malignant cells. These pathways include: B-cell receptor signaling in both normal and malignant cells[135,136], the p38 MAPK pathway[137,138], expression of the anti-apoptotic proteins Bcl-2 and Bcl-$_{XL}$[137-141], the NF-κB pathway[138,139,142,143], c-Myc mRNA and protein expression[139], Raf-MEK-ERK signaling[135,138,139,144] and the Akt pathway[138,145].

While the relative contribution of ADCC, CDC and direct signaling to the anti-cancer effects of rituximab is contentious, all of these mechanisms depend on CD20 expression at the cell surface of the target B-cell. This is important because loss of CD20 expression has been implicated as a mechanism of resistance to rituximab-containing treatment. Approximately a quarter of patients who relapse on rituximab-containing combination

chemotherapy lose extracellular CD20 protein expression. This is accompanied by a concomitant reduction in CD20 mRNA levels. Evidence from preclinical models suggests that epigenetic regulation may underlie the observed CD20 down-regulation[146,147]. This will be covered in greater detail in the introduction to chapter two.

**1.7 Acute Myeloid Leukemia (AML):** AML constitutes a heterogeneous group of malignancies arising from cells at different stages of myeloid development. Chapter four of this thesis will focus on a sub-type of AML characterized by inversion of chromosome 3 ("inv(3)"). AML with inv(3) is a rare disease, accounting for only about 1-2% of all AML cases[148]. Based on the estimated incidence of leukemia in Canada in 2012, fewer than 100 people will be diagnosed with inv(3) AML per year[2]. Patients with inv(3) AML are generally younger than other AML patients at diagnosis and present with higher counts of white blood cells and platelets at diagnosis. AML inv(3) has a very unfavorable prognosis with an overall survival at five years of only 5.7% despite treatment with combination chemotherapy[148].

The chromosomal inversion that is pathognomonic in AML inv(3) places the oncogene, ecotropic viral integration site 1 (*EVI1*), under the control of regulatory elements of a housekeeping gene, resulting in increased expression of *EVI1*[149]. EVI1 is a transcription factor and plays a role in the development of several organ systems, including the hematopoietic system. EVI1 mediates its effects on gene expression via several mechanisms,

including interaction with HDACs and HATs as well as through recruitment of DNA methyltransferases, resulting in a characteristic hypermethylation signature[149,150].

Overall, AML inv(3) represents a molecularly well-defined disease category with a very severe prognosis. At present, no targeted therapy is available for these patients. Chapter four describes a case report outlining our investigations into the potential use of arsenic-containing drugs in the setting of AML inv(3).

**1.8 Introduction to arsenicals:** Compounds containing arsenic have a long history of use in medicine, being employed in the treatment of human ailments ranging from syphilis to cancer[151]. In modern medicine, the inorganic arsenical, arsenic trioxide (ATO), has been approved for use in patients with relapse of acute promyelocytic leukemia (APL). ATO also shows great promise in combination with all-*trans* retinoic acid as first line therapy against APL[152]. Efforts to enhance the anti-cancer activities of arsenic by joining it to carbon-containing compounds have led to the development of organic arsenicals. One such organic arsenical is darinaparsin, which is made up of dimethyl arsenic joined to glutathione[153].

ATO and darinaparsin share some mechanistic similarities. Both induce reactive oxygen species (ROS) and the generation of ROS appears to play an important role in the subsequent induction of apoptosis[153]. In addition, ATO and darinaparsin share similarities in signal transduction

pathways upstream of the induction of apoptosis. These include activation of the JNK pathway and of caspase cleavage[153].

However, there also appear to be important differences between ATO and darinaparsin. Due to the different chemical structures, ATO and darinaparsin probably enter and exit cells via different mechanisms, as suggested by the fact that cells treated with darinaparsin accumulate higher concentrations of arsenic than cells treated with ATO (at equimolar arsenic concentrations)[154,155]. The differences between these two arsenic-containing compounds are underscored by the fact that darinaparsin has activity against ATO-resistant cells[155].

Arsenicals have been tested in a number of different malignancies; however, to date consistent effect has only been demonstrated in APL. Anecdotal evidence from pre-clinical models and one small early-phase clinical trial suggests that arsenicals, specifically ATO, may have activity in cancers with overexpression of EVI1[156,157]. This prompted us to investigate the response of AML inv(3) to arsenicals.

**1.9 Closing remarks:** It is hoped that the above chapter will serve as an introduction to the ideas and results upon which much of the work in this thesis is built. The concepts of translational research and personalized medicine are the common denominator for the body of work presented herein.

As mentioned in the preface, chapters two and three will describe our investigations into the effects of HDACi, alone and in combination with rituximab, in DLBCL and this introductory chapter should help the reader understand why we are interested in this particular treatment in this particular setting. These two chapters together constitute an example of how data in preclinical models can be translated to the clinic. In addition, our data describing the quality and yield of biomaterials from lymph node biopsies, presented in chapter three, constitute an example of knowledge that can help the lymphoma field adopt better practices. Our method of lymph node biopsy processing can easily be adapted to any B-NHL trial where the investigators are interested in tumor profiles. As such, I hope that this information will help encourage the use of tumor biopsies in lymphoma trials and that this will lead to a better understanding of lymphoma biology and response/resistance mechanisms to specific agents.

In addition to chapters two and three, I have included a chapter describing the treatment of AML with an organic arsenical because, although not in lymphoma, it illustrates an aspect of translational medicine not otherwise demonstrated by the work presented in lymphoma namely, the translation of knowledge from the clinic to the bench.

Finally, a few thoughts on what has been learned about translational research will be presented in chapter five.

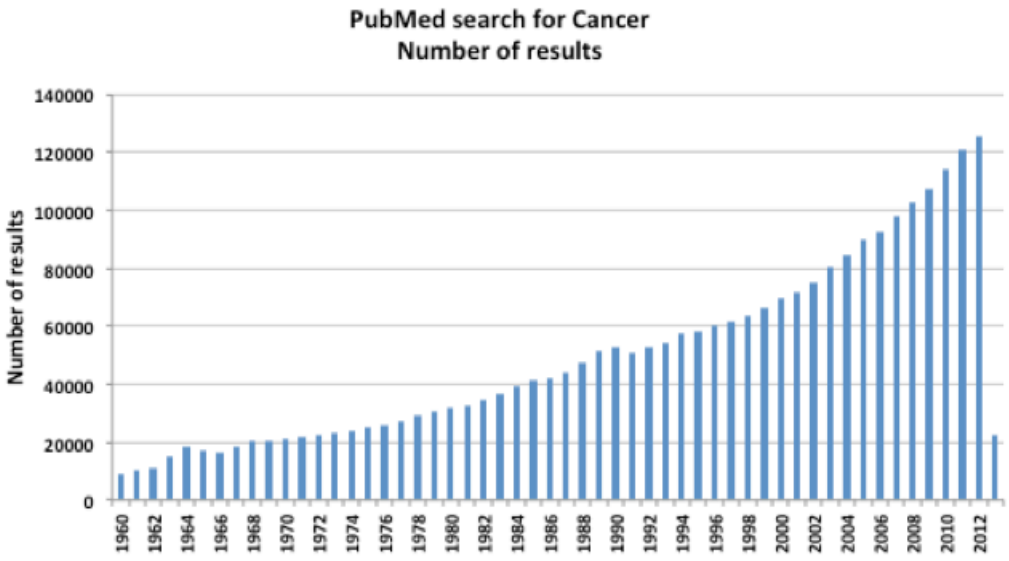


**Figure 1.1:** Number of results on PubMed for the search term "cancer". The search was performed on Feb. 28th 2013.

# Chapter 2

# "From the bench"

## Investigating the effect(s) of HDACi and rituximab in preclinical models of lymphoma

### 2.1 Introduction:

**2.1.1 Background and rationale:** Relapsed DLBCL is a grave disease with a poor prognosis and no accepted standard treatment. At the same time, DLBCL is a relatively common malignancy, thus the population of patients with relapsed disease constitutes a sizeable cohort. The data presented in this chapter represent our initial efforts to investigate whether histone deacetylase inhibitors (HDACi) show effect in preclinical models of DLBCL, either alone or in combination with rituximab. The idea to more closely investigate the effect(s) of HDACi in DLBCL stems from a clinical trial of an HDACi, mocetinostat (MGCD0103), for which Sarit Assouline, Division of Hematology, Jewish General Hospital, Montreal was an investigator[119]. This trial demonstrated one complete response and 3 partial responses in a cohort of 17 patients with relapsed DLBCL. These responses approximate the overall response rates described in several other malignancies where HDACi have been investigated, including cutaneous T-cell lymphoma for which two

HDACi are approved[113-116]. It seems that HDACi treatment results in good, but infrequent, responses in several types of cancer and the challenge thus becomes to either increase the proportion of patients who respond to HDACi treatment or to better define the mechanism(s) by which HDACi exert their anti-cancer effects in order to predict which patients will benefit from treatment. Ideally, both objectives could be met by a greater understanding of how HDACi work in a particular malignancy.

One way to potentially increase the proportion of patients who respond to HDACi treatment is to combine them with a drug with a mechanism of action that either potentiates that of HDACi or is itself potentiated by HDACi treatment. Combination chemotherapy with an HDACi as one of the constituent drugs is a fertile area of research with over 200 clinical trials listed on clinicaltrials.gov at the time of writing. This chapter will primarily be devoted to preclinical investigations into HDACi treatment, alone or in combination with the anti-CD20 antibody rituximab, in DLBCL. Data from a phase II clinical trial investigating panobinostat with or without rituximab will be discussed in chapter three.

Rituximab was chosen as a rational combination partner for HDACi for three main reasons: First, rituximab has revolutionized the treatment of several CD20-expressing malignancies and the incorporation of rituximab into standard first-line therapy for DLBCL has significantly increased the overall survival[34,35]. Second, the literature suggests several mechanisms whereby HDACi and rituximab could synergize, either through an HDACi-

induced effect on CD20 expression and/or through mutual effects on multiple intracellular signaling pathways.

Several groups have provided evidence that CD20 expression is subject to epigenetic control. Tomita *et al.* described a cell line established from a patient whose disease transformed from CD20-positive follicular lymphoma to CD20–negative DLBCL while on rituximab-containing chemotherapy treatment. Treatment of the CD20-negative cells with an HDACi resulted in a marked increase in expression of CD20 mRNA and protein suggesting that the decreased CD20 observed was due to an epigenetic mechanism of repression. No data on viability or cell death induced by HDACi plus rituximab was reported[147]. This same group subsequently quantified the frequency of transformation from CD20-positive to –negative in the population of patients who relapse or progress on rituximab-containing combination chemotherapy. Approximately 30% of patients on rituximab-containing combination chemotherapy relapsed. Out of the relapsed patients who were re-biopsied, about 25% showed loss of CD20 expression. The mechanism of CD20 loss appears to be diverse as evidence of mutation of *MS4A1*, the gene encoding CD20, was found in some patients. In others, no mutation was detected; instead, CD20 expression was shown to be increased by treatment with a DNA methyltransferase inhibitor, suggesting an epigenetic mechanism of CD20 loss. It is interesting to note that in all cases where CD20 loss was documented, the CD20-negative cells were found in the bone marrow or cerebro-spinal fluid, not in a lymph node biopsy[146].

Shimizu *et al.* found that treatment with two different HDACi induced an increase in cell surface CD20 in one of two DLBCL cell lines tested (neither of which are included in the DLBCL cell line panel of this thesis), as well as in several Burkitt's lymphoma cell lines. The authors present data to support increased acetylation of histones and recruitment of the transcription factor SP1 at the *MS4A1* promoter. Finally, they demonstrate enhanced anti-cancer effects *in vitro* and *in vivo* with combination treatment in preclinical models of Burkitt's lymphoma[158]. These data corroborate the initial finding of Tomita *et al.* that CD20 expression can, in some cases, be subject to epigenetic repression that is amenable to treatment with HDACi or other epigenetic therapy[146,147].

As was mentioned in chapter one, both rituximab direct signaling, through binding to CD20, and HDACi treatment, through acetylation of numerous histone and non-histone targets, can impact many different signaling pathways. Significant overlap exists between the targets of these drugs and therefore, it is tempting to speculate that combination treatment may result in enhanced anti-cancer effects. Zhao *et al.* found a synergistic increase in cell death when the HDACi vorinostat and rituximab were combined in both a DLBCL cell line (SU-DHL4) and a Burkitt's lymphoma cell line. The authors proposed the mechanism underlying this synergy to be the result of a combined inhibitory effect of both drugs on several anti-apoptotic proteins (Bcl-2, Bcl-XL), the NF-κB pathway, MAP kinase pathway signaling and c-Myc. Furthermore, this study demonstrated that SAHA and rituximab

in combination had synergistic effects on growth inhibition of primary B-NHL cells treated *ex vivo* and on survival of nude mice xenotransplanted with Burkitt's lymphoma cells[139]. Recently, a report investigating the use of HDACi plus rituximab in mantle cell lymphoma (MCL) found that this combination leads to synergistic cell death. No change in CD20 expression was reported, instead, the mechanism of synergy was posited to be due to combined inhibition of several mediators of survival including: Bcl-2, NF-κB, AKT, ERK and p38 MAPK. Xenograft studies showed prolonged survival of mice treated with HDACi plus rituximab compared to controls and mice treated with either single agent alone[138]. The data from Shi *et al.* in MCL overlap somewhat with what was found by Zhao *et al.* in DLBCL and Burkitt's lymphoma, with the results from both groups implicating Bcl-2 downregulation, decreased MAP kinase pathway signaling and inhibition of the NF-κB pathway. Thus, the literature on combination of HDACi with rituximab in B-NHL is currently divided into two main mechanisms of synergy. One supports a mechanism involving epigenetic de-repression of CD20, while the other supports the inhibition of several survival pathways as the mechanism of synergy. These mechanisms need not be mutually exclusive, however, the only report to have looked at both, found that the two did not occur together[138].

A final, more theoretical argument for the selection of rituximab as the combination partner of choice with an HDACi, is related to the molecular targets of the two drugs. As mentioned in the introductory chapter, HDACi

have been described to exert their anti-cancer activity through pleiotropic effects, which makes sense given the large number of proteins that are targets of acetylation[94]. The relative importance of acetylation targets and the pathways they impact remains to be defined and may well depend on cell/treatment context. Rituximab, on the other hand, targets a very well defined membrane spanning protein, namely, CD20. From the antibody binding CD20, intracellular signals are propagated downstream, which affect multiple pathways. Theoretically at least, one should be able to trace the effects of rituximab back to CD20. Combining a drug with many cellular targets with one that has only one may facilitate the elucidation of the mechanism whereby they synergize. In addition, determining the mechanism(s) of synergy between these two drugs may shed some light on which of the many effects of HDACi are important for their anti-cancer properties in DLBCL.

Here, we present data to suggest that HDACi synergize more frequently in GCB-type than ABC-type DLBCL. Contrary to some previously published reports, we do not find that this synergy is dependent on increased expression of CD20 at the cell surface. In addition, we find very scant evidence of modulation of a list of targets curated from among targets shared by HDACi and rituximab. Using an unbiased approach, looking at changes in gene expression, our data point toward a mechanism involving B-cell receptor signaling.

## 2.2 Materials and Methods:

**2.2.1 Cells:** ABC-type DLBCL cell lines HBL-1, OCI-LY3, RIVA, SU-DHL2 and U2932 were generously provided by Riccardo Dalla-Favera, Columbia University, NY, USA. All are grown in Iscove's Modified Dulbecco's Medium (Life Technologies) supplemented with 10% fetal bovine serum (Wisent) and antibiotics (50 IU/mL penicillin and 50 μg/mL streptomycin (Wisent)). The GCB-type DLBCL cell lines OCI-LY1, OCI-LY7, OCI-LY8 and SU-DHL4 were generously provided by Raquel Aloyz, McGill University, Montreal, Canada. OCI-LY1, OCI-LY7 and OCI-LY8 grow in RPMI 1640 media (Wisent) supplemented with 10% fetal bovine serum, antibiotics (as above) and 50 μM β-mercapto-ethanol (Sigma). SU-DHL6 cells were a kind gift from Ari Melnick, Weill Cornell Medical College, NY, USA. Toledo cells were purchased from the American Type Culture Collection (ATCC.org). The CD20-negative multiple myeloma cell line U266 was generously provided by Michael Witcher, McGill University, Montreal, Canada. SU-DHL4, SU-DHL6, Toledo and U266 cells are grown in RPMI 1640 media supplemented with 10% fetal bovine serum and antibiotics (as above).

**2.2.2 Drugs:** Panobinostat (LBH589) was provided by Novartis Pharma AG. Vorinostat (zolinza, SAHA) was provided by Merck. For both HDACi, a stock solution was produced by dissolving in DMSO and aliquots were kept at -20°C to avoid repeated freeze-thaw cycles. Rituximab (10

mg/mL, Roche) was purchased from the Jewish General Hospital Pharmacy and aliquots were kept at 4°C in the dark. The chemical inhibitor of p38 MAPK, SB203580, was purchased from Tocris biosciences.

**2.2.3 Propidium iodide (PI) stain:** All cell lines were seeded at 200,000 cells/ml prior to each experiment and treated as indicated, except OCI-LY1, OCI-LY7 and OCI-LY8 which were seeded at 100,000 cells/ml. All drug concentrations were seeded in triplicate. After treatment for 48 hours, cells were harvested and washed once with FACS wash buffer (5mM $NaN_3$ in PBS supplemented with 5% fetal bovine serum) followed by staining with 50 µg/mL PI (Sigma) in hypotonic buffer (0.1% sodium citrate and 0.1% Triton X-100 in ddH20). Approximately 500,000 cells/condition were stained with 0.5 mL PI stain and analyzed using a BD Biosciences FACSCalibur flow cytometer. At least 7,000 events were measured per condition. Cell death was measured as the percentage of cells with sub-G0 DNA content using FCS Express v3.0.

**2.2.4 Calculation of $LD_{50}$ and synergy using CalcuSyn:** Both $LD_{50}$ and synergy were calculated using CalcuSyn version 2.0 (Biosoft)[159,160]. Cell death was adjusted for baseline cell death by subtracting the percentage of sub-G0 cells in untreated controls from the cell death in all other conditions prior to calculation of $LD_{50}$ and synergy. For the calculation of synergy, four concentrations of each drug are tested, alone and in combination, keeping a

constant ratio between the two drug concentrations as recommended by the manufacturer of the software. Synergy is shown as the combination index (CI). A CI of less than one indicates synergy while a CI greater than one indicates antagonism. A CI of one indicates an additive effect. For the purposes of analysis in this thesis, a CI of less than 0.9 in at least three out of four combinations per cell line is considered to indicate synergy while cell lines with three out of four CI values above 1.1 will be classified in the antagonism category. Cell lines with three out of four CI values between 0.9 and 1.1 are considered to have an additive response to the combination of panobinostat and rituximab.

**2.2.5 Measurement of CD20 cell surface expression:** Cells were treated as described in section 2.2.3 (cells from the same well were used for both PI stain and CD20 stain). One hundred thousand cells/condition were used for CD20 quantification. Cells were washed once in FACS wash buffer (same as in section 2.2.3), incubated with 2μL antibody (either anti-CD20-FITC from Miltenyi Biotec or anti-IgG1-FITC isotype control from BD) for 20 minutes on ice in the dark, washed again with FACS wash buffer and fixed with 4% paraformaldehyde in PBS. Quantification of bound antibody was performed using a BD Biosciences FACSCalibur flow cytometer. At least 10,000 events were measured per condition. Binding of isotype control was used as a measure of non-specific binding. CD20 surface expression is shown as overlays of the geometric mean fluorescence.

**2.2.6 Immunoblots:** Whole cell extracts were made using the following protein lysis buffer: 50 mM Tris-HCl (pH 8.0), 150 mM NaCl and 1% Triton X-100 supplemented with aprotinin, leupeptin, PMSF, $NaVO_4$ and phosphatase inhibitors. Proteins were separated by SDS-PAGE and transferred to nitrocellulose membrane. Primary antibodies used: Bcl-2 (Santa Cruz, sc-7382), BCL6 (Santa Cruz, sc-858), CD20 (Santa Cruz, sc-70582), p38 (Santa Cruz, sc-535), phospho-p38 (Cell Signaling, #4511), p62/SQSTM1 (Santa Cruz, sc-28359), PARP (Calbiochem, #512739) and GAPDH (Cell Signaling, #2118). Specific binding was detected with horseradish peroxidase-labeled secondary antibodies and visualized with enhanced chemiluminescence.

**2.2.7 Microarray analyses:** SUDHL6 cells, representing cells with strong synergy between panobinostat and rituximab, and Toledo cells, representing cells where no synergy is observed, were analyzed for changes in gene expression by microarray analysis. All cells were treated for 12 hours followed by RNA isolation using a Qiagen Allprep DNA/RNA mini kit according to the manufacturers instructions. A time point of 12 hours was chosen because acetylation and gene expression changes are apparent at this time while cell death is not yet detectable. SUDHL6 cells were treated as follows: CTL (untreated), 7.5 nM panobinostat alone, 0.075 μg/mL rituximab and 7.5 nM panobinostat plus 0.075 μg/mL rituximab. Toledo cells were

treated as follows: CTL (untreated), 12.5 nM panobinostat alone, 1.25 μg/mL rituximab and 12.5 nM panobinostat plus 1.25 μg/mL rituximab. These doses were picked so they would result in approximately 30% cell death at 48 hours with panobinostat alone and addition of rituximab would lead to a synergistic increase in cell death in SUDHL6. An aliquot of cells from each condition were kept in the incubator for 48 hours to ascertain supra-additive cell death in SUDHL6 and additive cell death in Toledo in the samples from which RNA was isolated. All experiments were performed in duplicate. RNA was sent to the McGill University and Genome Quebec Innovation Center for analysis using Agilent GE 8x60K one-color arrays.

Raw data from the microarrays were normalized and gene lists compiled using FlexArray by Koren Mann, McGill University. Gene lists from each condition showing two-fold or greater changes in expression compared to CTL with a p-value of 0.02 or less were analyzed for commonly modulated pathways using Ingenuity Pathway Analysis.

### 2.2.8 Processing of primary B-NHL samples for *ex vivo* treatment:

Lymph node tissue from patients undergoing diagnostic (excisional) lymph node biopsies was collected with patient consent. Lymph node tissue was macroscopically dissociated using scalpels followed by passage through a syringe attached to needles of decreasing diameter. These manipulations liberate lymphocytes from the lymph node connective tissue into a single-cell suspension. Lymphocytes were isolated by Ficoll gradient separation. Cells

were plated at 500,000 cells/mL and treated with HDACi and/or rituximab as indicated. Cell death was assessed by PI stain (see section 2.2.3).

## 2.3 Results:

**2.3.1 Panobinostat treatment in DLBCL cell lines:** In order to define the effects of panobinostat monotherapy in DLBCL and to investigate a possible difference in sensitivity among DLBCL subtypes, we screened a panel of 11 DLBCL cell lines for sensitivity to panobinostat (labeled as "LBH" in all figure legends). Cell lines representing both ABC-type and GCB-type DLBCL were included in this screen to investigate if cell of origin subtype conferred differential sensitivity to HDACi. As shown in figure 2.1 and 2.2, the mean lethal dose ($LD_{50}$) of panobinostat at 48 hours varies from approximately 7 nM (OCI-LY3 cells) to about 30 nM (OCI-LY8 cells) in the DLBCL cell lines tested. Cell death was measured by flow cytometry as the percentage of cells with sub-G0 DNA content following propidium iodide stain. All cell lines tested had an $LD_{50}$ of panobinostat below what is clinically achievable in humans (peak plasma concentrations in excess of 40 nM can safely be achieved after panobinostat administration, personal communication – Sarit Assouline, Jewish General Hospital). While the average panobinostat $LD_{50}$ for the GCB-type cell lines was higher than that of the ABC-type cell lines, this difference did not reach statistical significance ($p = 0.4199$) and so we conclude that cell of origin subtype does not correlate with differential sensitivity to panobinostat alone in our panel (figure 2.3).

### 2.3.2 Combining panobinostat and rituximab in DLBCL cell lines:

Having established that panobinostat has cytotoxic effects at clinically achievable concentrations in cell line models of DLBCL, we investigated the effect of combining panobinostat with rituximab.

Representative graphs of cell death with panobinostat alone, rituximab alone and the combination are shown for ABC cell lines in figure 2.4 and GCB cell lines in figure 2.5. In addition, cell death data from the multiple myeloma cell line U266 are included as a control (figure 2.6). U266 cells do not express CD20 on their cell surface (figure 2.7) and therefore would be expected to be insensitive to rituximab, both as monotherapy and in combination with panobinostat. This fits well with the data observed in U266 cells (figure 2.6 and 2.7).

Combination of panobinostat and rituximab results in a synergistic increase in cell death in five out of six GCB-type cell lines, while such synergy is only observed in one of five ABC-type cell lines tested. Applying Fisher's exact test to the observed distributions yields a p-value of 0.0801, which, while not below the commonly accepted 5% risk of seeing such a result by chance, might suggest that there could be differences in the way DLBCL subtypes respond to combination treatment with panobinostat and rituximab.

### 2.3.3 *Ex vivo* treatment with HDACi and rituximab in primary lymphoma cells:

We wanted to ascertain if our cell line data could be

replicated using an alternative preclinical model of B-NHL, namely *ex vivo* treatment of primary cells isolated from lymph node biopsies from patients suspected of/diagnosed with lymphoma. The primary objective of these experiments was to investigate the effects of HDACi treatment on B-NHL cell death at clinically achievable concentrations as a prelude to the clinical trial described in chapter three. In total, nine biopsies from patients with several types of B-NHL (table 2.1) were treated with two different HDACi (vorinostat (SAHA) and panobinostat (LBH)) and analyzed for cell death at 48 hours (figure 2.8 and 2.9). All concentrations of both HDACi tested induced significant cell death in all samples compared to untreated control cells. Note that the basal cell death in untreated cells was quite variable and often high. Encouragingly, the two HDACi induced very similar responses across a range of clinically achievable concentrations, suggesting that the results are representative of a shared "HDACi effect".

In order to test our hypothesis that HDACi and rituximab make good combination partners, we treated primary B-NHL cells with rituximab 50 μg/mL, alone and in combination with the highest dose of HDACi used. Rituximab had only a minimal effect on cell death as monotherapy and only increased HDACi induced cell death in one of the patient samples tested and only with one of the two HDACi (figure 2.10). This sample was from a patient diagnosed with Small Lymphocytic Lymphoma/Chronic Lymphatic Leukemia. Addition of rituximab did not augment HDACi induced cell death in any of the DLBCL patient samples in our cohort (data not shown). It should be noted

that only one concentration of rituximab was investigated in primary patient cells. This decision was based on the limited number of cells isolated from some lymph node biopsies. Having data from only one concentration of one of the drugs used in combination precludes calculation of combination indices and so we cannot formally evaluate whether synergy was present or not. However, given the fact that only one patient sample showed significantly more cell death with panobinostat plus rituximab than with panobinostat alone, it seems unlikely that a strong synergistic effect was elicited.

The cell of origin subtype of DLBCL samples included in this screen is unknown. Likewise, the clinical history of the patients from which each biopsy was derived is, for most samples, unknown. All diagnoses indicated in table 2.1 have been verified by a hemato-pathologist. The fact that we only observe significantly increased cell death with combination treatment in one out of nine samples serves to further highlight the need to molecularly characterize patient populations in order to better understand differences between patients with good and poor responses.

**2.3.4 Expression of potential mediators of synergy – CD20:** In an effort to better understand the mechanism of synergy observed between panobinostat and rituximab, expression of potential mediators of this effect was assessed in cell lines. As synergy is rarely observed in ABC-type cell lines but quite commonly in those of GCB-type, we decided to focus on the latter.

The first target we chose to investigate was cell surface expression of CD20. We hypothesized that treatment with an HDACi might induce up-regulation of CD20 at the cell surface. As mentioned in section 2.1.1, this hypothesis is supported by the work of others[147,158]. As shown in figure 2.11, panobinostat treatment did not increase surface CD20-expression in any of the cell lines in our panel. On the contrary, it resulted in a marked decrease in CD20 at the cell surface in two cell lines (OCI-LY1 and OCI-LY8). Interestingly, synergy between panobinostat and rituximab was still observed despite decreased expression of the target of rituximab. A moderate decrease in CD20 was also seen in Toledo cells, where panobinostat and rituximab do not synergize. However, this was only observed at the highest dose tested. In an effort to further test the importance of CD20 to the mechanism of synergy, we attempted to knock down CD20 in OCI-LY8 cells using specific anti-*MS4A1* (the gene coding for CD20) shRNAs. While knock down of global CD20 protein level was successful (figure 2.12, top), no decrease in cell surface CD20 was apparent in cells treated with *MS4A1*-targeting shRNAs compared to cells treated with mock shRNAs (figure 2.12, middle and bottom). As expected given the equal levels of surface CD20 expression, no difference in response to combination treatment between "mock" and "on-target" shRNA treated cells was observed (figure 2.13). Based on our flow cytometry results, CD20 expression does not appear to be increased with panobinostat treatment in our cell line panel. The knock down data are inconclusive, as knock down at the cell surface was not achieved.

**2.3.5 Expression of potential mediators of synergy – other targets:** After ruling out increased CD20 expression as a likely mechanism of synergy, we were interested in exploring expression levels of other molecular targets which might be impacted on by both HDACi and rituximab and which might play a role in cell survival in DLBCL. Based on the literature on combination treatment with HDACi and rituximab, we initially decided to investigate Bcl-2, BCL6 and p38 MAPK as targets which are commonly down-regulated by both HDACi and rituximab and which have previously been implicated in the mechanism by which these two drug classes synergize[138,139]. In addition, our laboratory has a strong interest in the effects of HDACi treatment on autophagy and so the autophagy marker p62 was also included for analysis[106]. To narrow down the number of cell lines to be investigated, we picked two with robust synergy (OCI-LY8 and SUDHL6) and one without synergy (Toledo) as a model system in which to compare expression of potential mediators of synergy. Immunoblots of the aforementioned targets of interest are shown in figure 2.14 in cells treated as indicated (the panobinostat concentrations used result in about 30% cell death as monotherapy). Based on these results, no change in Bcl-2 is observed with either drug alone or with combination treatment. BCL6 expression was decreased by panobinostat treatment in both cell lines displaying robust synergy, however, this decrease was unaltered by addition of rituximab. Curiously, BCL6 expression was greatly decreased by combination treatment

in cells where no synergy was observed. These results suggest that decreased BCL6 expression does not play a major role in the observed mechanism of synergy. Expression of the autophagy marker p62 is decreased in all three cell lines treated with panobinostat regardless of combination with rituximab (p62 levels are inversely related to autophagic activity so a decrease in p62 indicates induction of autophagy by panobinostat). The fact that this expression pattern is also seen in cells where no synergy is observed suggests that induction of autophagy is not an underlying mechanism of synergy in DLBCL cell lines or that cells with no synergy are somehow resistant to increased induction of autophagy. Activation of p38 MAPK by phosphorylation at threonine 180 and tyrosine 182 was induced by panobinostat (mono-) therapy in cells with synergy. This activating mark was noticeably increased when rituximab was added in combination with panobinostat. In cells where synergy was absent, neither panobinostat alone nor combination therapy induced phosphorylation of p38 MAPK. However, rituximab treatment alone did seem to have some activating effect. Based on these results, we decided that activation of p38 MAPK, as a potential mechanism of synergy, merited further investigation. To test the significance of this finding, p38 MAPK activity was inhibited using a chemical inhibitor, SB203580. In OCI-LY8 cells, which show robust synergy when treated with panobinostat plus rituximab, inhibition of p38 MAPK activation modestly but significantly inhibited cell death caused by combination treatment with panobinostat and rituximab (figure 2.15). To confirm that SB203580 did,

indeed, inhibit p38 MAPK, levels of phosphorylated HSP-27, a downstream target of p38 MAPK were investigated by immunoblot (figure 2.16). As expected, inhibition of p38 MAPK activation had no effect in cells where synergy was absent (Toledo). Surprisingly, co-treatment with SB203580 in SU-DHL6 cells had no effect on synergy (figure 2.15). It seems, therefore, that p38 activation may play a modest part in the mechanism of synergy but that this mechanism is cell line dependent.

**2.3.6 Microarray analyses:** Having been unsuccessful in determining a robust mechanism of synergy using a list of candidate targets curated from the literature, we next explored an unbiased approach to investigate differences in gene expression between cells that show synergistic cell death in response to combination treatment and cells that do not. Changes in gene expression in SUDHL6 and Toledo cells were analyzed using Agilent GE 8x60K arrays. By picking a cell line with robust synergy between panobinostat and rituximab (SUDHL6) and one where no synergy is observed (Toledo), we hoped to be able to define which pathways play a role in the mechanism of synergy.

A preliminary analysis of the gene expression levels of cells treated with panobinostat plus rituximab compared with expression levels in untreated cells revealed that 193 genes were upregulated in SUDHL6 in response to combination treatment, while 187 genes were downregulated. For Toledo, the corresponding numbers were 559 genes up and 435 genes

down in treated cells compared with controls. A number of these genes were regulated in a similar fashion in the two cell lines and were removed for the initial analysis. Looking at genes uniquely regulated in SUDHL6 or Toledo, we analyzed the lists for common pathways using Ingenuity Pathway Analysis. One of the interesting findings from this analysis relates to B-cell receptor signaling. In both the SUDHL6 unique gene list and the Toledo unique gene list, the B-cell receptor pathway features as one of the pathways that is significantly enriched. However, in SUDHL6 cells, the pathway members immediately downstream of the B-cell receptor are unperturbed by treatment while in Toledo cells, these genes are downregulated (figure 2.17). This suggests that B-cell receptor signaling may be required in order to achieve synergy. These findings will be validated with qPCR and if they are confirmed, we will test the effect of modulating B-cell receptor signaling on synergy.

## 2.4 Concluding remarks:

**2.4.1 Lessons learned from testing HDACi with and without rituximab in preclinical models of B-NHL:** The experiments described in this chapter have yielded several useful pieces of information. First, we demonstrated that HDACi treatment at clinically achievable concentrations has cytotoxic effects in all cell lines and all primary patient samples tested thus far.

Second, we have shown that combination treatment with panobinostat and rituximab leads to supra-additive cytotoxic effects in a subset of DLBCL cell lines. The majority of cell lines where this drug combination showed synergistic cytotoxic effects were of GCB subtype. However, this division was not complete as we also saw synergy in one ABC cell line and had one GCB cell line in which combination treatment was merely additive. As such, the observed distribution of cells with synergy did not reach significance, but there seems to be a trend worth investigating.

*Ex vivo* treatment of primary B-NHL samples, with concentrations of HDACi achievable *in vivo*, increased cell death in all samples. Curiously, we only saw one instance of improved cytotoxicity with combination treatment in primary patient samples treated *ex vivo*. The primary patient samples represent a broad range of B-NHL sub-types. For those samples that have been diagnosed as DLBCL, the cell of origin sub-type is not known. Assuming that preclinical models provide an accurate approximation of *in vivo* treatment on the whole organism level, our results suggest that DLBCL, and more broadly, B-NHL, is sensitive to HDACi treatment with and without rituximab (see below for caveats to this assumption).

Third, we found that rituximab, as monotherapy, without the addition of complement or immune effector cells, was cytotoxic in a subset of DLBCL cells. This effect was limited to GCB-type cell lines (SUDHL4 and SUDHL6) and suggests that some (GCB) cell lines are acutely sensitive to direct signaling effects of rituximab. This has previously been shown for SUDHL4[Ref]

[139], however, results from ABC-type cell lines have, to our knowledge, not yet been reported. Translating these results to R-CHOP treatment in the clinic, they might explain some of the differences in response observed between patients with ABC subtype and GCB subtype lymphoma, where GCB DLBCL patients fare better[20,161,162]. It is noteworthy that synergistic effects on cell death are still seen in cells where rituximab monotherapy has very limited cytotoxicity. This might suggest that a signaling mechanism downstream of CD20 is activated by binding of rituximab and collaborates with signals induced by HDACi to induce cell death.

A brief discussion of one of the limitations of the model system we are using is in order here: We add neither complement components, nor immune effector cells to our assays with rituximab, therefore, we are only testing direct signaling effects induced by rituximab binding to CD20. Specifically, the rituximab effector mechanisms antibody dependent cytotoxicity (ADCC) and complement dependent cytotoxicity (CDC) are not evaluated in our investigations. The decision to focus on direct signaling effects was motivated by our wish to determine where HDACi and rituximab signaling intersect to produce synergistic cell death. We hope that this will help pinpoint pathways of import to HDACi-mediated cell death. However, it should be borne in mind that *in vivo* experiments with rituximab will result in activation of ADCC, CDC and direct signaling and so may not exactly mirror our results *in vitro*.

Analysis of gene expression data is still ongoing by our bioinformatician, however, a preliminary analysis has revealed some

interesting differences in expression induced by combination treatment in cells with synergy versus those where no synergy is seen. Our data suggest that B-cell receptor signaling is active in cells with synergy, while some pathway members are downregulated in cells without synergy. Interestingly, chronic B-cell receptor activation has been implicated in ABC-type DLBCL lymphomagenesis and survival[45]. This subtype-specific dependence on B-cell receptor signaling may underlie the difference in synergy between DLBCL subtypes observed in our results.

Another interesting finding from our preliminary analysis is that p38 MAPK family members seem to be differentially regulated in cells with and without synergy. In cells with synergy, p38β (MAPK11) is induced by combination treatment, while in cells without synergy, p38δ (MAPK13) is downregulated. These results, implicating differences in p38 MAPK signaling in the mechanism of synergy support the hypothesis that signaling through the p38 family of kinases is important in this context. However, our results using a chemical inhibitor of p38 MAPK activation showed only a very modest and cell line specific effect on synergy.

We have not yet elucidated the mechanism behind the observed synergy in our panel of cell lines, however, we were able to discount several potential mechanisms of action. The best studied of these is the hypothesis that treatment with an HDACi leads to an increase in CD20 expression which increases cell death from treatment with rituximab[158]. Other hypotheses, which seem less likely to be true based on our work include: decreased

expression of Bcl-2 and BCL6 and induction of autophagy. Our results with a chemical inhibitor of p38 MAPK suggest that activation of p38 MAPK may play a small role in response to combination treatment however, only in some cell lines. Interestingly, gene expression data described in the previous paragraph may point towards an explanation of the somewhat disappointing results of p38 inhibition. The p38 inhibitor we used, SB203580, is a 10-fold more potent inhibitor of p38α than p38β, but does not have strong activity against p38γ (MAPK12) or p38δ (MAPK13)[163-165]. It is therefore possible that the slight inhibition of synergy we see when co-treating with SB203580 is due to inhibition of p38β.

**2.4.2 Future perspectives:** The potential mechanisms of synergy that we have explored thus far were all suggested by looking for overlapping functions of HDACi and rituximab reported in the literature. Several other hypotheses that we have yet to test can be generated following this approach. These include investigation of the role of calcium flux induced by HDACi and/or rituximab alone and in combination. Both HDACi and rituximab have been reported to induce an increase in intracellular calcium and it is possible that a convergence of two calcium-stimulating signals could be cytotoxic to B-cells[166-171]. B-cell receptor signaling is also a powerful calcium-stimulating pathway and if we are able to corroborate our microarray data supporting a role of B-cell receptor signaling in the mechanism of synergy, it will be interesting to investigate the effect our experimental treatment has on

calcium levels. As mentioned above, this is particularly intriguing given the reported differences among DLBCL subtypes in their dependence on the B-cell receptor pathway.

To try to understand the effects of treatment with panobinostat, rituximab and the combination, we are pursuing more unbiased approaches than the hypothesis-based efforts described above. As outlined in sections 2.3.6 and 2.4.1, comparison of gene expression profiles in cells with synergy versus cells where no synergy is observed have pointed us in the direction of the B-cell receptor signaling pathway as a potentially important component of synergy. As mentioned above, these data may also offer an explanation for our results with chemical inhibition of p38 MAPK. The convergence of hypothesis-driven work and more unbiased approaches on p38 MAPK may cause us to investigate the role this family of kinases plays further. Current work is focusing on validating the array data by qPCR.

Based on work with the *ex vivo* treated primary patient samples, we conclude that both panobinostat and vorinostat have cytotoxic effects at 48 hours in a number of different types of B-NHL. Rituximab alone was not cytotoxic in *ex vivo* models of B-NHL while combination of HDACi plus rituximab only augmented cell death in one *ex vivo* treated sample. No further experiments are planned with these samples, however, the *ex vivo* treated samples provided a means to practice working with primary patient samples, which has been very useful in designing the biopsy processing protocols for the clinical trial (chapter three). Furthermore, having data from

primary samples was probably helpful for the negotiation of sponsorship for the clinical trial.

In conclusion, our preclinical work has yielded several results and it will be interesting to see whether these are recapitulated *in vivo* in the clinical trial. Results to be investigated include: whether there is a bias towards GCB-type DLBCL in cells with a synergistic response to combination treatment, the role of induction of CD20 expression in the mechanism of synergy and the implication of p38 MAPK signaling and B-cell receptor signaling in the mechanism of synergy.

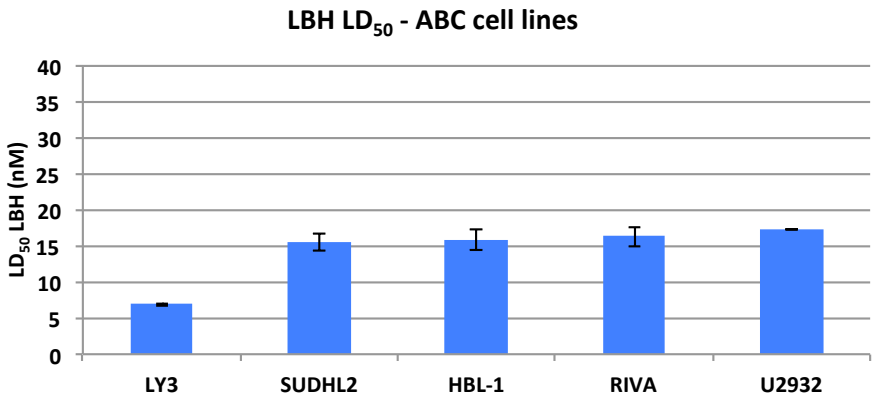


**Figure 2.1:** Lethal dose 50% ($LD_{50}$) of panobinostat (LBH) in activated B-cell (ABC) type DLBCL cell lines after 48 hours treatment. Cell death was assessed by flow cytometry using propidium iodide stain.

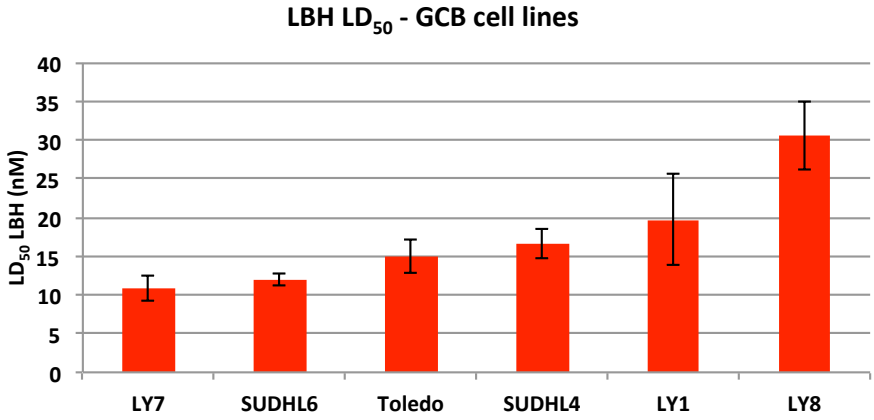


**Figure 2.2:** Lethal dose 50% ($LD_{50}$) of panobinostat (LBH) in germinal center B-cell (GCB) type DLBCL cell lines after 48 hours treatment. Cell death was assessed by flow cytometry using propidium iodide stain.

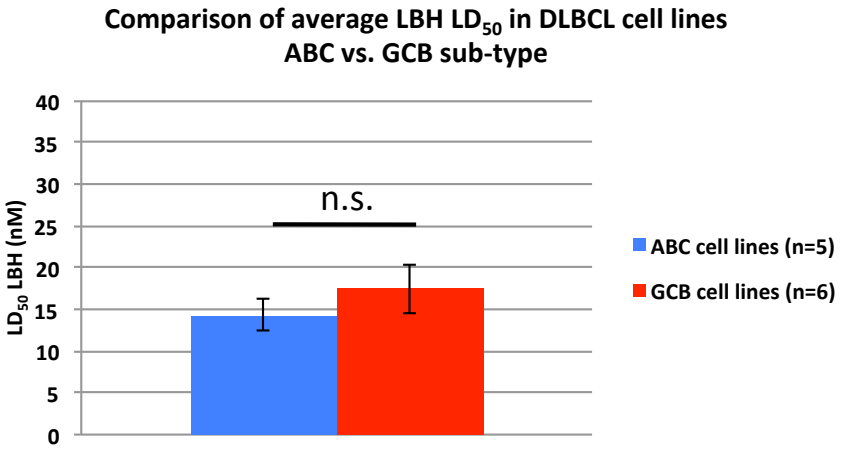


**Figure 2.3:** There's no statistically significant difference between the average LBH $LD_{50}$ in ABC- and GCB-type DLBCL in our panel of cell lines. Treatment time = 48 hours. n.s. = not significant.

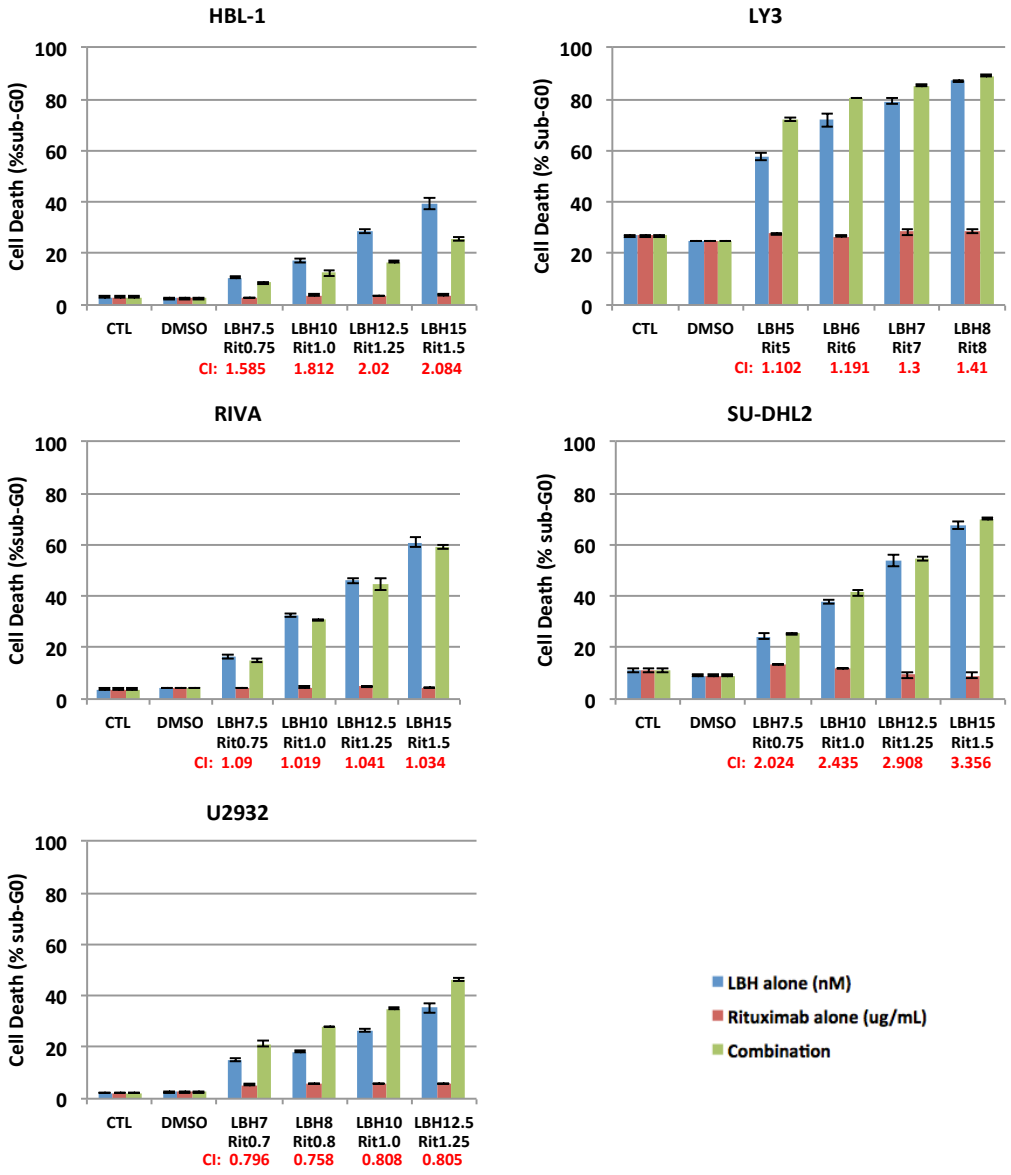


**Figure 2.4:** Cell death in ABC-type DLBCL cells treated with LBH alone, rituximab alone or the combination for 48 hours. The combination index (CI) values, calculated using CalcuSyn, are indicated in red.

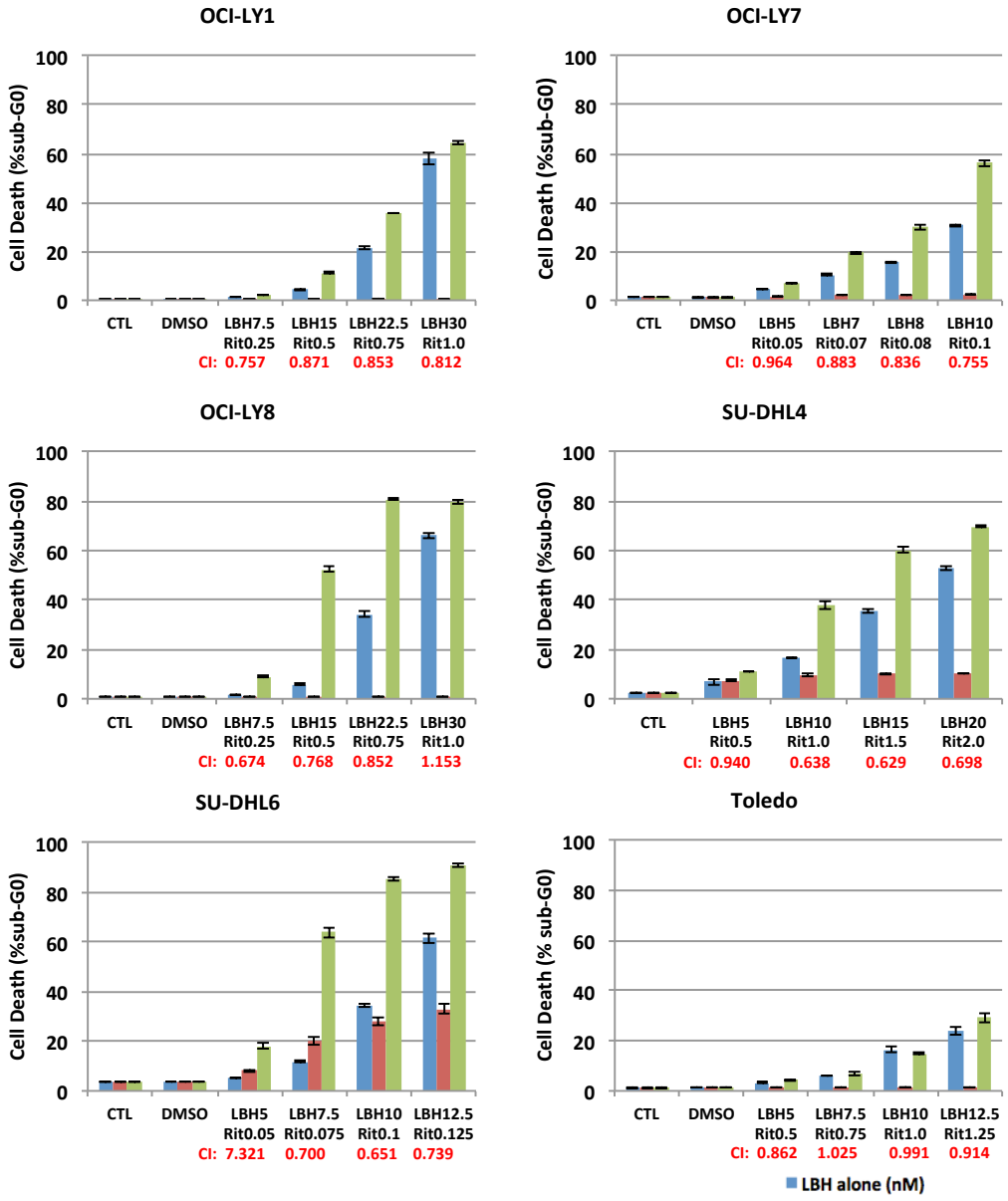


**Figure 2.5:** Cell death in GCB-type DLBCL cells treated with LBH alone, rituximab alone or the combination for 48 hours. The combination index (CI) values, calculated using CalcuSyn, are indicated in red.

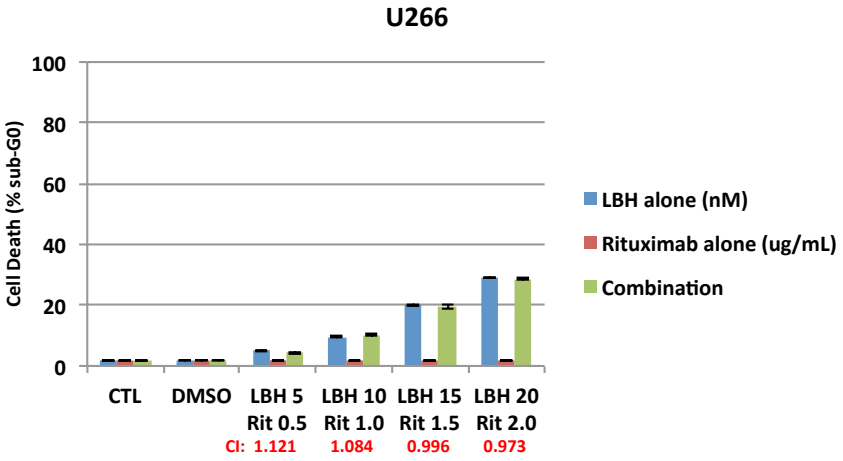


**Figure 2.6:** Cell death in the CD20-negative multiple myeloma cell line, U266 after 48 hours treatment with LBH, rituximab or both drugs. The combination index (CI) values, calculated using CalcuSyn, are indicated in red.

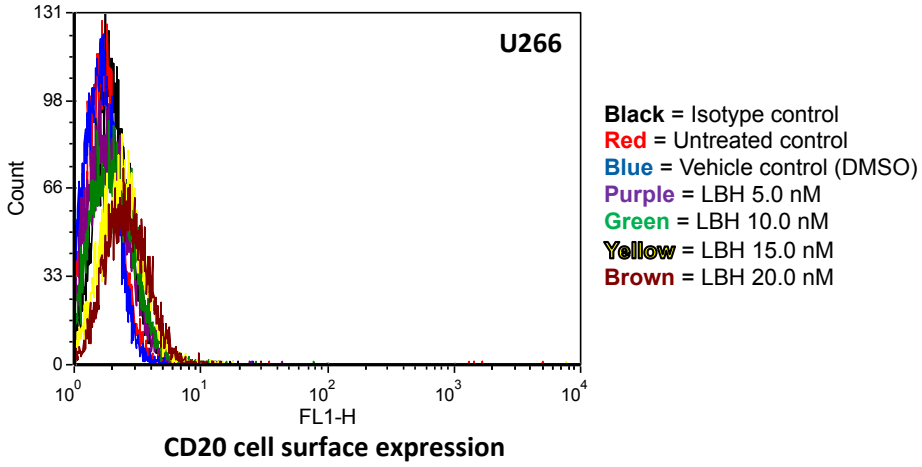


**Figure 2.7:** CD20 cell surface expression in U266 cells following LBH treatment. The fact that CD20 signal never exceeds the signal in isotype control stains suggests that these cells are CD20-negative. Treatment with LBH does not increase CD20 cell surface expression.

| Patient # | DIAGNOSIS |
|---|---|
| Patient 6 | Follicular Lymphoma |
| Patient 7 | Follicular Lymphoma |
| Patient 8 | Follicular Lymphoma |
| Patient 9 | Nodal Marginal Zone Lymphoma |
| Patient 10 | Hairy Cell Leukemia |
| Patient 14 | Small Lymphocytic Lymphoma (Chronic Lymphatic Leukemia) |
| Patient 15 | Diffuse Large B-Cell Lymphoma |
| Patient 17 | Diffuse Large B-Cell Lymphoma |
| Patient 22 | Small Lymphocytic Lymphoma (Chronic Lymphatic Leukemia) |

**Table 2.1:** List of primary patient samples treated *ex vivo* with HDACi and rituximab. Patient samples are numbered consecutively upon receipt in the lab and so not all samples pertain to the lymphoma project described in this chapter.

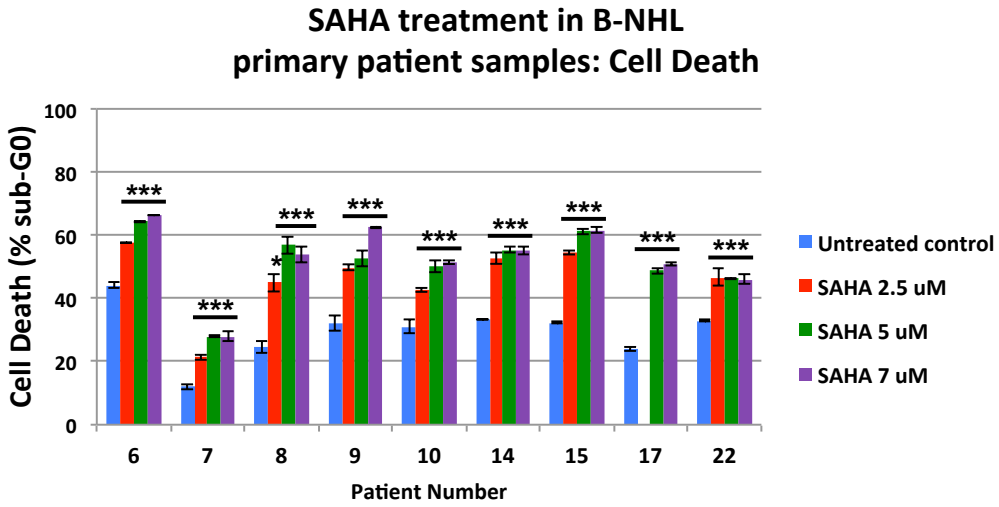


**Figure 2.8:** Cell death after 48 hours treatment *ex vivo* with vorinostat (SAHA). Data shown represent the mean of three experimental replicates, error bars = SEM. * = P<0.05 compared to control, *** = P<0.001 compared to control. Please note that there are no data for either cell viability or cell death from Patient number 17 treated with 2.5 μM SAHA.

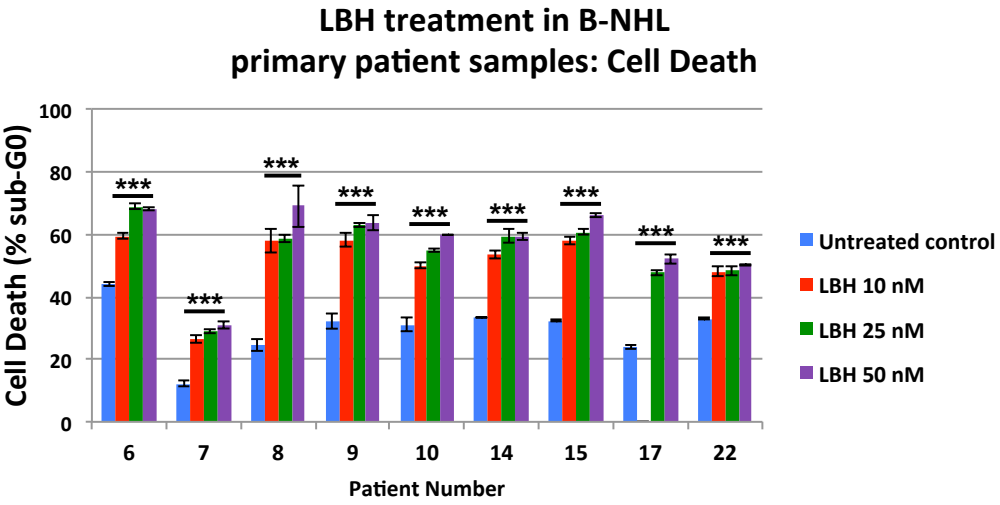


**Figure 2.9:** Cell death after 48 hours treatment *ex vivo* with panobinostat (LBH). Data shown represent the mean of three experimental replicates, error bars = SEM. *** = P<0.001 compared to control. Please note that there are no data for either cell viability or cell death from Patient number 17 treated with 10 nM LBH.

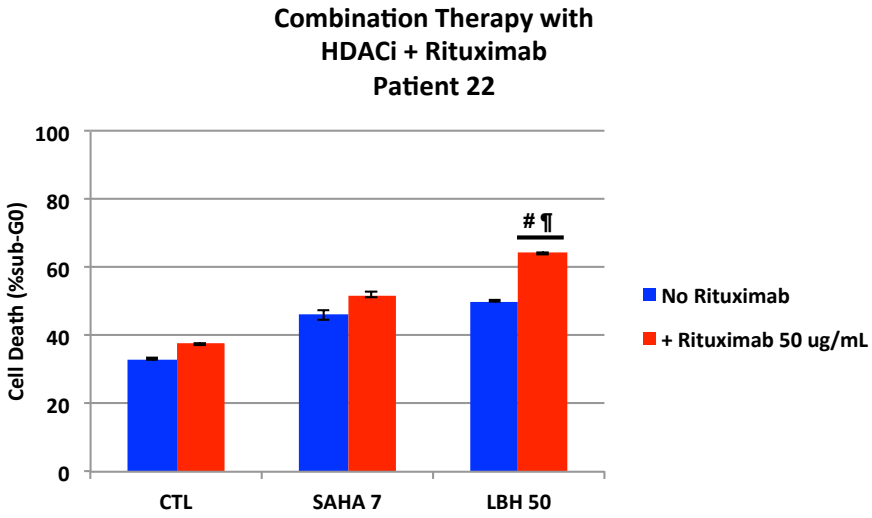


**Figure 2.10:** Co-treatment with SAHA and rituximab shows an additive effect on cell death in patient sample number 22 (Small Lymphocytic Leukemia), while co-treatment with LBH and rituximab potentiates the effect of LBH alone on cell death even further.
Treatment time: 48 hours.
Data shown represent the mean of three experimental replicates, error bars = SEM.
# = P<0.001 compared to rituximab treated control. ¶ = P<0.001 compared to LBH 50 nM (without rituximab).

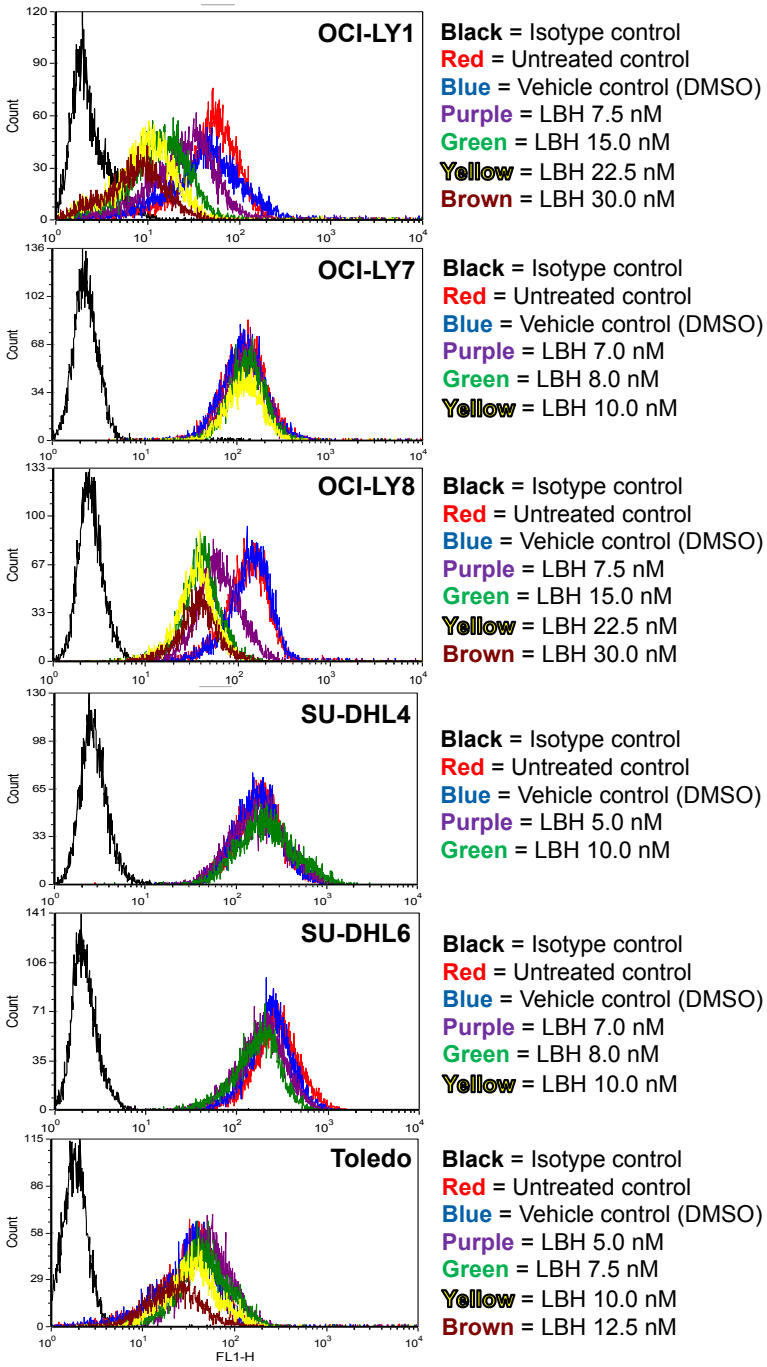


**Figure 2.11:** CD20 cell surface expression in GCB-type DLBCL cell lines treated with LBH for 48 hours.

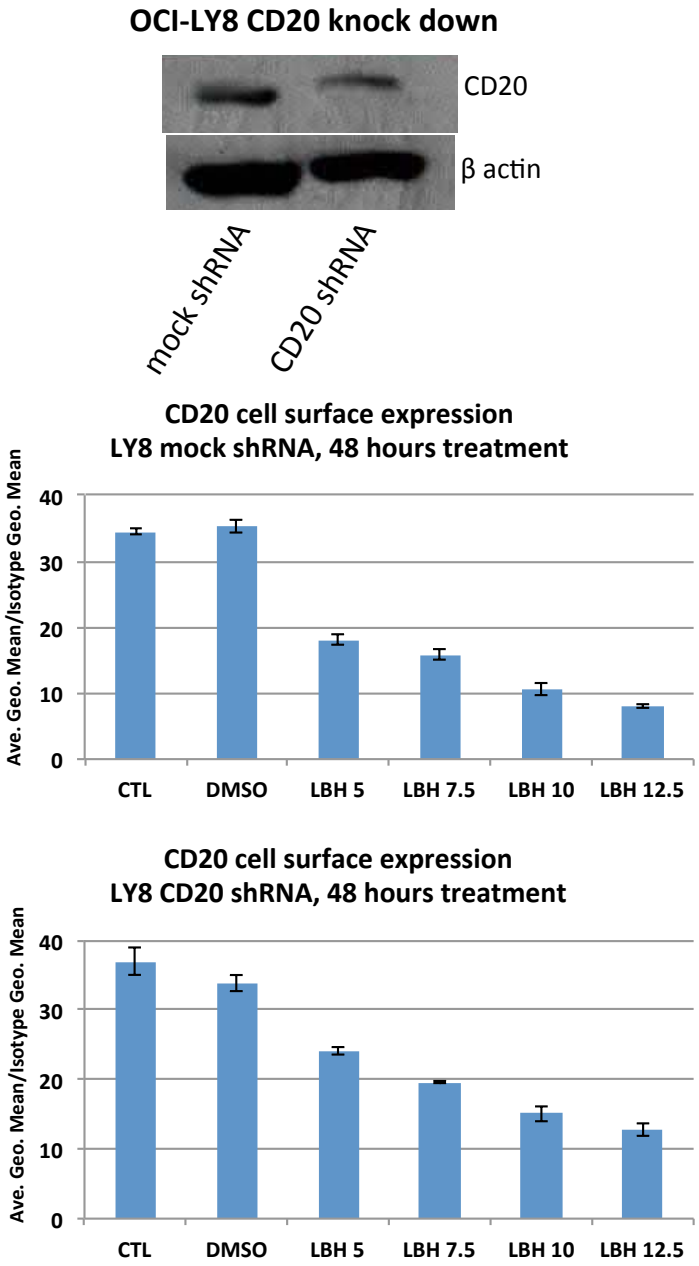


**Figure 2.12:** Top: Immunoblot of whole cell lysates from OCI-LY7 cells treated with either mock shRNA or CD20 shRNA. β actin is included as a loading control.
Middle and bottom: CD20 cell surface expression depicted as average geometric mean over isotype control geometric mean. CD20 cell surface expression is reduced regardless of the kind of shRNA treatment however, cells treated with shRNA against CD20 (bottom) do not show reduced levels of surface CD20 compared to mock shRNA treated cells (middle).

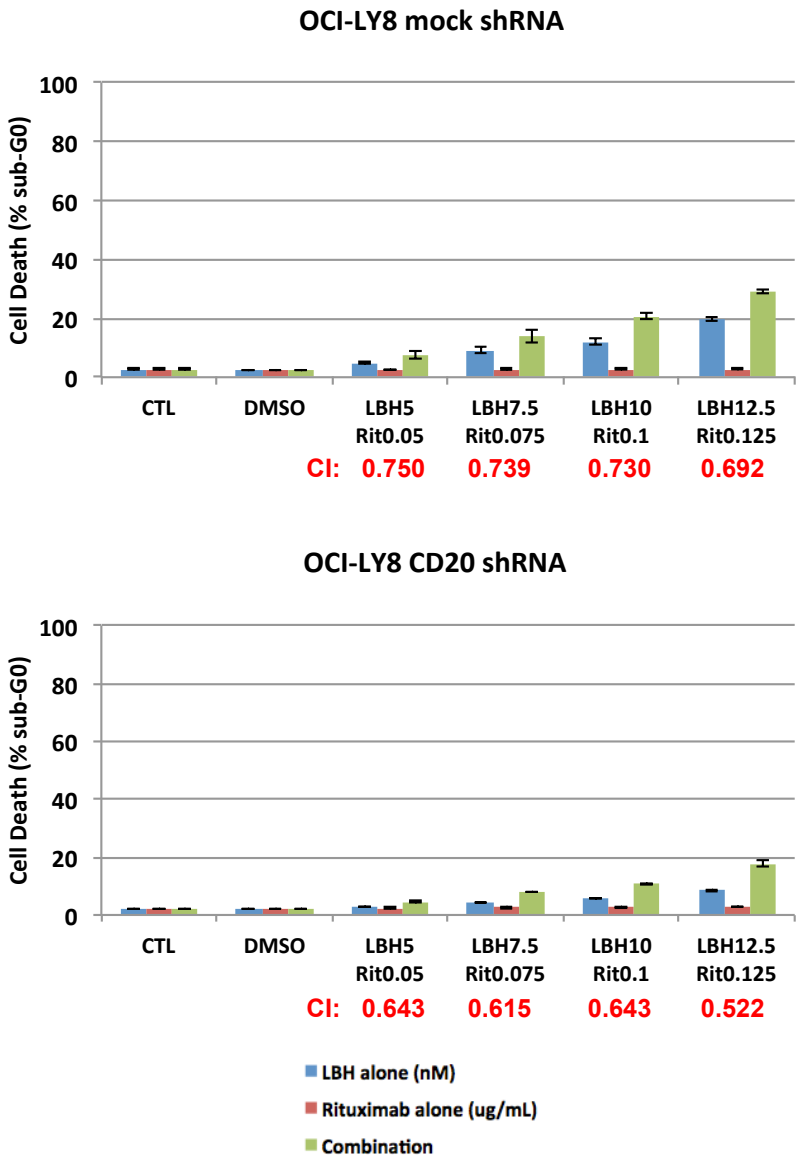


**Figure 2.13:** Cell death in OCI-LY8 cells treated with LBH alone, rituximab alone or the combination for 48 hours. The combination index (CI) values, calculated using CalcuSyn, are indicated in red. There is robust synergy regardless of the kind of shRNA added suggesting that CD20 surface levels are more important to this effect than total CD20 protein levels (see figure 2.12).

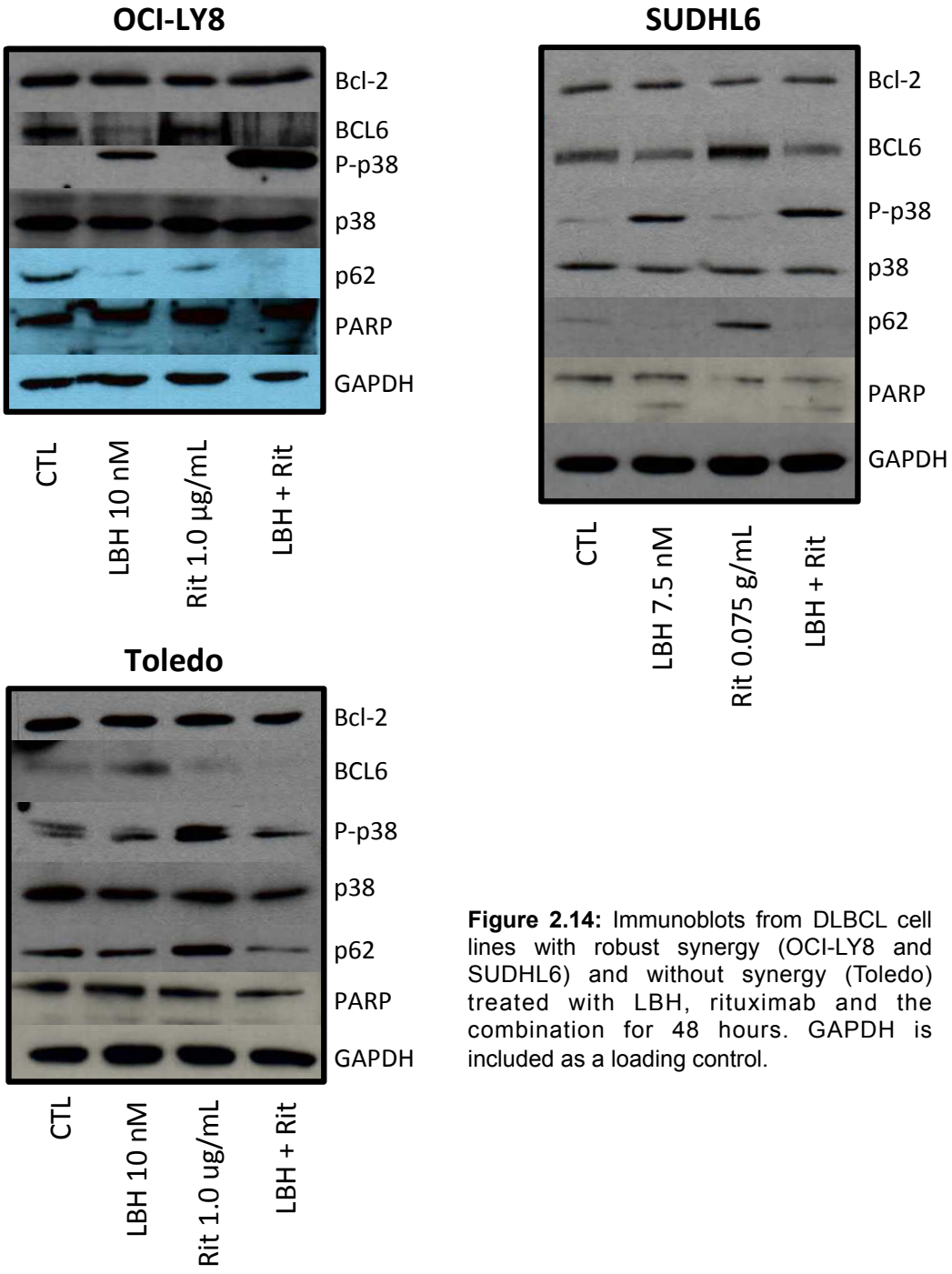


**Figure 2.14:** Immunoblots from DLBCL cell lines with robust synergy (OCI-LY8 and SUDHL6) and without synergy (Toledo) treated with LBH, rituximab and the combination for 48 hours. GAPDH is included as a loading control.

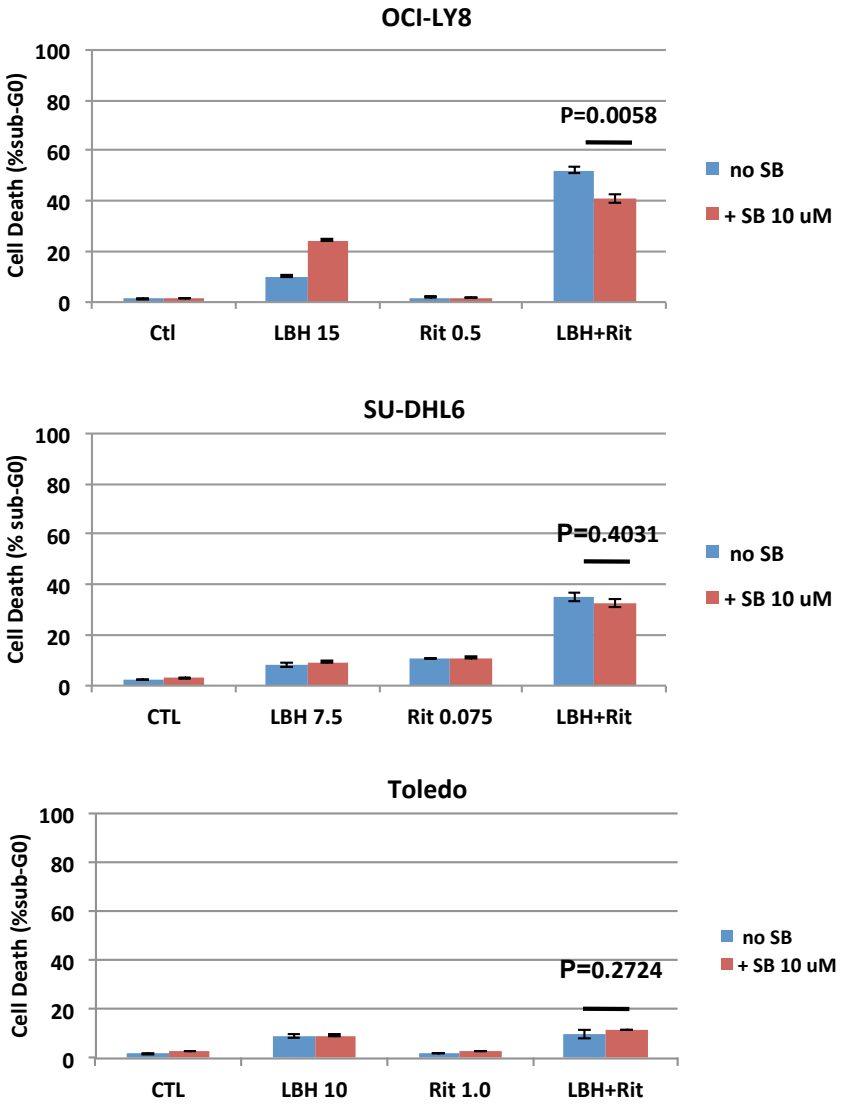


**Figure 2.15:** Cell death in OCI-LY8, SUDHL6 and Toledo cells treated with LBH alone, rituximab alone or the combination for 48 hours, with or without a chemical inhibitor of p38 MAPK (SB = SB203580).

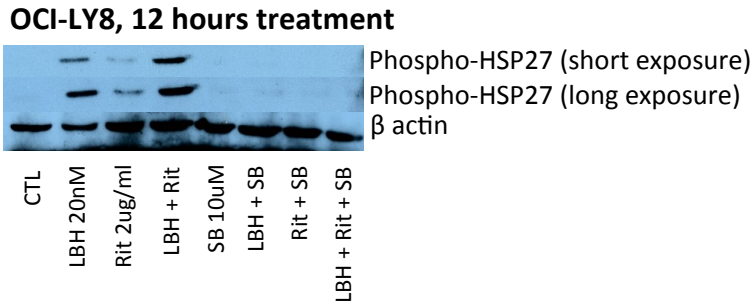


**Figure 2.16:** Immunoblot in OCI-LY8 cells to confirm that the dose of SB (SB203580) used is sufficient to inhibit p38 MAPK activity. HSP27 is a downstream target of p38 MAPK. Note that phosphorylation levels of HSP27 are increased with both LBH and rituximab alone and that the combination appears to further increase this mark of p38 MAPK activation in these cells.

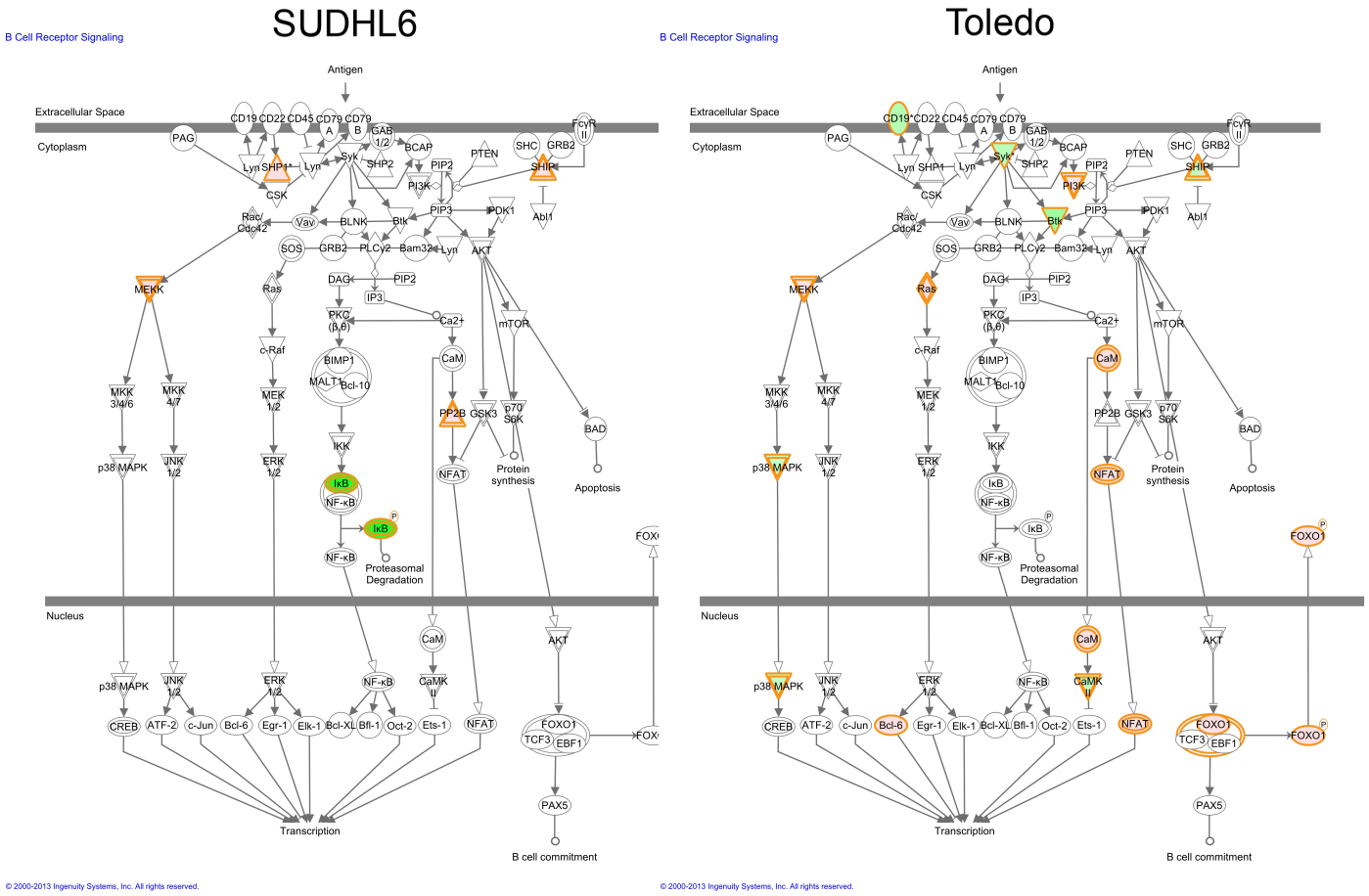


**Figure 2.17:** Ingenuity Pathway Analysis comparing gene expression changes in cells with robust synergy (SUDHL6) and cells without synergy (Toledo). The pathway shown represents gene expression levels in cells treated with LBH plus rituximab over levels in untreated cells. Red indicates increased gene expression levels in treated cells while green indicates decreased gene expression levels in treated cells.

# Chapter 3

# "To the bedside"

## QCROC-02: A Phase II Study of Oral Panobinostat (LBH589) and Rituximab to Treat Diffuse Large B Cell Lymphoma

### 3.1 Introduction:

Current standard treatment of DLBCL, with combination chemo- and immunotherapy (R-CHOP), achieves 50-80% survival[34,35]. However, for patients who progress or relapse on R-CHOP, no accepted second-line therapy exists. This is particularly true for the majority of relapsed patients who are not eligible for autologous stem cell transplant. Based on our data from preclinical models of DLBCL (chapter two), we decided to test HDACi treatment, both alone and in combination with rituximab, in the clinic. Current standard treatment was deemed to be sufficiently beneficial that denying patients the opportunity to try R-CHOP would be unethical. For this reason, we chose patients who had failed R-CHOP and who were not candidates for autologous stem cell transplant, as the patient population in which to study the effects of HDACi with or without rituximab.

The initial idea that made us interested in testing HDACi in the context of DLBCL was closely linked to promising data from preclinical models showing synergistic effects of HDACi combined with rituximab in B-NHL[138,139,147,158]. Thus, we hypothesized that HDACi plus rituximab might be a

superior treatment to HDACi alone. However, it was felt that the clinical effect of monotherapy with HDACi in general, and with panobinostat in particular, was not sufficiently well characterized in patients with relapsed DLBCL to provide a good reference for comparison. Therefore, we decided on a trial design with two arms: one where patients were treated with panobinostat alone and one where patients were treated with panobinostat in combination with rituximab. Patients will be assigned to one treatment arm or the other based on a computer-generated randomization list.

It can be surmised from the fact that a large proportion of relapsed DLBCL patients are not candidates for stem cell transplant and that older patients tend to fare worse on R-CHOP than younger patients[33-35], that many relapsed DLBCL patients constitute a frail patient category who are not expected to tolerate aggressive treatment regimens well. We felt that the side-effect profiles of HDACi (including the HDACi chosen for this study, panobinostat) and rituximab were sufficiently benign to be considered as treatment options, even in a fragile patient population.

Despite promising data in preclinical models, previous clinical trials investigating the effects of HDACi in DLBCL have repeatedly demonstrated that only a minority of the treated population derives significant benefit[117-119]. Interestingly, each of these studies has reported occasional partial and complete responses. It therefore seems that there exists a subset of DLBCL patients who derive measurable benefit from HDACi treatment, while most patients with DLBCL will not. We hypothesized that differences in response

could be due to different molecular aberrations present in different tumors. In order to investigate this, we included tumor biopsies in the trial design as a means to assay tumor characteristics.

The incorporation of biopsies for correlative studies of tumor aberrations is a relatively new field and, to the best of our knowledge, the QCROC-02 trial is the first biopsy-driven trial to be conducted in lymphoma. Due to a lack of literature on the practicalities of conducting biopsy-driven clinical trials in lymphoma, we developed our own protocol for obtaining tumor-derived tissue from lymph node biopsies.

The trial is designed as a multi-center trial, involving four hospitals in Canada at the time of writing: the Jewish General Hospital, Montreal, Quebec, Princess Margaret Hospital, Toronto, Ontario, Queen Elizabeth II Health Sciences Centre, Halifax, Nova Scotia and Sacré-Coeur Hospital, Montreal, Quebec. The decision to enroll patients at multiple sites stems from the realization that accrual of patients with relapsed DLBCL who are candidates for experimental treatment would be quite slow if limited to one site. In order to eliminate as much bias associated with processing of samples as possible, all biopsy specimens and blood samples are sent to the Miller/Mann lab at the Jewish General Hospital for processing. Samples collected at sites other than the Jewish General Hospital were delivered overnight and were processed within approximately 30 hours of the time the biopsy or blood sample was taken. By measuring the quality and yield of biological materials isolated using our protocol, we were able to assess, not only the yield and

quality of RNA and DNA from biopsies and blood samples which could be expected by following the QCROC02 protocols, but also the impact of transportation and delay in processing on these samples. Thus, we have developed a platform for processing lymphoma samples from a multi-center trial. We believe this will serve as an example for future lymphoma trials where biopsies are included as a means to investigate tumor heterogeneity and treatment responses.

In summary, the following chapter details our efforts to develop protocols for the isolation of biomaterials from lymph node biopsies and peripheral blood in order to thoroughly characterize individual patient responses to experimental treatment. When planning the trial, we were interested in investigating the following tumor/blood characteristics: protein expression in tumor tissue by immunohistochemistry (IHC), gene expression levels by microarray analysis, tumor and germline DNA aberrations by exome sequencing, protein expression in peripheral blood mononuclear cells (PBMCs) by immunoblot and levels of circulating metabolites in serum by mass spectroscopy. Results presented in this chapter include our preliminary tests to establish the optimal methods of obtaining biomaterials, as well as results from the clinical trial to validate the quality and yield of the actual biomaterials acquired.

## 3.2 Institutions involved:

Due to the scale and relative complexity of the study, many different people and institutions are, and have been, involved in the design and execution of this trial. The trial was initiated and is run through a collaboration between the Lady Davis Institute for Medical Research, McGill University and the Division of Hematology, Segal Cancer Center, with support from members of the Departments of Pathology and Radiology at the Jewish General Hospital, Montreal. The study is part of the Quebec Clinical Research Organization in Cancer (QCROC) umbrella organization for clinical research in cancer. Princess Margaret Hospital, Toronto, ON, Jewish General Hospital, Montreal, QC, Queen Elizabeth II Health Sciences Centre, Halifax, NS and Sacré-Coeur Hospital, Montreal, QC have all contributed patients to the study. Funding for the trial has been provided by Novartis, the manufacturer of panobinostat. Hoffmann-La Roche, the manufacturer of rituximab, provides this drug free of charge to patients randomized to combination therapy in provinces where such experimental treatment is not covered by the provincial health insurance. The clinical trial is managed by Ozmosis Research.

## 3.3 Ethics:

All treatments and correlative science procedures are performed with

informed consent from the patients on the study. The trial described herein has been approved by the University Health Network Research Ethics Board and Health Canada. It is registered at clinicaltrials.gov under the identifier: NCT01238692.

**3.4.1 Dosing:** All patients on this trial are treated with panobinostat 30 mg three times per week (Monday, Wednesday and Friday). Panobinostat is taken *per os*. For patients randomized to combination treatment, rituximab is administered intravenously at a dose of 375 mg/m$^2$ every 21 days.

**3.4.2 Samples for correlative studies:** As mentioned in the introduction to this chapter, previous studies of HDACi have demonstrated good results in a minority of patients, while the majority of patients do not achieve clinical benefit. For this reason, biopsies and blood samples taken prior to treatment start and at day 15 of treatment, were included in the trial design in order to thoroughly profile tumor and blood characteristics. Tissue from lymph node biopsies was used for IHC analysis and isolation of tumor derived DNA and RNA. Blood samples provided plasma for metabolomics studies, as well as PBMCs from which germline DNA, RNA and whole cell extracts were isolated. It is hoped that these samples will help us gain a better understanding of which patient/tumor characteristics are important for response. They should also provide valuable information on changes induced by treatment in responding vs. non-responding patients and thus

contribute clues concerning target pathways that play a role in HDACi sensitivity. A schematic of the timing of treatments and biopsies/blood samples is shown in figure 3.1.

We were unsure of the best time to biopsy the tumor after treatment start; therefore, we initially included a lymph node biopsy at day two of treatment. However, this was deemed to be impractical after the first patient was biopsied and no subsequent patients have undergone a day two biopsy.

## 3.5 Materials and methods for correlative science project:

Given the scarcity of literature describing sequential biopsies for lymphoma trials, we developed our own "QCROC-02 protocol" for the isolation of DNA, RNA and material for IHC from biopsies. For this protocol, a total of four needle core biopsies were taken from an accessible lymph node. The first tissue core was placed in formalin and processed for use in IHC analyses while the last three cores were pooled together to have enough tissue to isolate DNA and RNA from B-cells using a commercial kit (see Appendix for detailed SOPs). Biopsy types other than needle cores are acceptable; the choice of biopsy type is left to the discretion of the treating physician and the radiologist/surgeon performing the procedure. The QCROC-02 protocol has successfully been adapted to process tissue from both excisional biopsies and skin punch biopsies. In addition, a protocol for the isolation of plasma from peripheral blood samples as well as RNA, DNA

and whole cell extracts from peripheral blood mononuclear cells (PBMC) has been developed (Appendix).

**3.5.1 Optimization efforts:** Prior to starting the trial, a number of tests were run in order to determine the most useful way to collect samples. The assays we were primarily interested in, exome sequencing and gene expression analysis by cDNA microarray, require isolation of DNA and RNA respectively from lymphoma cells, as well as DNA from germline cells for sequencing. In addition, we wanted to investigate protein expression in biopsy material by immunohistochemistry.

To get an idea of the potential RNA yield from needle core biopsies, we "biopsied" a mouse liver using needles of varying gauges. A total of eight cores were taken with each needle and pooled for RNA isolation with a Qiagen Allprep DNA/RNA mini kit. The results are shown in table 3.1. While mouse liver tissue is perhaps not the perfect surrogate for a human lymph node, the results demonstrate that useful amounts of RNA can be isolated from small pieces of tissue.

Another concern we had prior to starting the trial was how to best ship samples harvested at other hospitals. Peripheral blood from normal volunteers was exposed to a variety of conditions to mimic transport, followed by isolation of protein extracts and RNA from PBMCs. Initially, we evaluated the effect of mock shipping with dry ice. Blood samples were stored for two hours or overnight in a Styrofoam box with dry ice followed by

isolation of PBMCs and extraction of proteins. Centrifuged samples showed massive hemolysis. The signal on immunoblots compared to that from freshly isolated PBMCs was not ideal for either of the conditions exposed to sub-zero temperatures (figure 3.2). This, along with the fact that packaging with dry ice might not be routine practice at some participating hospitals, prompted us to test other shipping conditions: PBMCs exposed to mock shipping for 24 hours on ice and at room temperature were compared with freshly isolated PBMCs. In addition to the effects of shipping at different temperatures, we investigated the best way to isolate PBMCs by comparing Ficoll gradient separation with red blood cell lysis (see figure 3.3, top for a schematic of the experimental design). Each mock transport and PBMC isolation method was evaluated with respect to: number of PBMCs isolated from 10 mL blood, quality and yield of RNA isolated and quality of protein isolated (figure 3.3). Based on these results, we picked transportation at room temperature followed by isolation of PBMCs by Ficoll gradient separation as the most promising protocol. From the yield of RNA, we concluded that a blood volume greater than 10 mL should be collected. Finally, to test which anti-coagulation system would be best suited for isolation of protein for immunoblots, we compared blood drawn in EDTA tubes with blood from heparin tubes. Based on results shown in figure 3.4, we selected heparin tubes for use in the trial. Note that heparin tubes were also used for the experiments shown in figure 3.2 and 3.3.

In order to assay changes in tumor cells with minimal contamination of the signal from normal cells, we investigated the possibility of enriching our samples for B-cells using a negative selection kit (EasySep human B cell enrichment kit without CD43 depletion, StemCell Technologies). This technology removes unwanted cells using antibodies tagged with magnetic beads targeted towards non-B-cell epitopes. The unwanted cells can thus be separated out using a magnet without touching the B-cells of interest. To test the ability of such a kit to enrich for B-cells, we stained PBMCs from a healthy volunteer with the B-cell marker CD19, before and after negative selection. As shown in figure 3.5, the percentage of CD19 positive cells was greatly increased in the sample after negative selection, suggesting enrichment of the B-cell population. Thus, tissue from needle core lymph node biopsies were treated with the negative selection kit prior to isolation of DNA and RNA. This ensured that down-stream analyses were performed on tissue, which has been enriched for tumor cell content. For biopsy samples where a sufficient number of cells were isolated after negative selection, a portion was stained with CD19 to evaluate the B-cell content.

Our efforts to separate out tumor tissue from biopsy material should not be interpreted as a disregard for the role the tumor microenvironment plays in lymphoma biology. However, most of our hypotheses concerning how HDACi, with or without rituximab, work in DLBCL involve mechanisms directed at the tumor cells so we were interested in investigating the tumor cells directly first. We have entertained the thought of keeping the tissue that

was separated out during negative selection as a "tumor microenvironment-enriched" sample, but no practical work was done to assess the feasibility of this.

In addition to isolation of tissue for DNA and RNA extraction, a separate needle core from each biopsy is taken for use for IHC analyses. Currently, work is ongoing to find suitable positive and negative (or normal expression) controls for each protein target for which we wish to determine expression. Targets include: Bcl-2, BCL6, CD20, c-Myc and acetylated histone H3. The planned controls are normal human tonsils for Bcl-2, BCL6 and CD20 (for both positive and negative/normal expression levels), and a biopsy from a confirmed Burkitt's lymphoma patient for c-Myc positive expression (normal tonsil for c-Myc negative). For acetylated histone H3, we have prepared cell blocks from tonsil cells in single cell suspension. Cells used for positive controls have been treated with panobinostat for 15 hours while cells for negative/normal expression are untreated. Increased acetylation is readily apparent in the treated sample.

**3.5.2 Gene expression profiling:** RNA isolated from biopsies (pre-treatment and Day 15) was sent to the McGill University and Genome Quebec Innovation Centre, Montreal for analysis of gene expression using microarray technology (Agilent, one-color, 8x60K arrays). The data files are analyzed by our collaborator Éric Paquet, McGill University. Analysis is still ongoing and no data on gene expression are currently available.

**3.5.3 Exome sequencing:** Exome sequencing of DNA from pre-treatment biopsies and pre-treatment PBMCs was performed at the Institut de Recherche en Immunologie et Cancérologie, Université de Montréal. Exomic DNA was enriched using Illumina exome capture and sequenced using Illumina HiSeq. Thus far, 11 patients (22 DNA samples total) have been sequenced. Data was analyzed by Ryan Morin, Simon Fraser University and Nathalie Johnson, McGill University. Analysis is still ongoing and no data on mutational status will be presented here.

## 3.6 Results:

**3.6.1 Patient enrollment:** A total of 25 patients have been enrolled at four cancer centers across Canada thus far. Of these, Princess Margaret Hospital, Toronto, ON has contributed 13 patients, Jewish General Hospital, Montreal, QC has contributed nine patients, Queen Elizabeth II Health Sciences Centre, Halifax, NS has enrolled two patients, while one patient has been enrolled at Sacré-Coeur Hospital, Montreal, QC (figure 3.6). Enrollment started in December 2010, which means that the trial is accruing approximately one new patient per month.

Patients on the QCROC-02 trial were identified by a trial number starting with 021 (the number of the trial in the Ozmosis Research trial

management system), followed by the enrollment number of the patient. It should be noted that the very first patient scheduled to go on the QCROC-02 trial never received any study treatment because no lymphoma cells were found in his/her pre-treatment biopsy material. Patient 021-001 has therefore been excluded from all analyses. Due to this fact, results discussed in this thesis include patients numbered 021-002 to 021-026.

**3.6.2 Collection of biopsies:** The trial protocol mandates biopsy of accessible lymph nodes whenever deemed safe by the investigator. Biopsies are performed before the start of the study treatment and on Day 15 of treatment. Peripheral blood is taken at the same time points. To date, 18 out of 25 patients (72%) enrolled on the QCROC-02 protocol have had a pre-treatment biopsy performed and of these, eight (32% of all patients on trial, 44% of patients who had a pre-treatment biopsy done) have also had a Day 15 biopsy (figure 3.7, top).

There appears to be some variation among hospitals with regard to the proportion of patients that undergo biopsy (figure 3.7, bottom). Especially the Day 15 biopsy seems to be successfully consented and performed with varying frequency. At Princess Margaret Hospital, nine out of 13 patients (69%) have had a pre-treatment biopsy performed, while only one of these 13 patients (8%) also had a Day 15 biopsy. At the Jewish General Hospital, seven out of nine patients (78%) underwent a pre-treatment biopsy while five out of nine (56%) of these patients also had a Day 15 biopsy done.

Of the two patients from Queen Elizabeth II Health Sciences Centre, one had both pre-treatment and Day 15 biopsies done, while the other did not have any biopsies performed. Thus, biopsy consent rate is 50% for both pre-treatment and Day 15 biopsies. The sole patient enrolled at Sacré-Coeur Hospital had both a pre-treatment and a Day 15 biopsy done. Possible reasons underlying the variation in biopsy collection will be discussed in section 3.7.

**3.6.3 Collection of blood samples:** Pre-treatment blood samples have been collected from all patients on this study, while Day 15 blood samples have been obtained from 24 out of 25 patients (96%). The one patient from whom no Day 15 blood sample was collected (patient 021-009) suffered an adverse event and was removed from the study prior to receiving 15 days of treatment.

### 3.6.4 Yield and quality of biomaterials isolated from biopsies:

Quality and yield of DNA from both biopsy material and blood samples was measured using a Nanodrop 1000 spectrophotometer. This instrument gives a concentration (ng/μl), which is multiplied by the volume of each sample to give the yield (ng). Analysis by Nanodrop also provides the ratio of absorbance at 260nm and 280nm, which is a measure of the purity of nucleic acids in the sample. A DNA sample with no contamination should have an

A260/280 ratio of 1.8, while the A260/280 ratio of a pure RNA sample is 2.0[Ref 172].

The fact that we received samples from multiple institutions, allowed us to investigate the effect of transportation on the quality and yield of the isolated biomaterials.

**3.6.4.1 Yield of DNA isolated from biopsies:** As a first comparison, we were interested in whether the yield of DNA from biopsy material differed between pre-treatment biopsies and Day 15 biopsies. As shown in figure 3.8, the average yield from pre-treatment biopsies is about twice the average yield of Day 15 biopsies however, due to the relatively high variability in biopsy DNA yield, this difference did not reach statistical significance. We require 2200ng of DNA to perform exome-sequencing analysis, which is the down-stream application for which we were using the isolated DNA. Only one out of the 26 total biopsies performed to date (18 pre-treatment and eight Day 15 biopsies) yielded an insufficient amount of DNA for sequencing analysis to be carried out (This was a Day 15 biopsy from patient 021-011). As a point of clarification, it should be noted that we are not planning to sequence DNA from Day 15 biopsies since we do not hypothesize that the DNA sequence is being altered after two weeks treatment with panobinostat.

To investigate possible deleterious effects of transportation on the amount of DNA isolated from each biopsy, we compared the yield of biopsies

performed at the Jewish General Hospital (JGH) with that of biopsies from all other hospitals. Furthermore, in order to get an idea of what yield to expect from the QCROC-02 protocol, we excluded biopsies that were taken using different biopsy techniques (excisional or skin punch) or where the QCROC-02 protocol was clearly neglected (we received material from two patients where only two, instead of three, needle core biopsies had been collected for DNA and RNA isolation). We found no statistically significant difference in DNA yield between pre-treatment biopsies collected using the QCROC-02 protocol (figure 3.9A). It should be noted that the p-value was close to 0.05 and so it is possible that we may see a difference once we accrue more samples.

If we include all pre-treatment biopsies, regardless of biopsy technique, in the analysis, we again find that transport does not seem to impact the amount of DNA isolated from the lymph node biopsies (figure 3.9B).

Comparison of Day 15 biopsies performed at the Jewish General Hospital versus at all other hospitals recapitulates the pattern seen with pre-treatment biopsies. Transportation and/or the delay in processing associated herewith, does not appear to influence the DNA yield of biopsies collected using the QCROC-02 protocol (figure 3.10A) or all biopsy techniques (figure 3.10B).

**3.6.4.2 Quality of DNA isolated from biopsies:** All the comparisons investigated above for DNA yield were repeated using data on the DNA A260/280 ratio as a measure of DNA quality. As shown in figures 3.11, 3.12A and B and 3.13A and B, no statistically significant differences were found, suggesting that both pre-treatment and Day 15 biopsies consistently yield good quality DNA and that transportation does not influence quality of either pre-treatment or Day 15 biopsy DNA.

**3.6.4.3 Yield of RNA isolated from biopsies:** Due to the more dynamic and fragile nature of RNA compared to DNA, we were particularly keen to ascertain the RNA quality and yield we could expect from our samples. A comparison of the RNA yield from all pre-treatment biopsies with all Day 15 biopsies shows no significant difference in yield between these groups (figure 3.14). The RNA we isolate will be used to investigate gene expression profiles in tumor cells from all biopsies with sufficient material using Agilent 8x60K one-color arrays. Microarray analysis requires 200 ng of RNA. Three of 26 total biopsies performed to date (12%) yielded insufficient material to analyze by microarray. Of these, one was a pre-treatment biopsy (from patient 021-017) and two were Day 15 biopsies (from patients 021-011 and 021-018).

We were curious to see if transportation had an effect on the amount of RNA isolated from biopsies. As described above for DNA, we split these analyses into pre-treatment and Day 15 biopsies and also did a separate

comparison for all biopsies performed in compliance with the QCROC-02 protocol. These results, shown in figures 3.15A and B and 3.16A and B, reveal that transportation does not appear to influence the yield, regardless of the timing of the biopsies or the biopsy protocol used. It should be noted that the difference in yield for pre-treatment biopsies isolated by the QCROC-02 protocol was close to reaching significance (figure 3.15A). In future analyses, when larger numbers of biopsies are available, we may find that transportation is, in fact, associated with lower yield. Another point worth noting is that the average yield from Day 15 biopsies isolated using the QCROC-02 protocol is low and close to the limit of what is needed for the designated down-stream application.

**3.6.4.4 Quality of RNA isolated from biopsies:** The quality of RNA isolated from biopsies in this project will be measured using two different techniques: 1) A260/280, discussed above (section 3.6.4) and 2) RNA integrity Number (RIN). The RIN is determined by applying a software algorithm to an electrophoretic trace of the RNA in a sample. The software will then rank the sample on a scale from 1 to 10 with 1 indicating RNA of poor quality and 10 indicating intact RNA[173]. RIN measurements are performed at Genome Quebec as a prelude to microarray analysis. For this reason, RIN-data are only available for those samples that have been sent to Genome Quebec.

Quality measurements of the A260/280 ratio show no difference between the RNA quality of pre-treatment biopsies and Day 15 biopsies (figure 3.17A). Data using the RIN as a quality parameter are in agreement with this (figure 3.17B).

Using the A260/280 ratio as an indicator of RNA quality, it does not appear that transportation influences the quality of the isolated RNA regardless of the timing of the biopsy (pre-treatment or Day 15 biopsy) or the procedure by which it was taken (QCROC-02 protocol compliant or all biopsies) (figure 3.18A and B and figure 3.19A and B). For pre-treatment biopsies, the conclusion reached by looking at the RIN values is the same as for the A260/280 ratio: transportation does not influence the quality of the RNA isolated (regardless of biopsy method) (figure 3.20A and B). We only have RIN-data from one Day 15 biopsy from a non-JGH hospital processed according to the QCROC-02 protocol. Therefore, it is not possible to statistically evaluate the effect of transportation for Day 15 biopsies on samples processed according to the QCROC-02 protocol (figure 3.21A). However, based on the RIN values for biopsies isolated by any method, we conclude that the RNA from Day 15 biopsies taken at hospitals where the samples require transportation prior to processing is of significantly lower quality than RNA from samples that are not transported (figure 3.21B).

**3.6.5 Yield and quality of biomaterials isolated from blood samples:** PBMCs are isolated from heparinized peripheral blood and used to

prepare DNA and RNA and to make whole cell extracts for immunoblotting. DNA from PBMCs will be used as a source of germline DNA for comparison with sequencing results from tumor-derived DNA. At this time, we have no specific plans for the RNA isolated from PBMCs, however, it is collected and stored at -80 in case future projects/collaborations find a use for it. Plasma is also isolated from blood samples for use in a project run by a collaborator (Leandro Cerchietti). This plasma metabolomics project will be briefly discussed in the conclusions section of this chapter, however, no data for this project have been generated in our lab and so no results are presented here.

**3.6.5.1 Yield of DNA isolated from blood samples:** Isolation of DNA from both pre-treatment and Day 15 blood samples yields sufficient DNA for sequencing analysis. No difference in the amount of isolated DNA was observed between pre-treatment and Day 15 blood samples (figure 3.22). Transportation does not influence the amount of DNA yielded from blood samples, either at pre-treatment or at Day 15 of treatment (figure 3.23A and B).

**3.6.5.2 Quality of DNA isolated from blood samples:** In general, DNA isolated from blood appears to be of very good quality. There is no difference in DNA quality between pre-treatment and Day 15 blood samples (figure 3.24) and transportation does not impact the quality of DNA isolated

from either pre-treatment blood samples (figure 3.25A) or Day 15 blood samples (figure 3.25B).

**3.6.5.3 Yield of RNA isolated from blood samples:** Although we do not currently have a use for RNA isolated from blood, the quality and yield were still determined to help gauge the usefulness of the collected materials. Average yields from both pre-treatment and Day 15 samples were high enough to run, for example, a microarray analysis. Curiously, we found that Day 15 blood samples yielded significantly more RNA than pre-treatment samples (figure 3.26). We also found that pre-treatment blood samples that were transported yielded significantly lower amounts of RNA than pre-treatment samples that were processed immediately after being taken (figure 3.27A). Lower yield of transported samples was not found in Day 15 samples (figure 3.27B).

**3.6.5.4 Quality of RNA isolated from blood samples:** No differences in RNA quality were demonstrated between pre-treatment and Day 15 blood samples (figure 3.28) or between samples that were or were not transported (figure 3.29A and B). One sample (the first pre-treatment blood sample, patient 021-003) was sent for analysis by microarray to demonstrate suitability for this application. The RIN of this sample was 9.9 (excellent quality). No further RNA samples derived from blood are planned to be analyzed in this way at the moment.

**3.6.5.5 Whole cell extracts from blood samples:** An aliquot for making whole cell extracts is taken from samples where more than 3 million PBMCs are isolated. Thus far, whole cell extracts have been made from all but three of 49 blood samples (94%). Test immunoblots of acetylated histone H3 and acetylated tubulin have, unfortunately, been of disappointing quality. One problem is that loading of proteins appears to be quite uneven despite quantification of protein concentration prior to starting the experiment. Varying degrees of erythrocyte "contamination" derived from the isolation of PBMCs probably plays a role in this. Due to the poor quality of these blots, they are not informative in terms of measuring changes in acetylation levels of known protein targets of HDACs (figure 3.30). We hope that needle core lymph node biopsy material for IHC can be used as an alternative approach to measure changes in acetylation status (which would have the added benefit that any acetylation changes observed would be from the tumor milieu rather than peripheral blood).

**3.6.5.6 Plasma isolated from blood samples:** On average, we collect 4.8 mL plasma from each patient sample (approximately 15mL peripheral blood). Currently, these samples are used by our collaborator, Leandro Cerchietti, for profiling lymphoma associated plasma metabolites. The plasma samples that have undergone metabolomics profiling to date have all been of sufficiently high quality that mass spectrometry was successful.

**3.6.6 Preliminary results from exome sequencing:** No data on mutations from the 11 patient samples sequenced thus far will be presented in this thesis, however, one important point can still be made: Mutations of genes that are known to occur with high frequency in DLBCL have been detected in all 11 samples. This is important because it strengthens our hypothesis that the DNA and RNA we isolate via our biopsy processing protocol is indeed derived from malignant B-cells and as such provides representative study material for the investigation of each individual tumor. Previously described, recurrent DLBCL-mutations found in our cohort include mutation of: Bcl-2, CCND3, CREBBP, EP300, EZH2, FAS, IKZF3, MLL2, MLL3, P2RY8, SGK1, TET2 and TP53, among others[65,66,174-177].

## 3.7 Conclusions:

This project has been designed to address two key questions: 1) Is HDACi therapy, alone or in combination with rituximab, an effective treatment for patients with relapsed DLBCL and 2) if so, is it possible to predict which patients will benefit from such treatment based on tumor profiles? Much of the work to answer these questions is still ongoing, however, some progress has already been made. This chapter describes the development of protocols to obtain useful biological materials, from tumor biopsies and normal PBMCs, which can be used to profile each individual

patient's disease in detail. As such, the work presented here represents a requisite first step on the way to answering the more important question: who will benefit from treatment?

**3.7.1 Conclusions on biopsy participation:** A protocol was developed for obtaining tumor-derived tissue using needle core lymph node biopsies. This type of biopsy was felt to be a sufficiently minor trauma to not discourage patients from participating in the trial and also to be both safe and ethically permissible. At the same time, needle core biopsies would permit serial sampling of the same lymph node both pre-treatment and after starting therapy. An excisional biopsy would preclude any further sampling of the particular node in question. Serial sampling of the same node will help us avoid some of the complexities associated with intertumoral heterogeneity discussed in chapter one. This strategy, however, does not allay the issue of intratumoral heterogeneity. The uncertainty, of whether the biopsy hit a representative part of the tumor containing enough of the particular malignant clone that our therapy targets to detect, is an inherent challenge in any biopsy driven trial. Inclusion in the protocol of a B-cell enrichment step (discussed in section 3.5.1) as well as results from sequencing (described in section 3.6.6) provides some reassurance that, at least, each biopsy tested contains mutations in genes that are frequently mutated in DLBCL. From this, we are fairly certain that the biological material isolated contains tumor cells. Whether these cells and the mutations they

harbor faithfully represent the cells that respond and thus provide useful information on sensitivity to HDACi treatment in DLBCL remains to be seen.

Another issue with tumor heterogeneity arises in patients with more than one lesion. We only sample the most accessible enlarged lymph node and so it is theoretically possible that the node we biopsy does not respond while another node does. We have not yet correlated biopsy site with response data from CT scans however, this should be possible based on the information we collect from biopsies and CT imaging respectively.

Given that this is the first DLBCL trial at our institution to collect biopsies for tumor profiling, we were quite anxious to see how well such a trial would be received by our patients. Due to the fact that biopsies are encouraged but not mandatory for enrollment, we were curious to see how many patients would consent to this procedure. The published literature on patient willingness to undergo biopsies solely for research use varies considerably. El-Osta *et al.* found that in only 4.4% of patients participating in trials where biopsies were optional would a biopsy be performed, while Gomez-Roca *et al.* found 68% of patients on optional biopsy protocols had at least one biopsy done and 44% had sequential biopsies[178,179]. The proportion of biopsies in the latter study is in relatively good agreement with our data: We find that 72% of patients enrolled in the QCROC-02 trial have had a pre-treatment biopsy and 32% had sequential biopsies. Apparent from these numbers is the fact that the proportion of patients who have more than one biopsy done on our trial falls somewhat short of what has been reported

previously in the literature. Several reasons may be behind this difference: First of all, it is possible that it is due to chance. We are still looking at quite small numbers of patients where the occurrence of random adverse events, for example, could skew the number of patients who have a Day 15 biopsy performed. This happened for patient 021-009, who went off study before having received 15 days of treatment. It is also possible that the patient population on this protocol is sicker than that referenced by Gomez-Roca et al. Overall, a sicker patient population would make the completion of biopsies less likely, however, this would probably be equally true for both pre-treatment biopsies and Day 15 biopsies. A third possibility is that the somewhat disappointing rate of Day 15 biopsy success is due to a difference in culture or attitude among patients and/or the clinical staff involved in the recruiting. It is possible that some sites do not feel that an extra biopsy contributes enough knowledge to warrant the added risk and discomfort to the patient. The rather disparate rates of completion of Day 15 biopsies between the different hospitals participating in this trial suggest that this may be the case. A pedagogical effort to educate both patients and clinical staff on the merits of sequential biopsies may be required to increase post-treatment biopsy rates. A fourth reason that may explain why we see so relatively few Day 15 biopsies is related to logistics and resources. Biopsy of most lesions associated with DLBCL requires either the involvement of an interventional radiologist or a surgeon. The coordination of such procedures is no simple task, especially for the Day 15 biopsy, which must be scheduled

within a narrow window of intervention. It is therefore possible that this biopsy is the first to be dropped due to constraints of time and resources. Likely, the overall biopsy rates are a reflection of influences from several of these challenges. It is worth noting, however, that the success rates of pre-treatment blood samples and Day 15 blood samples are both very high. This suggests that as long as the intervention performed is routine enough, it will be done. This holds a certain promise for future trials incorporating the use of biopsies: As all levels involved (including patients, clinicians, clinical research units and trial coordinators, processing labs, radiology, surgery and pathology) gain more experience with the process, it will hopefully improve both the attitudes towards biopsy driven trials and improve the logistics of running such trials. In the meantime, measures that could increase the proportion of patients who have a Day 15 biopsy done should be encouraged. In terms of safety, one patient reported pain in conjunction with the biopsy procedure. No other adverse events have been reported relating to biopsies.

A brief mention of a couple of ethical questions presented by this trial is in order here: One might speculate whether it is ethical to conduct a trial in which we know that probably only about 25% of patients will respond? Further one might wonder if it is ethical to conduct a trial that includes biopsy procedures (with their inherent risks and discomfort), which will almost certainly not benefit the patients enrolled on this study? I have no simple answer to these questions, however, the argument has been made that, precisely because not all patients will respond, it is imperative to

include biopsies, along with appropriate correlative science to investigate responders and non-responders, in early phase clinical trials in cancer[180].

**3.7.2 Lessons from the protocol project:** As briefly mentioned in section 3.6.1, the very first patient (021-001) we biopsied according to our newly developed protocol, yielded almost no B-cells. Review of the material taken for IHC corroborated this finding and the patient did not receive study treatment. Despite the inauspicious debut, subsequent biopsies have provided much more favorable results. However, even this inaugural setback provided a useful lesson: Had the pre-treatment biopsy not been performed, patient 021-001 would have been treated with experimental therapy despite what, we now know, was an uncertain diagnosis.

Based on the results on the quality and yield of biological material isolated from biopsies and blood samples, several conclusions can be made.

Concerning DNA and RNA isolated from biopsies, we were interested in measuring the yield and quality of nucleic acids isolated in compliance with the QCROC-02 protocol to assess the potential of this protocol. However, all samples, regardless of protocol, were also evaluated to give us an idea of the overall yield and quality of the materials isolated for this trial.

We were happy to find that the average DNA yield from biopsies, regardless of biopsy method or timing, was high enough to be used for DNA sequencing. No significant differences in yield were noted between samples that were transported versus those that were not (although, for pre-

treatment biopsies isolated using the QCROC-02 protocol, the p-value was close to 0.05). It should be mentioned that for Day 15 biopsies isolated according to the QCROC-02 protocol, the DNA yield was just on the threshold of what would be enough for sequencing (it should, however, also be noted that we do not plan to sequence DNA from Day 15 biopsies). In terms of quality, the DNA isolated from biopsies was uniformly of good quality, regardless of method of isolation, timing of biopsy or transport status. Thus, overall, adequate amounts of good quality DNA are isolated from biopsies.

No significant differences in RNA yield from biopsies were observed. This was true for both pre-treatment versus Day 15 biopsies and transported versus non-transported biopsies at both pre-treatment and Day 15 (and both for biopsies processed by the QCROC-02 protocol and for all biopsies). However, the high variability in RNA yield makes it difficult to compare the means. As was observed for DNA yield, the comparison of RNA yield of non-transported samples with transported samples isolated by the QCROC-02 protocol nearly reached significance. Day 15 samples isolated by the QCROC-02 protocol only yielded very low amounts of RNA. This is analogous to what was seen for DNA. In terms of quality, we measured both the A260/280 ratio (which for pure RNA should be close to 2.0) and the RIN. There was good agreement between the two measurements: the further from 2.0 the A260/280 ratio, the lower the RIN. Pre-treatment biopsies overall were found to be of good quality. RNA from Day 15 biopsies that had not been transported, was also of good quality. However, RNA from Day 15 biopsies

sent from other hospitals was of significantly poorer quality as measured by RIN.

Looking at the data from both DNA and RNA, there appears to be an issue with low (or borderline useful) amounts of nucleic acids isolated from Day 15 samples isolated with the QCROC-02 protocol and sent from hospitals where the biopsy needs to be transported. These values were not significantly lower than values from non-transported Day 15 samples because of the high variability; however, it is something to be aware of as we accumulate more samples. Furthermore, the RNA quality, as measured by RIN, of all transported Day 15 biopsies was significantly lower than that of biopsies not requiring transport. These findings all suggest that the Day 15 biopsies, particularly those that are sent from other hospitals, do not yield optimal results. A couple of reasons may be behind this: First, it is possible that the trauma of the pre-treatment biopsy in the area of the lesion still impacts the tissue two weeks later when the Day 15 biopsy is taken. If this were the case, we would expect to see problems in all Day 15 biopsies with no predilection for those requiring transportation. A second possibility is that treatment for 15 days with panobinostat, alone or in combination with rituximab, damages the malignant cells to such a degree that the yield from these biopsies is reduced. If this were the case, we would expect to see poorer yield and quality in Day 15 biopsies from patients with better responses. We have some evidence to support this hypothesis, however, in

order to avoid showing response data, this point will not be discussed further here.

In conjunction with the discussion of possible problems with Day 15 biopsies, it should be mentioned that we originally planned a biopsy on Day 2 of treatment. If the sub-optimal results seen at Day 15 are due to effects of treatment, it is possible that the timing of the post-treatment biopsy could impact quality and yield. Only one patient (021-003) underwent all three biopsies (pre-treatment, Day 2 and Day 15). The Day 2 and Day 15 biopsy quality and yield were similar for both DNA and RNA in this patient. The Day 2 biopsy was dropped after processing of patient 021-003 because it was deemed to be impractical to the point where it would influence patient enrollment. Thus, if we were given the opportunity to re-design the scheduling of the post-treatment biopsy, the ideal timing would probably be sometime between Day 2 and Day 15. This would avoid the logistics issues of having a re-biopsy at Day 2 and minimize the tissue damage seen at Day 15 in samples from patients who respond to treatment.

DNA and RNA isolated from PBMCs was found to be of excellent quality for both pre-treatment and Day 15 blood samples. Transportation did not appear to impact quality. In terms of yield, adequate amounts of nucleic acids for sequencing and microarray analysis were isolated from all samples. For DNA, no differences in yield were seen. For RNA, we found that the yield surprisingly was significantly higher in Day 15 samples than in pre-treatment samples. Looking at the effects of shipping, we found that transported pre-

treatment samples yielded significantly less RNA than non-transported pre-treatment samples. This suggests that some RNA degradation is taking place. No such difference was seen for Day 15 samples.

We also isolate plasma (section 3.6.5.6) and whole cell extracts (section 3.6.5.5) from PBMCs from blood samples. Plasma is sent to our collaborator Leandro Cerchietti who is studying the levels and types of plasma metabolites found in lymphoma patients and normal volunteers. We do not yet have data on quality of these plasma samples but this is under investigation. The quality of all samples thus far has been good enough to obtain data from the mass spectrometry analysis. In terms of quantity, approximately 500 μl of plasma are needed for the metabolomics project so sufficient amounts have been isolated from all samples for this application. We are currently exploring other uses for plasma samples.

The isolation of whole cell extracts from PBMCs has been disappointing. For the majority of blood samples, we isolate enough cells to use some for whole cell extracts, however, the quality of subsequent immunoblots using these extracts has been poor. We had planned to use immunoblots of acetylated histones from pre- and post-treatment blood samples to see if there was an increase in acetylation in the treated samples. An increase would confirm *in vivo* activity of panobinostat. Due to the poor quality of the initial blots, this is no longer deemed feasible, however, we still hope to be able to investigate levels of acetylated histones in tumor tissue by IHC.

In conclusion, we believe we have developed a protocol for the isolation of useful amounts of good quality DNA and RNA, as well as tissue for IHC, from lymph node biopsies. Incorporation of biopsies into the trial design has been well received by both patients and clinicians although the rate of Day 15 biopsy participation leaves room for improvement. The challenge now becomes to transform the biomaterials described in this chapter into useful information on disease response to treatment. We have several hypotheses, gleaned from preclinical work described in chapter two, which it will be interesting to test *in vivo*.

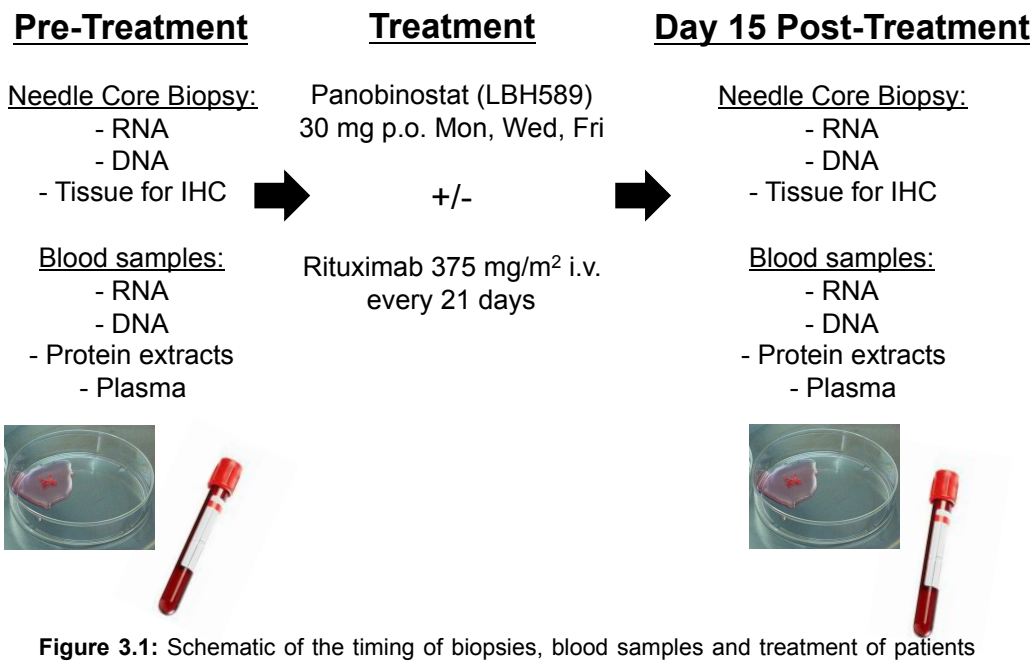


**Figure 3.1:** Schematic of the timing of biopsies, blood samples and treatment of patients enrolled in the QCROC-02 clinical trial. Note that biopsies are not mandatory so not all patients will have these performed.

| Needle size (gauge) | RNA concentration (ng/µl) | RNA quality A260/280 |
|---|---|---|
| 18G | 143.6 | 2.08 |
| 21G | 65.8 | 2.12 |
| 22G | 49.5 | 2.10 |
| 23G | 27.8 | 2.18 |

**Table 3.1:** RNA yield and quality from mock biopsy of a mouse liver using needles of varying lumen size. Samples were processed using the same commercial kit as patient biopsies.

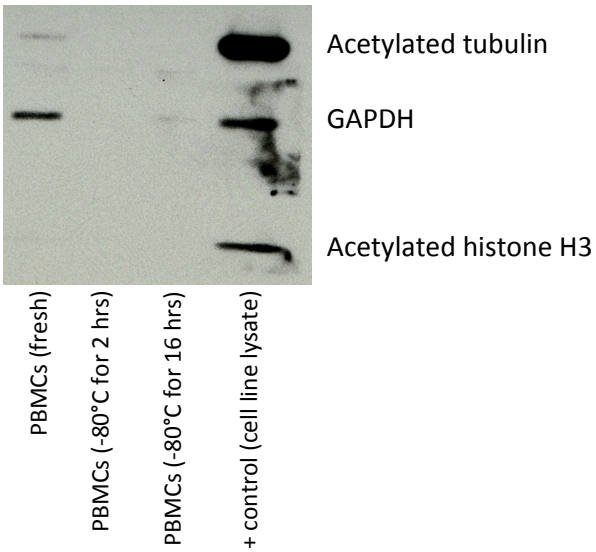


**Figure 3.2:** Immunoblot of acetylation targets in whole cell extracts from peripheral blood mononuclear cells (PBMCs) isolated from normal volunteers subjected to the indicated mock transport conditions. The positive control is cell lysate from a leukemia cell line (NB4) treated with an HDACi to increase acetylation levels. GAPDH is included as a loading control.

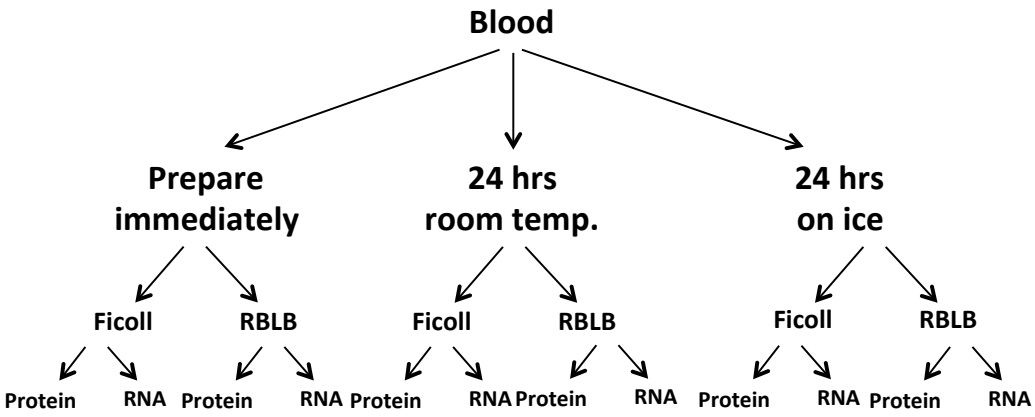


| Isolation method | Cell count (x 10,000) | RNA conc. (ng/µl) | A260/280 |
|---|---|---|---|
| Ficoll, prep. Immediately. | 390 | 16.1 | 1.86 |
| RBLB, prep. Immediately. | 2255 | 119.2 | 1.41 |
| Ficoll, room temp. 24 hrs. | 280 | 192.5 | 1.37 |
| RBLB, room temp. 24 hrs. | 1945 | 0.3 | 0.47 |
| Ficoll, ice 24 hrs. | 160 | 122.9 | 1.38 |
| RBLB, ice 24 hrs. | 1370 | 1.1 | 0.83 |

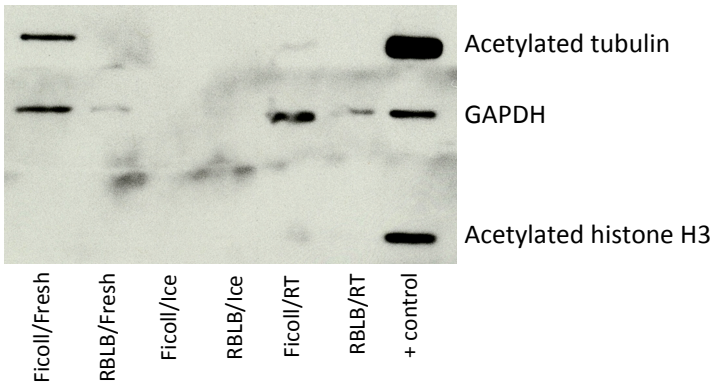


**Figure 3.3:** Top: Schematic of the different processing conditions evaluated in the experiment. The impact of mock transport temperature (room temperature (RT) versus 0°C) as well as the use of Ficoll gradient separation or red blood cell lysis buffer (RBLB) on the quality and yield of whole cell extracts and RNA from normal peripheral blood mononuclear cells (PBMCs) was investigated.
Middle: Cell counts, RNA yield and quality of each condition.
Bottom: Immunoblot to assess quality of protein extracts isolated. GAPDH is included as a loading control.

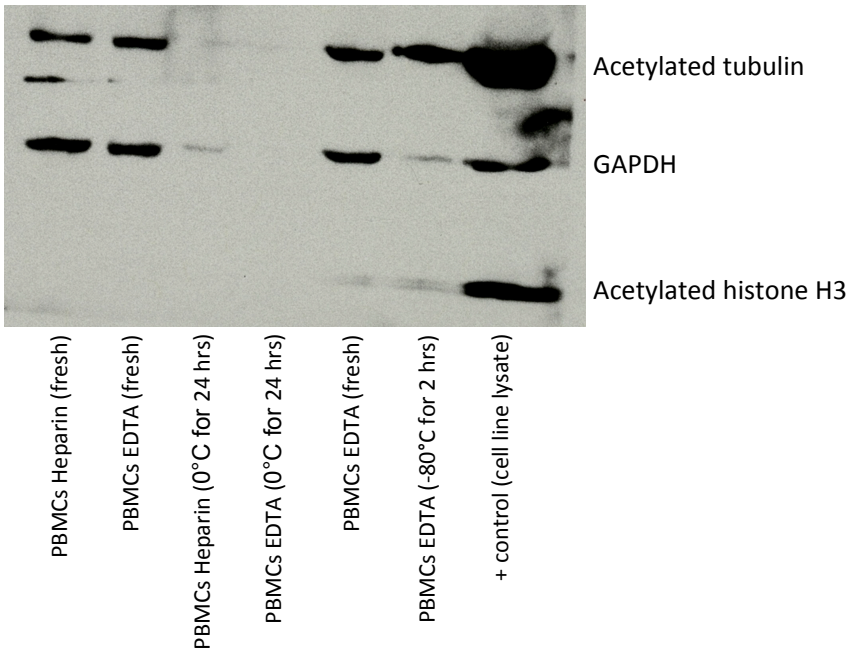


**Figure 3.4:** Evaluation of the impact of anti-coagulation treatment on the quality of the isolated protein extracts. Blood sample tubes with heparin were compared with tubes with EDTA.

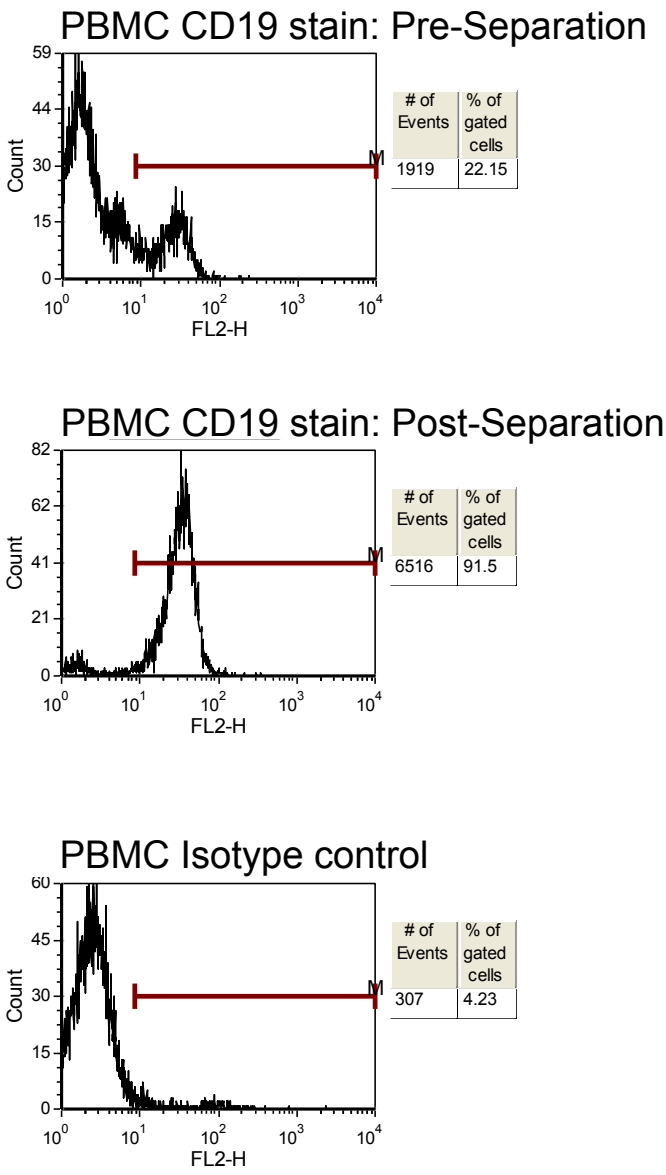


**Figure 3.5:** Evaluation of the efficacy of B-cell isolation using the EasySep kit from StemCell Technologies. Peripheral blood mononuclear cells from a normal volunteer were isolated by Ficoll gradient separation. CD19 stain of cells treated with and without the kit revealed enrichment of the CD19-positive population in cells where the kit was used. The isotype control was used to demarcate non-specific binding.

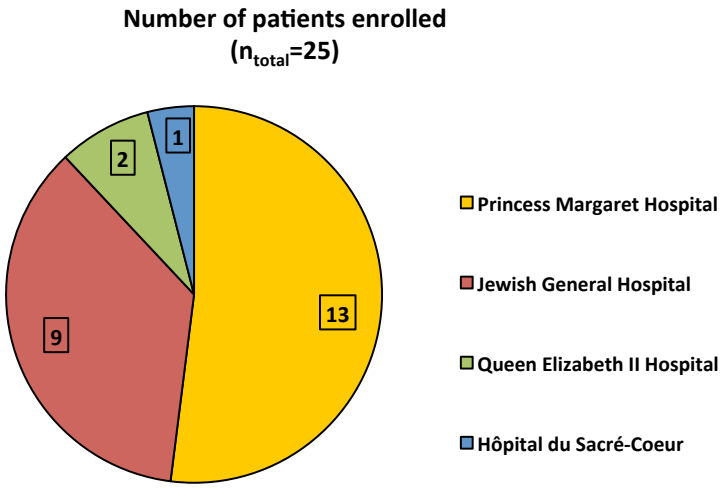


**Figure 3.6:** Number of patients enrolled at each of the four hospitals participating in the QCROC-02 clinical trial.

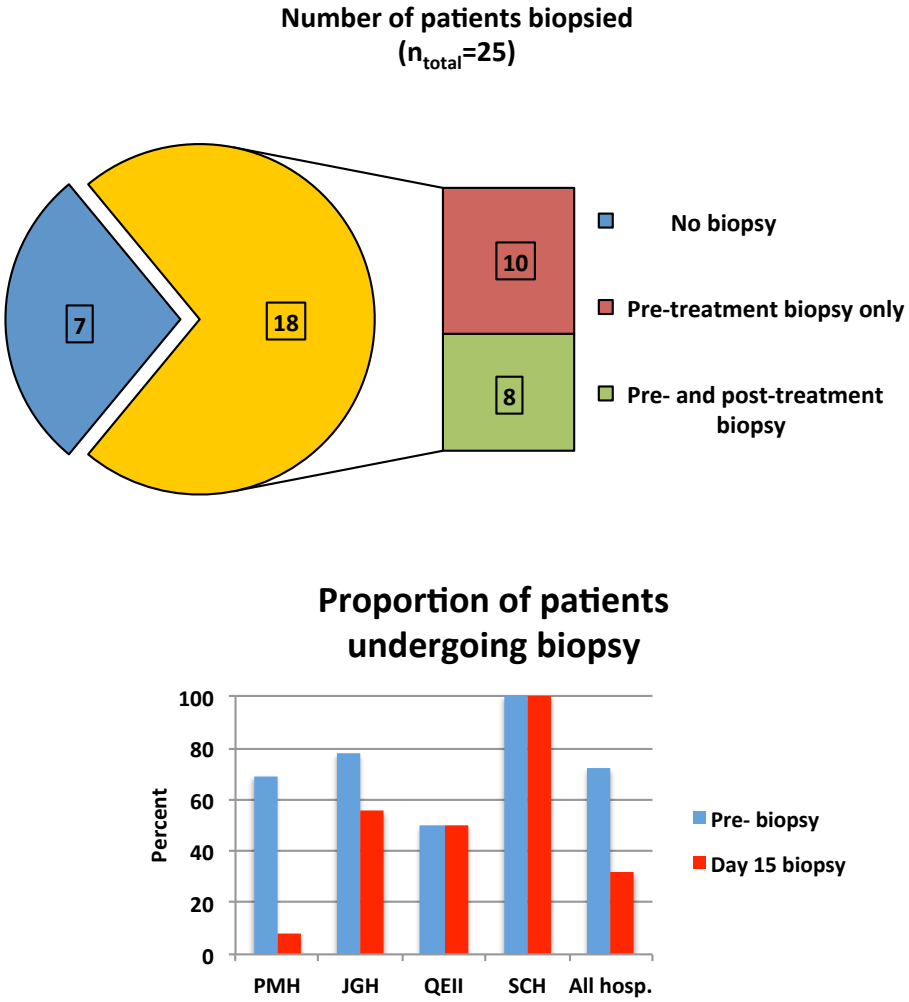


**Figure 3.7:** Top: Number of patients enrolled in the QCROC-02 trial where biopsy was performed. Of those who were biopsies, the number of patients receiving pre-treatment biopsy only and the number receiving both pre- and Day 15 biopsy is indicated.
Bottom: Site-specific biopsy rates. PMH = Princess Margaret Hospital, JGH = Jewish General Hospital, QEII = Queen Elizabeth II Hospital, SCH = Sacré-Coeur Hospital.

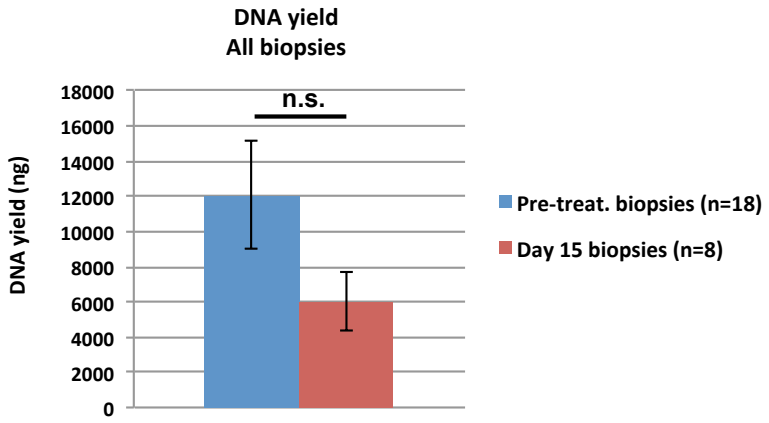


**Figure 3.8:** Comparison of DNA yield (ng) from Pre-treatment biopsies versus Day 15 biopsies. All biopsies, regardless of biopsy protocol used, are included in this graph. The number of biopsies in each group is indicated in parentheses.

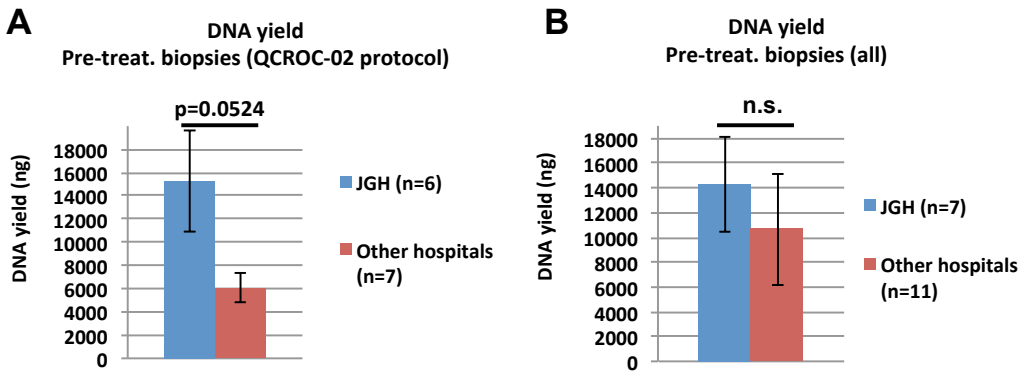


**Figure 3.9: (A)** Comparison of DNA yield (ng) of Pre-treatment biopsies from the Jewish General Hospital (JGH) versus all other hospitals for biopsies isolated in compliance with the QCROC-02 trial protocol. **(B)** Comparison of DNA yield (ng) from the JGH versus all other hospitals for all biopsies, regardless of biopsy protocol followed. The number of biopsies in each group is indicated in parentheses.

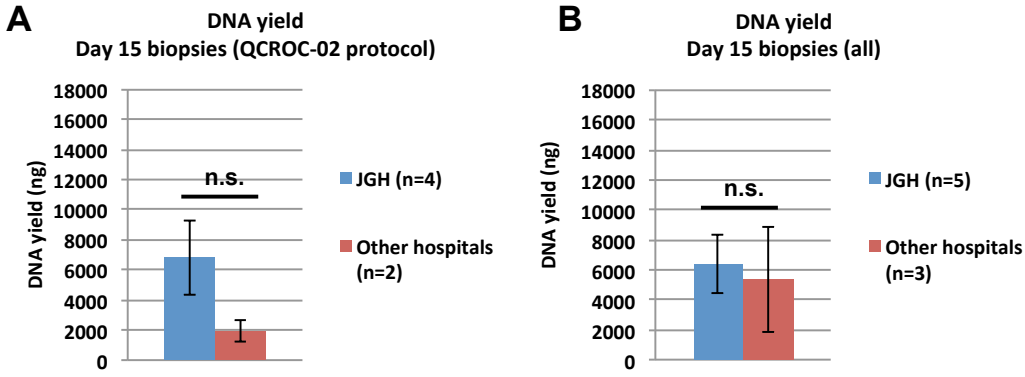


**Figure 3.10: (A)** Comparison of DNA yield (ng) of Day 15 biopsies from the Jewish General Hospital (JGH) versus all other hospitals for biopsies isolated in compliance with the QCROC-02 trial protocol. **(B)** Comparison of DNA yield (ng) from the JGH versus all other hospitals for all biopsies, regardless of biopsy protocol followed. The number of biopsies in each group is indicated in parentheses.

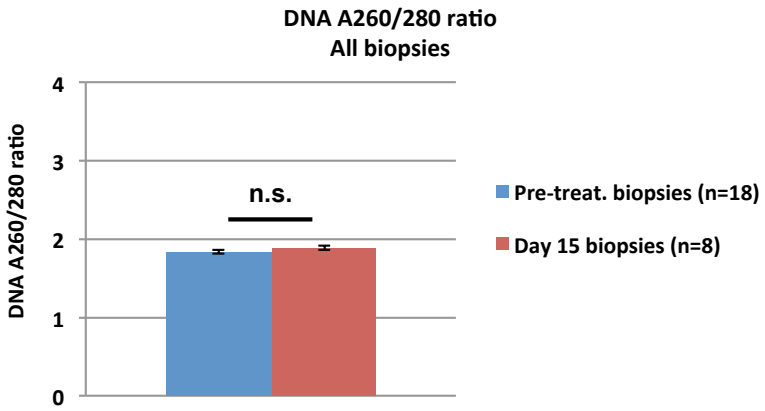


**Figure 3.11:** Comparison of DNA quality of Pre-treatment biopsies versus Day 15 biopsies. All biopsies, regardless of isolation protocol used, are included in this graph. The number of biopsies in each group is indicated in parentheses.

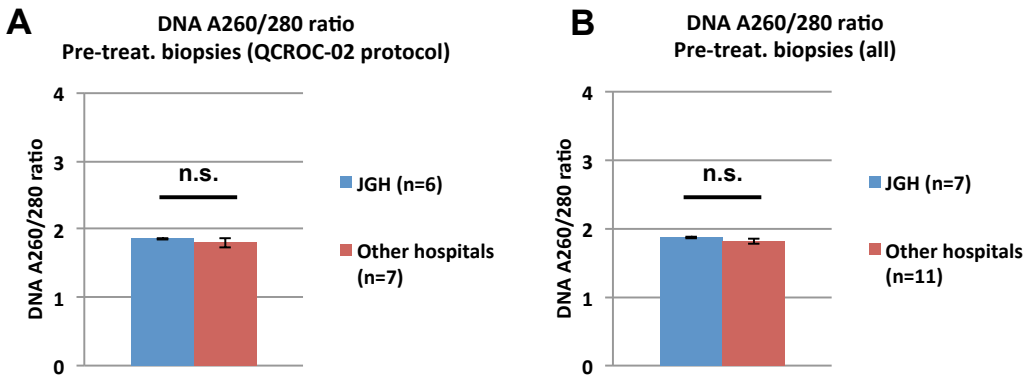


**Figure 3.12: (A)** Comparison of DNA quality of Pre-treatment biopsies from the Jewish General Hospital (JGH) versus all other hospitals for biopsies isolated in compliance with the QCROC-02 trial protocol. **(B)** Comparison of DNA quality from the JGH versus all other hospitals for all biopsies, regardless of biopsy protocol followed. The number of biopsies in each group is indicated in parentheses.

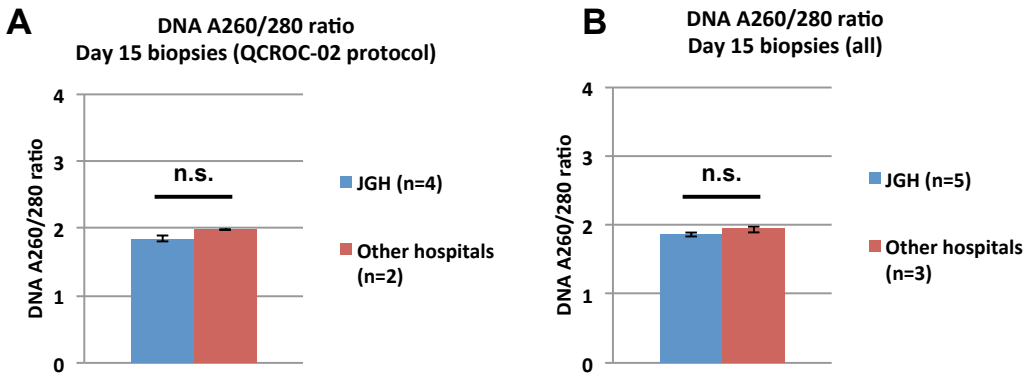


**Figure 3.13: (A)** Comparison of DNA quality of Day 15 biopsies from the Jewish General Hospital (JGH) versus all other hospitals for biopsies isolated in compliance with the QCROC-02 trial protocol. **(B)** Comparison of DNA quality from the JGH versus all other hospitals for all biopsies, regardless of biopsy protocol followed. The number of biopsies in each group is indicated in parentheses.

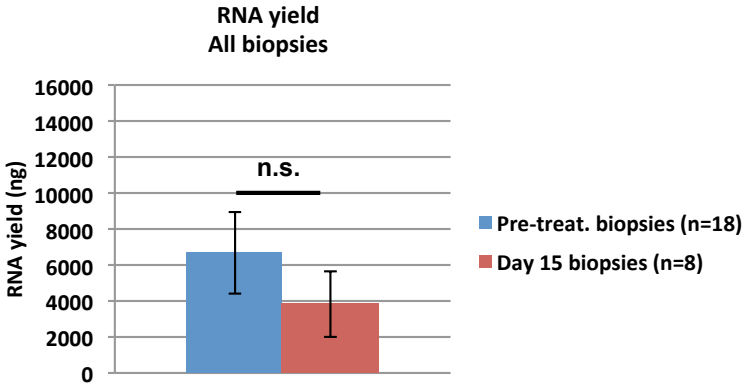


**Figure 3.14:** Comparison of RNA yield (ng) from Pre-treatment biopsies versus Day 15 biopsies. All biopsies, regardless of biopsy protocol used, are included in this graph. The number of biopsies in each group is indicated in parentheses.

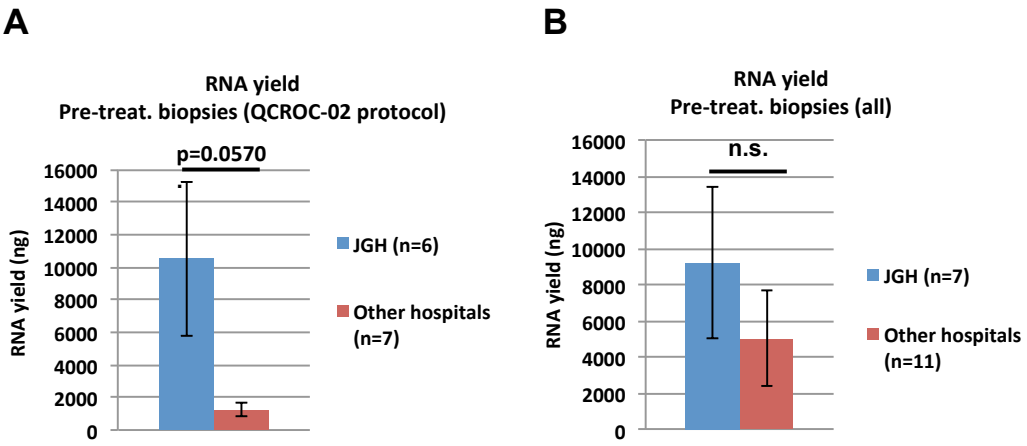


**Figure 3.15: (A)** Comparison of RNA yield (ng) of Pre-treatment biopsies from the Jewish General Hospital (JGH) versus all other hospitals for biopsies isolated in compliance with the QCROC-02 trial protocol. **(B)** Comparison of RNA yield (ng) from the JGH versus all other hospitals for all biopsies, regardless of biopsy protocol followed. The number of biopsies in each group is indicated in parentheses.

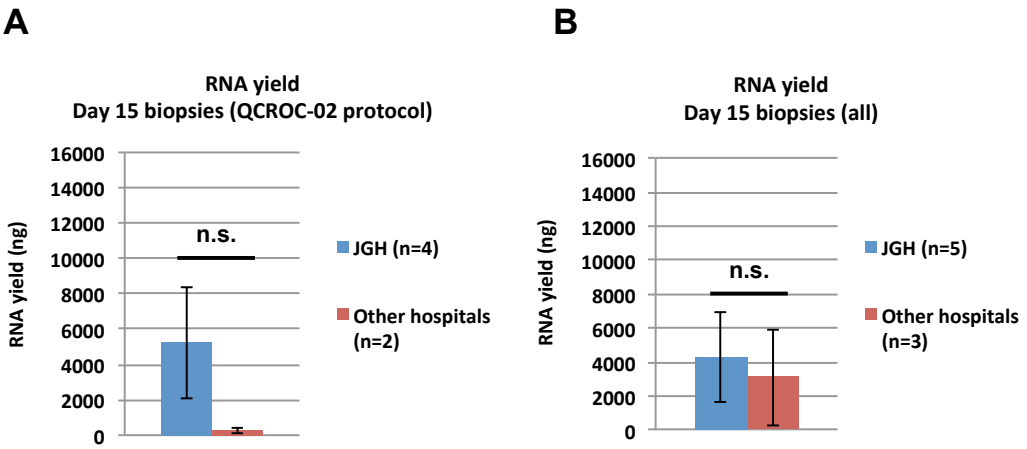


**Figure 3.16: (A)** Comparison of RNA yield (ng) of Day 15 biopsies from the Jewish General Hospital (JGH) versus all other hospitals for biopsies isolated in compliance with the QCROC-02 trial protocol. **(B)** Comparison of RNA yield (ng) from the JGH versus all other hospitals for all biopsies, regardless of biopsy protocol followed. The number of biopsies in each group is indicated in parentheses.

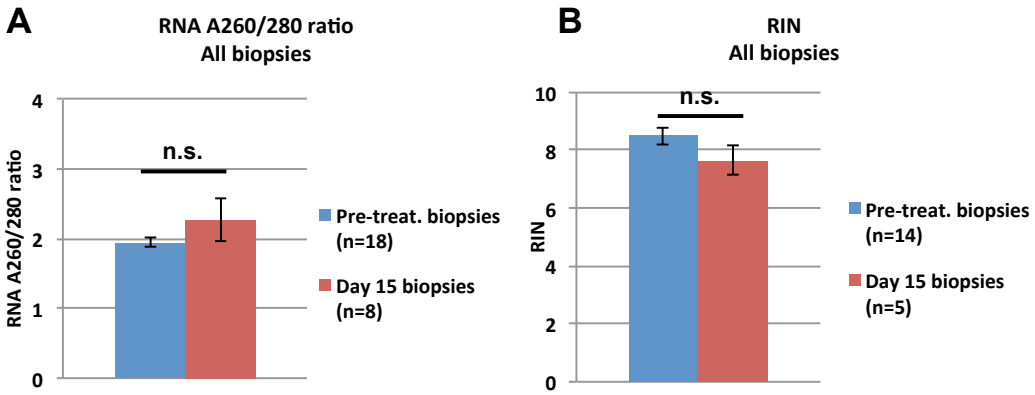


**Figure 3.17: (A)** Comparison of RNA yield quality of Pre-treatment biopsies versus Day 15 biopsies using A260/280 ratio. All biopsies, regardless of isolation protocol used, are included. **(B) )** Comparison of RNA quality of Pre-treatment biopsies versus Day 15 biopsies using the RNA integrity number (RIN). All biopsies, regardless of isolation protocol used, are included. The number of biopsies in each group is indicated in parentheses.

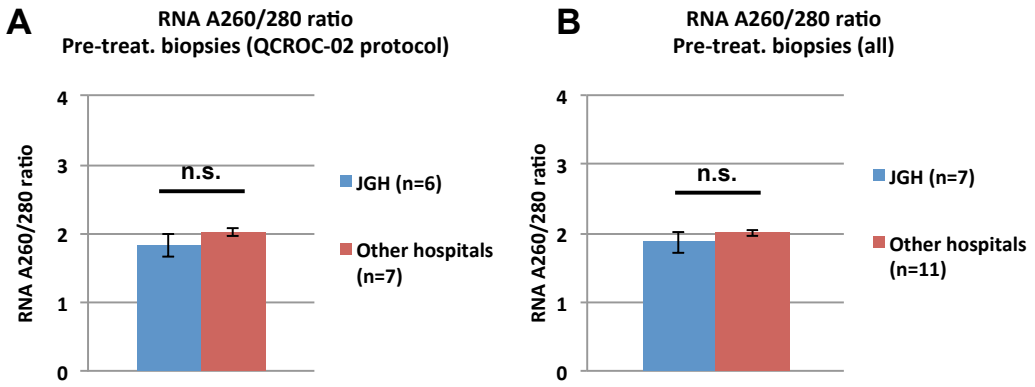


**Figure 3.18: (A)** Comparison of RNA quality (A260/280) of Pre-treatment biopsies from the Jewish General Hospital (JGH) versus all other hospitals for biopsies isolated in compliance with the QCROC-02 trial protocol. **(B)** Comparison of RNA quality (A260/280) from the JGH versus all other hospitals for all biopsies, regardless of biopsy protocol followed. The number of biopsies in each group is indicated in parentheses.

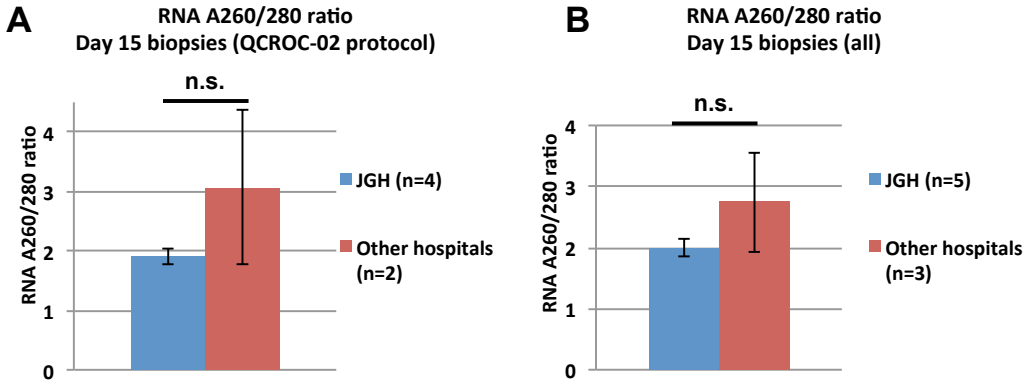


**Figure 3.19: (A)** Comparison of RNA quality (A260/280) of Day 15 biopsies from the Jewish General Hospital (JGH) versus all other hospitals for biopsies isolated in compliance with the QCROC-02 trial protocol. **(B)** Comparison of RNA quality (A260/280) from the JGH versus all other hospitals for all biopsies, regardless of biopsy protocol followed. The number of biopsies in each group is indicated in parentheses.

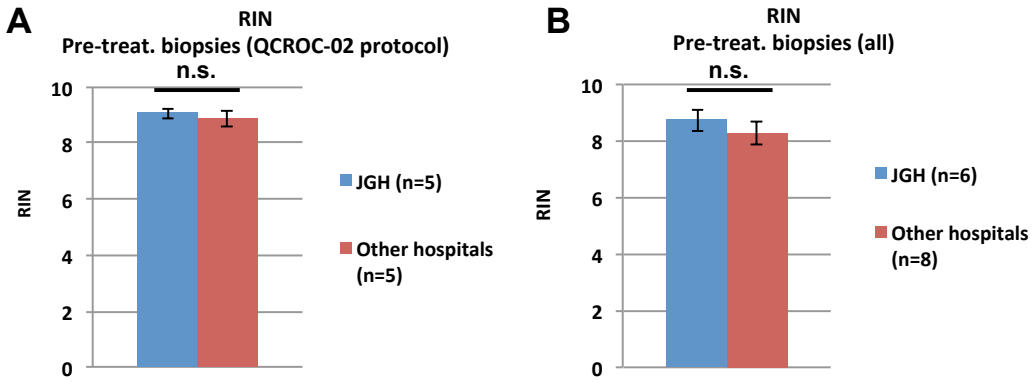


**Figure 3.20: (A)** Comparison of RNA quality (RIN) of Pre-treatment biopsies from the Jewish General Hospital (JGH) versus all other hospitals for biopsies isolated in compliance with the QCROC-02 trial protocol. **(B)** Comparison of RNA quality (RIN) from the JGH versus all other hospitals for all biopsies, regardless of biopsy protocol followed. The number of biopsies in each group is indicated in parentheses.

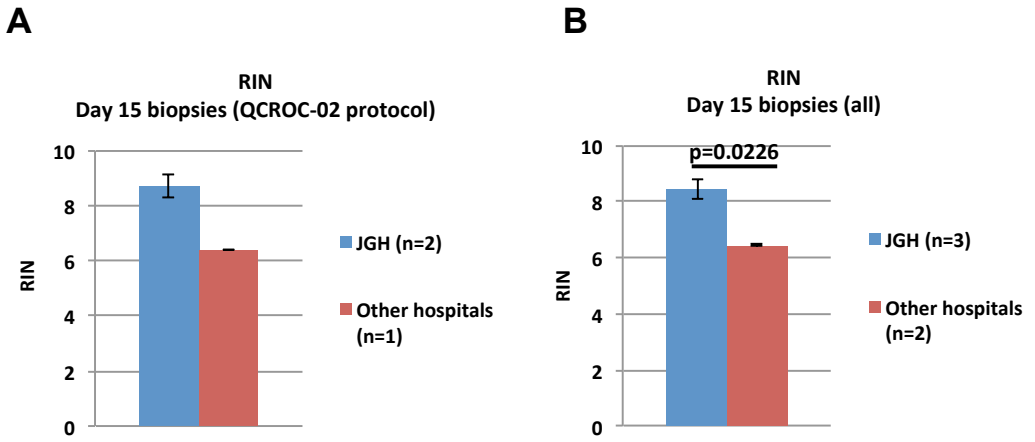


**Figure 3.21: (A)** Comparison of RNA quality (RIN) of Day 15 biopsies from the Jewish General Hospital (JGH) versus all other hospitals for biopsies isolated in compliance with the QCROC-02 trial protocol. **(B)** Comparison of RNA quality (RIN) from the JGH versus all other hospitals for all biopsies, regardless of biopsy protocol followed. The number of biopsies in each group is indicated in parentheses.

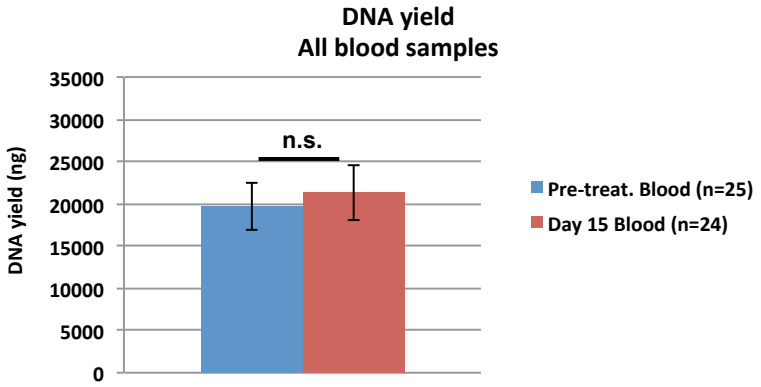


**Figure 3.22:** Comparison of DNA yield (ng) from Pre-treatment blood samples versus Day 15 blood samples. The number of blood samples in each group is indicated in parentheses.

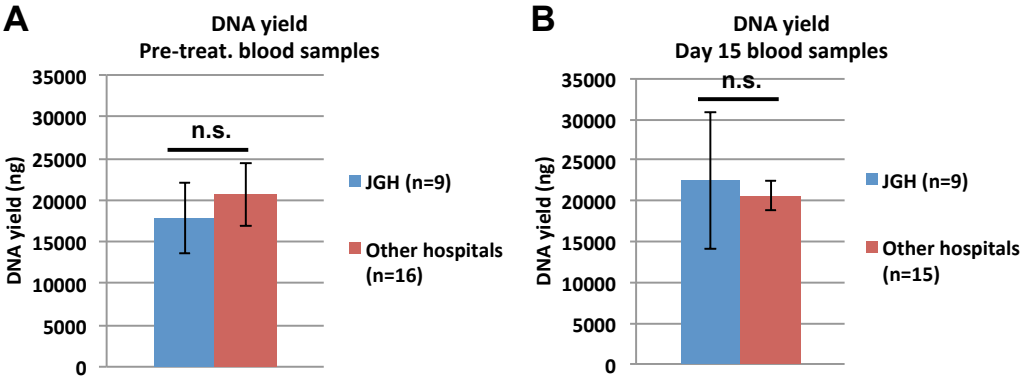


**Figure 3.23: (A)** Comparison of DNA yield (ng) of Pre-treatment blood samples from the Jewish General Hospital (JGH) versus all other hospitals. **(B)** Comparison of DNA yield (ng) of Day 15 blood samples from the Jewish General Hospital (JGH) versus all other hospitals. The number of samples in each group is indicated in parentheses.

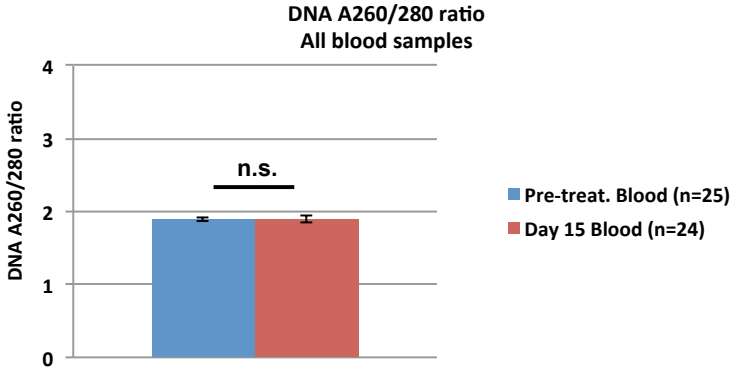


**Figure 3.24:** Comparison of DNA quality of Pre-treatment blood samples versus Day 15 blood samples. The number of blood samples in each group is indicated in parentheses.

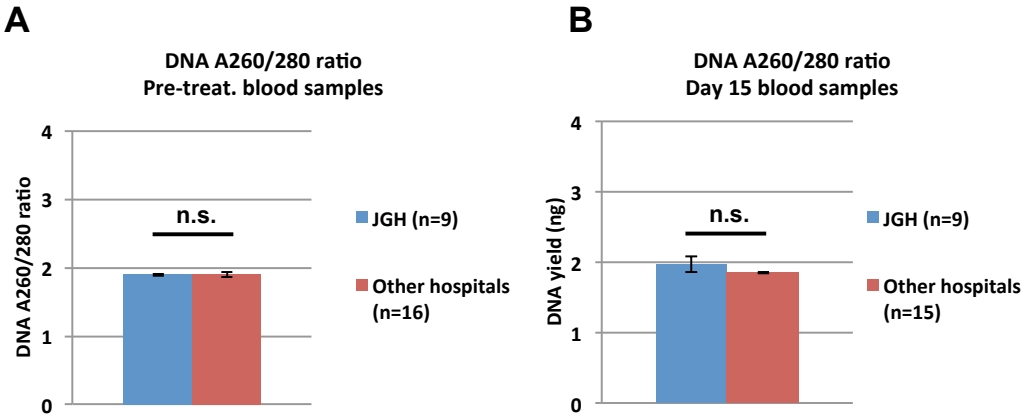


**Figure 3.25: (A)** Comparison of DNA quality of Pre-treatment blood samples from the Jewish General Hospital (JGH) versus all other hospitals. **(B)** Comparison of DNA quality of Day 15 blood samples from the Jewish General Hospital (JGH) versus all other hospitals. The number of samples in each group is indicated in parentheses.

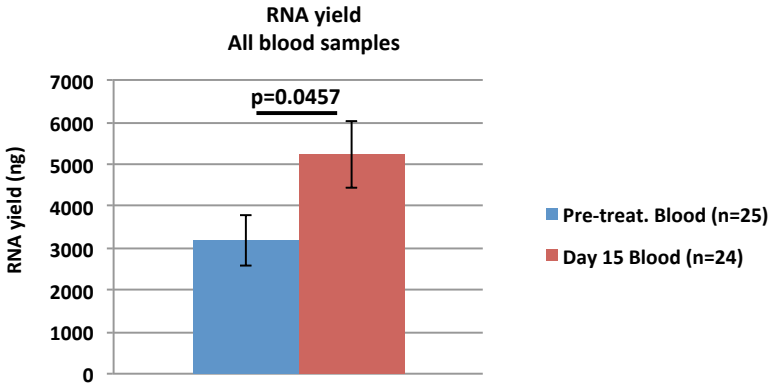


**Figure 3.26:** Comparison of RNA yield (ng) from Pre-treatment blood samples versus Day 15 blood samples. The number of blood samples in each group is indicated in parentheses.

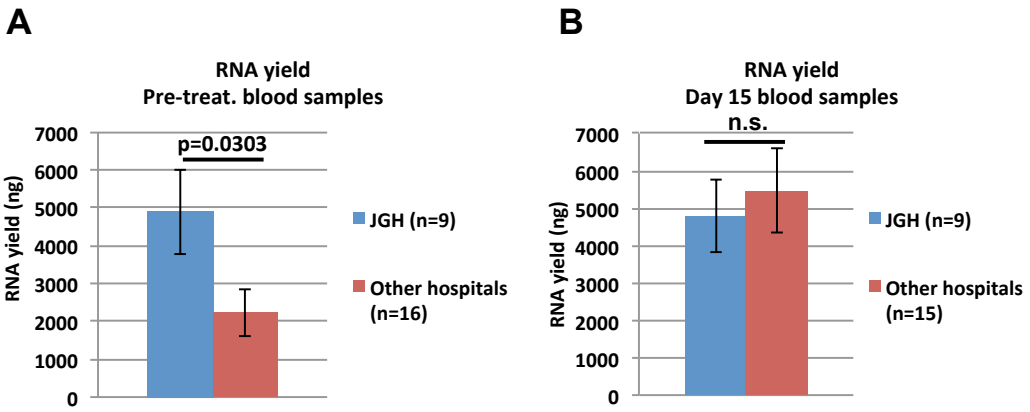


**Figure 3.27: (A)** Comparison of RNA yield (ng) of Pre-treatment blood samples from the Jewish General Hospital (JGH) versus all other hospitals. **(B)** Comparison of RNA yield (ng) of Day 15 blood samples from the Jewish General Hospital (JGH) versus all other hospitals. The number of samples in each group is indicated in parentheses.

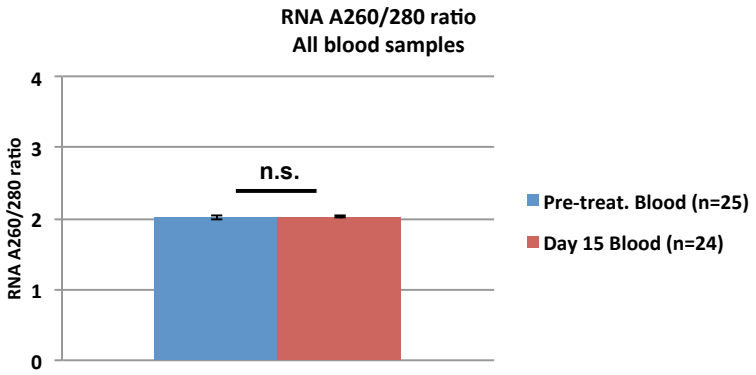


**Figure 3.28:** Comparison of RNA quality of Pre-treatment blood samples versus Day 15 blood samples. The number of samplesin each group is indicated in parentheses.

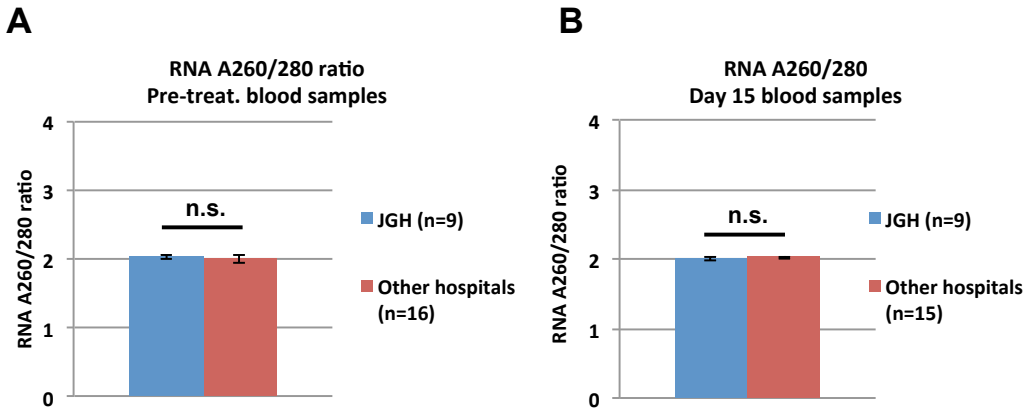


**Figure 3.29: (A)** Comparison of RNA quality of Pre-treatment blood samples from the Jewish General Hospital (JGH) versus all other hospitals. **(B)** Comparison of RNA quality of Day 15 blood samples from the Jewish General Hospital (JGH) versus all other hospitals. The number of samples in each group is indicated in parentheses.

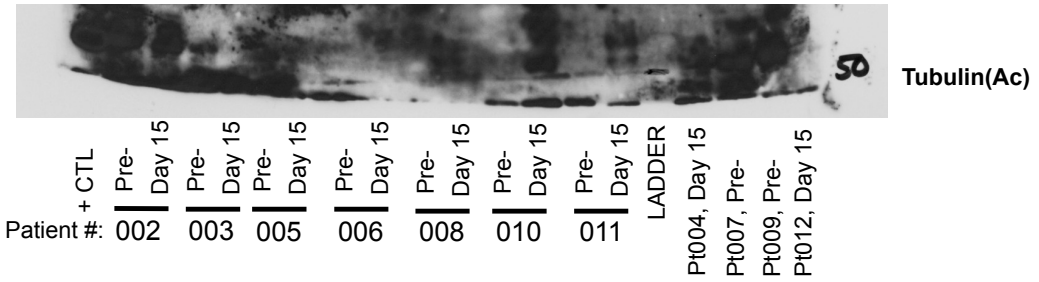


**Figure 3.30:** Immunoblot of acetylated tubulin using whole cell extracts from PBMCs from the QCROC-02 trial. As can be readily ascertained, the quality is poor with some lanes missing completely.

# Chapter 4

# "- and back again"

## Monitoring response and resistance to the novel arsenical darinaparsin in an AML patient

### 4.1 Introduction:

Translational research is often defined by the phrase "from the bench to the bedside", meaning that information learned in the lab is used to guide experimental therapy in the clinic. However, it is important to remember that this is only half of the story. Translational research is a bi-directional process where new insights learned in the clinic can equally be used to guide basic research efforts as the other way around. The previous two chapters of this thesis have described the "traditional" way of looking at translational research: Chapter two outlined our investigations of HDACi treatment plus rituximab in preclinical models of DLBCL while Chapter three described our efforts to translate these findings into a phase II clinical trial. The flow of information in this scenario is, very much, from the bench to the bedside. In the present chapter, we present data from a project that serves as an example of the reverse process: information learned in a clinical setting that has given rise to new hypotheses that will be tested in preclinical models in the lab.

The data presented in this chapter has recently been published in the journal Frontiers in Pharmacology of Anti-Cancer Drugs[181]. The article is reproduced below in its entirety, followed by a discussion of the preclinical

project to which it has led. The article has been formatted to fit the layout of this thesis.

## 4.2 Article:

**4.2.1 Abstract:** Acute myeloid leukemia (AML) with inversion of chromosome 3 is characterized by overexpression of EVI1 and carries a dismal prognosis. Arsenic-containing compounds have been described to be efficacious in malignancies overexpressing EVI1. Here, we describe a case of AML with inv(3)(q21q26.2) treated with the organic arsenical darinaparsin. Using a "personalized medicine approach," two different arsenicals were screened for anti-leukemic effect against the patient's cells *ex vivo*. The most promising compound, darinaparsin, was selected for *in vivo* treatment. Clinical effect was almost immediate, with a normalization of temperature, a stabilization of white blood cell (WBC) counts and an increased quality of life. Longitudinal monitoring of patient response and resistance incorporating significant correlative studies on patient-derived blood samples over the two cycles of darinaparsin given to this patient allowed us to evaluate potential mechanisms of response and resistance. The anti-leukemic effects of darinaparsin correlated with inhibition of the alternative NF-kB pathway and production of the inflammatory cytokine IL-8. Emergence of resistance was suspected during treatment cycle 2 and supported by xenograft studies in nude mice. Darinaparsin resistance correlated with an attenuation of the effect of treatment on the alternative NF-kB pathway. The results from this

patient indicate that darinaparsin may be a good treatment option for inv(3) AML and that inhibition of the alternative NF-kB pathway may be predictive of response. Longitudinal monitoring of disease response as well as several correlative parameters allowed for the generation of novel correlations and predictors of response to experimental therapy in a heavily pretreated patient.

**4.2.2 Introduction:** Acute myeloid leukemia (AML) with inversion or translocation of the long arm of chromosome 3 [inv(3)(q21q26.2)/t(3;3)(q21;q26.2)], hereafter referred to as "inv(3)/t(3;3) AML", accounts for 1-2% of AML cases and predicts an extremely poor prognosis, with a 5-year overall survival of 5.7%[148]. Due to the distinct clinicopathologic attributes associated with these chromosomal aberrations, inv(3)/t(3;3) AML has been included as a separate sub-category of "AML with recurrent genetic abnormalities" in the latest WHO classification[19]. Despite a characteristic clinical picture with a well-defined underlying molecular pathology, no targeted therapy currently exists for inv(3)/t(3;3) AML, although improved treatment regimens clearly are needed, as reflected by the poor overall performance of this patient category.

Molecularly, inv(3)/t(3;3) AML is characterized by the aberrant juxtaposition of the oncogene ecotropic viral integration site 1 (EVI1), with regulatory elements of ribophorin 1 (RPN1), resulting in overexpression of

EVI1[Ref 149]. EVI1 is a transcription factor with a well-recognized role in the normal development of the hematopoietic system. It has been reported to function primarily as a transcriptional repressor, however, examples of an activating role in gene expression have also been described[150,182]. Arsenic trioxide (ATO), an inorganic arsenical, has been investigated as a potential therapy for hematological diseases overexpressing EVI1. Shackelford *et al*. found that super-pharmacologic concentrations of ATO degrade EVI1, as well as several fusion proteins containing EVI1, in cell line models of AML[156]. A clinical trial investigating the effect of ATO in combination with thalidomide in myelodysplastic syndrome (MDS), reported hematologic responses in three out of five patients with overexpression of EVI1, including responses in two out of three patients with inv(3)/t(3;3)[157]. Here, we describe the treatment of a patient with inv(3) AML with the organic arsenical darinaparsin (reviewed in[153]). Although EVI1 expression was not modulated following treatment, we did monitor the response and development of resistance to darinaparsin. By assessing tumor gene expression longitudinally within the patient, we found changes in the alternative NF-κB pathway to be important correlates with response.

**4.2.3 Materials and Methods:** All clinical investigations and treatments were performed with patient consent under a compassionate use protocol approved by the Jewish General Hospital Research Ethics Committee and Health Canada.

**4.2.3.1 Cells:** K562 cells were purchased from ATCC and grown in IMDM medium supplemented with 10% fetal bovine serum and antibiotics.

**4.2.3.2 Standard cytogenetics and FISH:** G-banded karyotypes were obtained from bone marrow mononuclear cells according to standard cytogenetic procedures and described according to the International System for Human Cytogenetic Nomenclature 2009. FISH experiments were performed on interphasic nuclei and metaphases using the EVI1 Breakapart probe LPH036 (Cytocell, Cambridge, UK).

**4.2.3.3 Sample preparation:** Peripheral blood was collected in heparin tubes prior to starting treatment and every time the patient was seen in hospital. The blood was spun down to remove the plasma (stored at -80°C) followed by isolation of peripheral blood mononuclear cells (PBMCs) by Ficoll gradient separation. RNA, DNA and whole cell extracts were isolated as described below. Surplus PBMCs were frozen in 10% DMSO/90% fetal bovine serum at -80°C.

**4.2.3.4 Propidium Iodide (PI) stain of *ex vivo* treated bone marrow cells and PBMCs:** For a detailed description see Hardin *et al.*[183]. Briefly, cells were washed once in FACS wash buffer (5mM $NaN_3$ in PBS supplemented with 5% fetal bovine serum) and then stained with 50 μg/mL

PI (Sigma) in hypotonic buffer (0.1% sodium citrate and 0.1% Triton X-100 in dd$H_20$). Approximately 500,000 cells/condition were stained with 0.5 mL PI stain and analyzed on a BD Biosciences FACSCalibur flow cytometer. Cell death was measured as the percentage of cells with sub-$G_0$ DNA content.

**4.2.3.5 ICP-MS:** Elemental arsenic levels were measured in patient plasma and PBMCs by inductively-coupled plasma mass spectrometry (Chemical Solutions Ltd, Mechanicsburg, PA).

**4.2.3.6 Immunoblotting:** Whole cell extracts were made from patient samples and K562 cells using Tris/NaCl/triton x-100 buffer [50mM Tris-HCl pH 8.0, 150mM NaCl and 1% triton X-100 supplemented with protease inhibitor cocktail (Roche) and PhosStop (Roche)]. Proteins were separated by SDS-PAGE and transferred to nitrocellulose membrane. Primary antibodies for PTEN, EVI1, and GAPDH were all purchased from Cell Signaling. Specific binding was detected with horseradish peroxidase-labeled secondary antibodies and visualized with enhanced chemiluminescence.

**4.2.3.7 qPCR:** RNA was extracted from patient samples using Qiagen AllPrep DNA/RNA mini kit. RNA was converted to cDNA using Superscript II reverse transcriptase (Invitrogen). Specific qPCR amplification was performed using a 7500 Fast Thermocycler (Applied Biosystems) and either Taqman chemistry (*PTEN*, *18S*, and *GAPDH*) or SYBRgreen chemistry and

specific primers. *BIRC3*: 5'-TCC GTC AAG TTC AAG CCA GTT-3' and 5'-GGG CTG TCT GAT GTG GAT AGC-3'; *TNFSF1B*: 5'-GGC CAG ACC AGG AAC TGA AA-3' and 5'-GAT GAA GTC GTG TTG GAG AAC GT-3'; and *NFkB2*: 5'-ACG AGG GAC CAG CCA AGA T-3' and 5'-GCA CGA GGT GGG TCA CTG T-3'.

**4.2.3.8 Circulating cytokine determination:** Cytokine profiling of patient plasma samples was done using a Human Th1/Th2 11plex FlowCytomix Multiplex kit (eBioscience, San Diego, CA) according to the manufacturer's instructions.

**4.2.3.9 Mouse work:** Studies were performed with approval from the University of Rochester Institutional Review Board, IUCOC. NOD/SCID/IL2Rγc mice were sublethally irradiated with 2.7 Gy (270rad) using a RadSource X-ray irradiator (RadSource, Boca Raton, Fl) the day before transplantation. Cells to be assayed were thawed, counted and then injected via tail vein in a final volume of 0.2mL of PBS with 0.5% FBS. After 12 weeks, animals were sacrificed and BM was collected. To determine human cell engraftment the BM cells were labeled with antihuman CD45 (Becton Dickinson) and analyzed via flow cytometry.

**4.2.3.10 Gene expression profiling:** Microarray analyses were performed using Agilent (Mississauga, ON) Human 60K expression arrays at

Genome Quebec. Data were analyzed using FlexArray and Ingenuity Pathway Analysis Software.

Raw text files for the one-color Agilent array were imported in R version 2.14.0 using the package limma (PMID 16646809). We processed the data by first subtracting the background using normexp, took the log2 of the remaining intensity and applied quantile normalization to the entire set of arrays. Differential expression of genes was computed using limma (PMID 16646809). We considered genes as differentially expressed if the mean normalized signal of the two conditions is higher than 5 and the differential expression is greater than two fold change.

**4.2.3.11 Patient treatment protocol:** Darinaparsin (300mg/$m^2$) was administered by intravenous infusion on five consecutive days followed by 16 days off drug. Following the end of the first 21-day cycle, this protocol was repeated for cycle 2.

**4.2.3.12 Statistics:** For *in vitro* experiments, all error-bars represent the standard error of the mean of three replicates. Significance was determined by one-way analysis of variance followed by Newman–Keuls post-tests using Prism version 3.0 (GraphPad software, San Diego, CA, USA). For the mouse work, significance was calculated using an unpaired t-test (two-tailed).

*: p< 0.05; **: p<0.01, ***: p<0.001.

Pearson correlations in table 2 were calculated using the correlation function in Microsoft Excel with the data points shown.

### 4.2.4 Results:

**4.2.4.1. Medical history and pretreatment investigations:** The patient was diagnosed with AML in 2005 at the age of 30. The karyotype performed on bone marrow cells at diagnosis was 46,XX,inv(3)(q21q26.2)x2[21] (figure 4.1A). She initially underwent two induction regimens followed by an allogeneic stem cell transplant, resulting in a complete remission. After 5 years, the patient's AML relapsed and she received a total of seven different chemotherapy-containing regimens in an effort to try to control her disease (see table 4.1 for details). Fluorescent in situ hybridization experiments confirmed the presence of a biallelic inversion of chromosome 3 (figure 4.1B). Given previous reports suggesting that malignant cells with inv(3) might be sensitive to ATO, cells from the patient's bone marrow were collected to determine response to arsenicals *ex vivo*[156,157]. As shown in figure 4.2A, treatment with therapeutically attainable concentrations of darinaparsin induced significant cell death, while ATO treatment only resulted in a negligible increase in cell death[184]. Of note, ATO ($As_2O_3$) contains twice as much arsenic per mole as darinaparsin ($C_{12}H_{22}AsN_3O_6S$), thus, 1μM ATO contains equivalent amounts of arsenic as 2μM darinaparsin. Given these results, we requested approval from Health

Canada to treat the patient with darinaparsin. However, her leukemia progressed rapidly, requiring additional high-dose salvage chemotherapy to control her disease before approval to administer darinaparsin could be obtained. Following the last high-dose regimen, the patient was hospitalized with cytopenia, persistent fever and poor general condition corresponding to an ECOG performance status of 2. *Ex vivo* treatment of the patient's peripheral blood mononuclear cells (PBMCs) immediately prior to starting darinaparsin treatment confirmed that tumor cell sensitivity to darinaparsin was intact (figure 4.2B).

**4.2.4.2. Clinical response to darinaparsin treatment:** Peripheral white blood cell (WBC) counts were measured each time the patient was seen at the hospital. As shown in figure 4.3, darinaparsin immediately reduced the patient's WBC counts and this effect was maintained while the patient remained on drug. The wave-like pattern in WBC counts, with two troughs per treatment cycle, suggests that darinaparsin exerted both immediate anti-cancer effects and more delayed effects. Microscopy of peripheral blood smears, showing nuclear blebbing, suggests cells were dying by apoptosis (figure 4.4A). Induction of apoptosis has previously been described as a mechanism of anti-cancer activity of darinaparsin[154].

Within 10 hours of the first darinaparsin infusion, the patient's fever (figure 4.4B) and night sweats resolved and she regained her appetite and

energy. She was discharged home three days after receiving the last dose of the first cycle. She enjoyed a good quality of life, with an ECOG performance status of 1 for more than 30 days, while undergoing her second cycle of darinaparsin as an outpatient. Treatment was well tolerated with no observed side effects. The patient died from extramedullary manifestations and progression of her AML 36 days after receiving the first dose of darinaparsin.

Given the rapid resolution of the patient's symptoms following darinaparsin administration, we profiled levels of pro-inflammatory cytokines in plasma in response to treatment using a flow cytometry-based multiplex immunoassay kit. While all but three of the 11 cytokines investigated were below the limit of detection of the assay, high levels of interleukin (IL)-8 were detected prior to starting treatment (figure 4.4B). IL-8 has both pro-survival and pro-proliferative properties and has previously been shown to be increased in AML patients[185,186]. The patient's pre-treatment IL-8 levels were about ten times higher than what has been reported for normal controls[185]. Interestingly, the changes observed in IL-8 plasma levels in response to darinaparsin treatment mirror the changes seen in the patient's WBC counts (figure 4.3) and temperature (figure 4.4B), suggesting that darinaparsin impacts temperature, as well as levels of leukemic cells and inflammatory cytokines (these effects may well be related) and that this may underlie the marked subjective and objective

improvement in the patient's symptoms. Pearson correlation coefficients between IL-8 expression, temperature and WBC counts suggest that these three variables are indeed strongly positively related (table 4.2).

To determine whether the delayed effects were due to arsenic accumulation in the patient, we measured elemental arsenic levels in patient plasma and PBMCs. Arsenic levels in plasma increased within the first 24 hours of treatment and continually rose throughout the treatment period (figure 4.5A). After 4-5 days off drug, plasma arsenic levels returned to baseline. Arsenic levels in PBMCs rose slower than plasma levels and remained elevated for several days after discontinuation of darinaparsin (figure 4.5B). Thus, while it does not appear that arsenic accumulates in patient plasma under this dosing regimen, it seems that high arsenic levels in PBMCs are maintained several days after discontinuation of darinaparsin.

**4.2.4.3. Laboratory and correlative investigations:** By continuously sampling during the treatment of this patient, we were able to perform correlative studies to investigate potential markers of response and resistance. A defining molecular pathology of inv(3)/t(3;3) AML is the aberrant overexpression of EVI1. Previous studies suggested that arsenic could decrease EVI1 expression, potentially contributing to the cytotoxic effects[156,157]. To ascertain the effect of darinaparsin on EVI1, we first analyzed EVI1 protein expression levels in PBMCs by immunoblot. No change

in EVI1 protein was observed during the first 72 hours of darinaparsin treatment (figure 4.6A). After 72 hours, there was significant hemolysis of blood samples, preventing reliable quantification at later time-points. We also assessed whether the effect of darinaparsin observed in this patient was due to inhibition of EVI1's gene regulatory activity by analyzing the expression levels of the tumor suppressor PTEN, a target gene repressed by EVI1, by quantitative PCR and western blot[187]. No induction of PTEN mRNA or protein was observed during the first 72 hours of treatment (figure 4.6A and B).

In order to determine the reproducibility of our results obtained in a single patient, we treated the EVI1-expressing myeloid leukemia cell line K562 with ATO and darinaparsin for 24 and 48 hours. Analogous to what was observed in primary leukemic cells (figure 4.2A and B), K562 cells were more sensitive to darinaparsin than to ATO treatment (figure 4.6C) while neither darinaparsin nor ATO treatment modulated expression of EVI1 protein levels in K562 cells (figure 4.6D). Thus, our results do not support modulation of EVI1 expression or repressive activity as part of the anti-leukemic mechanism of darinaparsin in either EVI1-expressing primary cells or cell lines. Note that decreased EVI1 mRNA expression was only described after several months in MDS patients treated with ATO and thalidomide[157].

**4.2.4.4 Potential mechanism of sensitivity/resistance:** Comparison of the *in vivo* WBC response to darinaparsin during cycle 1 with the response

during cycle 2 suggests the emergence of resistance to darinaparsin (figure 4.3). In particular, the increase in WBC counts after darinaparsin infusion was stopped is greater in cycle 2 than in cycle 1. While the patient was still at home, enjoying a good quality of life at this time, these results suggest that resistance to darinaparsin was starting to develop. Further evidence of a resistant phenotype was provided by xenograft studies in nude mice (figure 4.7). In order to measure levels of leukemia initiating cells, we measured the engraftment of patient-derived PBMCs from a pre-treatment blood sample compared to PBMCs isolated during cycle 2. Engraftment is predictive of the number of leukemia initiating cells. Patient PBMCs isolated after 48 hours of darinaparsin treatment during cycle 2 showed greater levels of mouse marrow engraftment than pre-treatment PBMCs, suggesting elevated levels of leukemia initiating cells in the post-treatment sample from cycle 2.

To explore potential mechanisms of resistance to darinaparsin, we performed cDNA microarray analyses on PBMCs prior to and 48 hours after the start of each cycle of darinaparsin. The alternative NF-κB pathway was identified as one of the most modulated pathways during the course of darinaparsin treatment using Ingenuity Systems Pathway Analysis (figure 4.8, left panel). Expression patterns of three genes in the alternative NF-κB pathway were validated by quantitative PCR using gene-specific primers as shown in figure 4.9. There is good agreement between results obtained by microarray and quantitative PCR. Darinaparsin decreased expression of

several members of the alternative NF-κB pathway after 48 hours of treatment. This correlates with the observed decrease in production of IL-8 (figure 4.4B), a well-characterized NF-κB target gene. Furthermore, gene expression in PBMCs prior to the second cycle of darinaparsin revealed an upregulated alternative NF-κB pathway that was not inhibited by darinaparsin during the second cycle, perhaps foreshadowing the emergence of resistance (figure 4.8, center and right panels). The attenuation of the response of the alternative NF-κB pathway to darinaparsin treatment coincides with emergence of resistance, thereby strengthening the hypothesis that this pathway plays a role in the sensitivity/resistance of inv(3) AML cells to darinaparsin.

### 4.2.5 Discussion:

Herein, we describe for the first time the treatment of a patient with inv(3) AML with the organic arsenical darinaparsin. Darinaparsin stabilized disease in a heavily pretreated patient and greatly improved quality of life. Therapy was well tolerated with almost immediate clinical benefit and no observed side effects. Clinical benefit was suggested by a simple *ex vivo* cell-death assay performed prior to starting therapy, indicating that this may be useful as a predictive marker of *in vivo* response. Unexpectedly, we did not find evidence that treatment directly affected EVI1 levels or activity. Instead, our results indicate that inhibition of the alternative NF-κB pathway by darinaparsin correlated with response and plasma levels of the inflammatory

cytokine IL-8.

The strategy outlined here serves as an example of the power of a personalized medicine approach in patients for whom no accepted standard therapy is available. In particular, for patients suffering from uncommon types of malignancies, it is imperative to gather as much information on treatment effect, response and resistance at every given opportunity. This series of experiments highlights how multiple platforms can be used to assess mechanisms of response and resistance. Here, we included everything from genomics to *in vivo* stem cell analysis.

In this specific case, the literature suggested that arsenicals might be efficacious in malignancies with inv(3), thus we tested two arsenicals using a simple *ex vivo* death assay. Interestingly, the drug that performed the best in our *ex vivo* assay was not ATO (the drug for which activity in inv(3) malignancies had previously been reported), but rather the organic arsenical darinaparsin[153,156,157]. Darinaparsin has previously been tested in hematological malignancies, including acute leukemias (Clinical trial ID: NCT00592046). Encouragingly, the patient experienced marked subjective and objective improvement after starting darinaparsin, however, after about a month, her condition rapidly deteriorated. Our results highlight a key advantage of longitudinal sampling of the same patient over his or her entire disease trajectory. The availability of blood samples from both the time

during which the malignant cells exhibited sensitivity to treatment (cycle 1) and the time at which resistance was starting to become apparent (cycle 2) allowed us to compare treatment responses at these time points. Using an unbiased gene expression based approach, we identified the alternative NF-κB pathway as being constitutively activated in the patient's AML blasts prior to treatment and showed that this activation was attenuated after 48 hours of darinaparsin. However, prior to the start of cycle 2, the NF-κB pathway was upregulated further and was no longer responsive to darinaparsin treatment (figure 4.8). The abrogation of a putative mechanism of response at the time of emergence of resistance strengthens the hypothesis that this pathway plays an important role in resistance/sensitivity to darinaparsin in this patient. Levels of circulating IL-8 in plasma may function as a surrogate marker of NF-κB pathway activation and could conceivably be used to monitor treatment response in IL-8 secreting AML.

Based on the results outlined above, further investigation is warranted into 1) EVI1 overexpressing AMLs and 2) AMLs with activation of the alternative NF-κB pathway as potential targets for darinaparsin treatment.

**4.2.6 Conflict of Interest:** RAM is Senior Vice President, Regulatory Affairs & Quality/Pharmaceutical Development of ZIOPHARM Oncology, Inc.

and a stockholder of ZIOPHARM. ZIOPHARM is the licensee of darinaparsin and is developing darinaparsin for various indications in oncology.

**4.2.7 Acknowledgements:** The authors wish to thank Dr. Hugues de Thé for helpful suggestions. We also would like to acknowledge Christian Young for expert assistance with flow cytometric analyses and Genome Québec for assistance with gene expression microarray analysis. Finally, we wish to thank our patient for participating in clinical research.

Funding: This work was supported by a grant from the Canadian Institutes of Health Research and the Canadian Foundation for Innovation. THN holds a Cole Foundation fellowship. KPC holds a fellowship from the American Cancer Society. KKM is a chercheur-boursier of the Fonds de la Recherche en Santé-Québec (FRSQ).

**4.3 Conclusions:** The work outlined above demonstrates how an experimental treatment, guided by *ex vivo* assays of effect, can lead to a clinically useful, albeit short-lived, response in a heavily pre-treated patient. Correlative studies associated with this work have suggested several hypotheses, which are currently under investigation in the lab of Dr. Koren Mann. The main question we are interested in, based on the case reported above, is whether or not overexpression of EVI1, with or without inversion of chromosome 3, can serve as a marker of sensitivity to arsenicals, especially, darinaparsin. Patients with inv(3)(q21q26.2)/t(3;3)(q21;q26.2) make up

only 1-2% of the total AML patient population[148], however, overexpression of EVI1 mRNA is seen in up to 8-10% of AML and predicts a poor outcome[188-190]. Initial efforts in the lab have been focused on the development of an assay for EVI1 protein expression by flow cytometry for use in primary patient cells (figure 4.10). This assay is now functional and we are currently assessing EVI1 status and *ex vivo* sensitivity to the arsenicals ATO and darinaparsin in primary samples from AML patients (figure 4.11). These two assays should help determine if EVI1 expression correlates with sensitivity to arsenicals. One intriguing finding raised by the results shown in figure 4.10 is that only a sub-set of leucocytes expresses EVI1. It is possible that the EVI1-negative population represents normal circulating leucocytes or an EVI1-negative malignant population. Future analyses will investigate whether *ex vivo* treatment with arsenicals selectively depletes the EVI1-positive cells.

In the Frontiers manuscript, we found that darinaparsin neither modulated expression of EVI1 or expression of the EVI1 target gene PTEN[187]. While these findings do not directly implicate EVI1 expression or function in the mechanism of action of darinaparsin in this patient, we cannot exclude an effect on other EVI1 targets or EVI1 interacting proteins. Our work, as well as that of others[156], suggests there is something about EVI1-positive malignancies that may confer sensitivity to treatment with arsenicals. Therefore, we will investigate the role of EVI1 expression in sensitivity to ATO and darinaparsin more closely. EVI1 will be knocked down in the EVI1 expressing CML cell line K562 while EVI1 will be overexpressed in an EVI1-

negative cell line. Sensitivity to ATO and darinaparsin in this experimental system will help elucidate the role of EVI1 in arsenical sensitivity.

Finally, we will investigate whether modulation of the alternative NF-κB pathway correlates with response to arsenicals in AML patient samples and whether this effect is restricted to EVI1 positive patients or is a more general feature. If we find that the alternative NF-κB pathway plays a role in arsenic sensitivity, we will investigate if IL-8 expression is a useful marker of activity of this pathway, which could potentially serve as a predictor of response.

A brief note on the ethical and economic aspects of this type of research is in order here. Ethically, we feel that when it comes to patients with rare and serious diseases, such as AML inv(3), it is imperative to try to learn as much as possible from each case. Viewed in this light, we feel it is acceptable to perform the careful, in-depth studies described above. From an economic point of view, the incorporation of correlative science into clinical studies increases the cost significantly. For each project, a sound balance between which assays can be done versus what information each additional assay will yield should be sought at the very beginning. Obviously, the point of research is to test hypotheses. If the answer were given before starting the experiment, there would be no need to perform said experiment. It bears mentioning that the results of such work can be very difficult to predict. For example, in the work described in this chapter, we saw an initial effect of darinaparsin, however, the duration of response was shorter than expected.

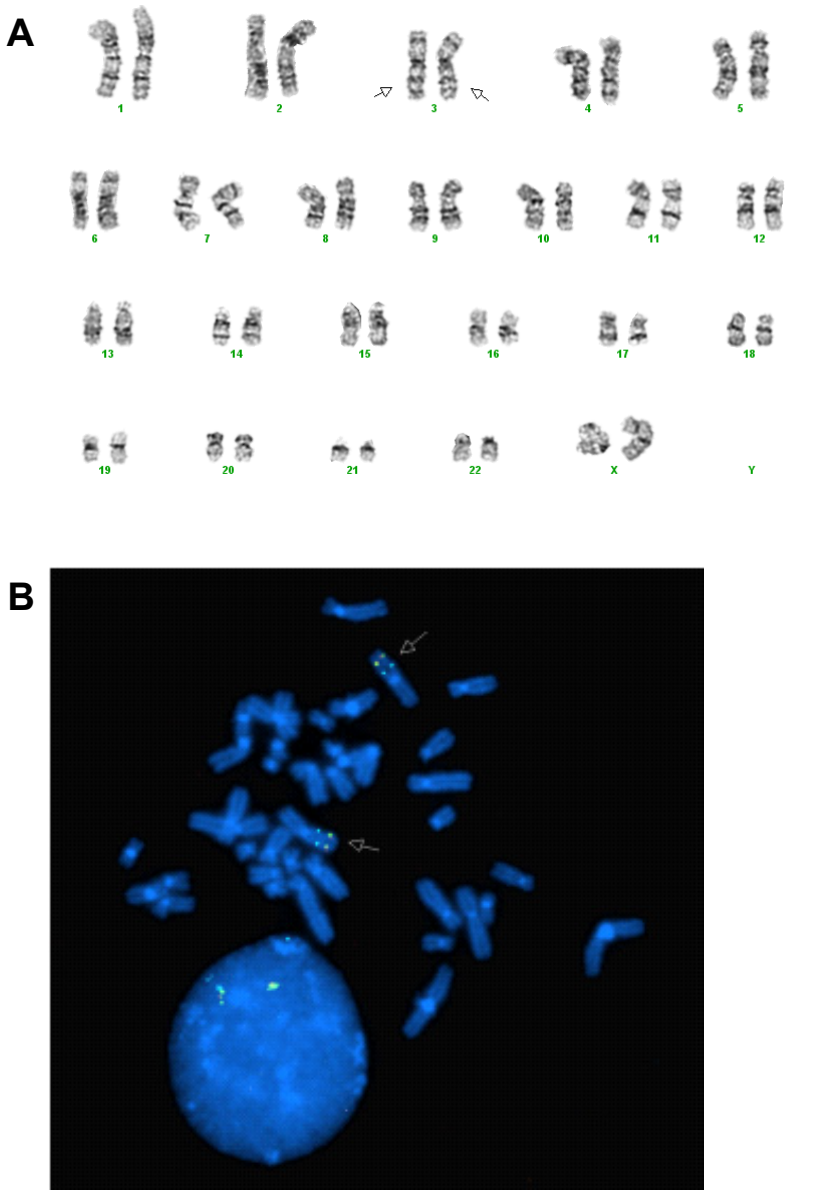


**Figure 4.1:** Metaphase karyotype from initial diagnosis **(A)** and fluorescence *in situ* hybridization performed at relapse **(B)** showing biallelic inversion of chromosome 3 (arrows). Also shown are two intact copies of chromosome 7 in this patient **(A)**.

| **Table 1: List of treatments** | |
|---|---|
| Date | Treatment |
| April to May 2005 | Two induction regimens: |
| | 1) Cytarabine + daunorubicin (7+3) |
| | 2) Cytarabine + idarubicin (4+3) |
| September 2005 | Pre-transplant mobilization: |
| | Cyclophosphamide + total body irradiation |
| September 2005 | Allogeneic stem cell transplant |
| August to September 2010 | Three high-dose regimens: |
| | 1) FLAG-Ida (fludarabine, cytarabine, G-CSF and idarubicin |
| | 2) High-dose cytarabine |
| | 3) Etoposide |
| November 2010 | Investigational treatment: |
| | Low-dose cytarabine + ribavirin |
| December 2010 | Three salvage chemotherapy regimens: |
| | 1) Mitoxantrone |
| | 2) Hydroxyurea |
| | 3) Etoposide + cyclophosphamide |
| January to February 2011 | Investigational treatment: |
| | Darinaparsin |

**Table 4.1:** List of regimens used to treat the patient.

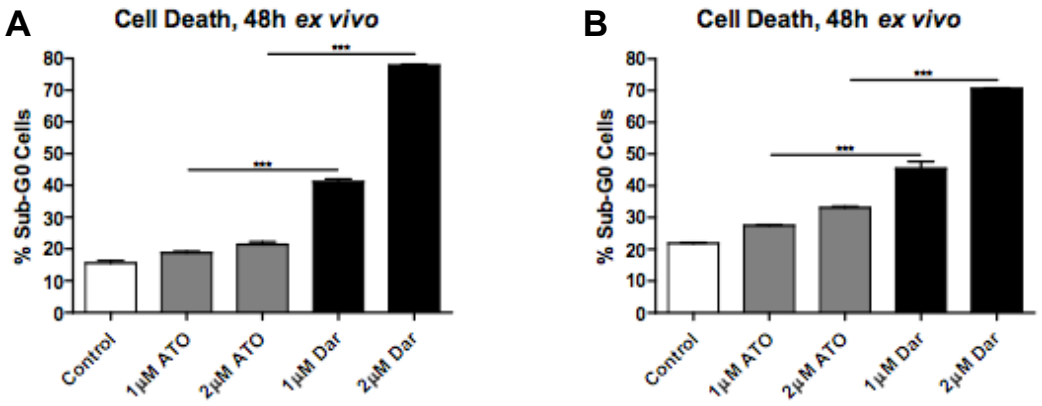


**Figure 4.2:** Mononuclear cells isolated by Ficoll gradient separation from bone marrow aspirate **(A)** and peripheral blood **(B)** were treated *ex vivo* for 48 hours with the indicated doses of arsenic trioxide (ATO) and darinaparsin (Dar) to assess sensitivity to arsenicals. Cell death was measured as the percentage of cells with sub-$G_0$ DNA content. Error bars indicate SEM.

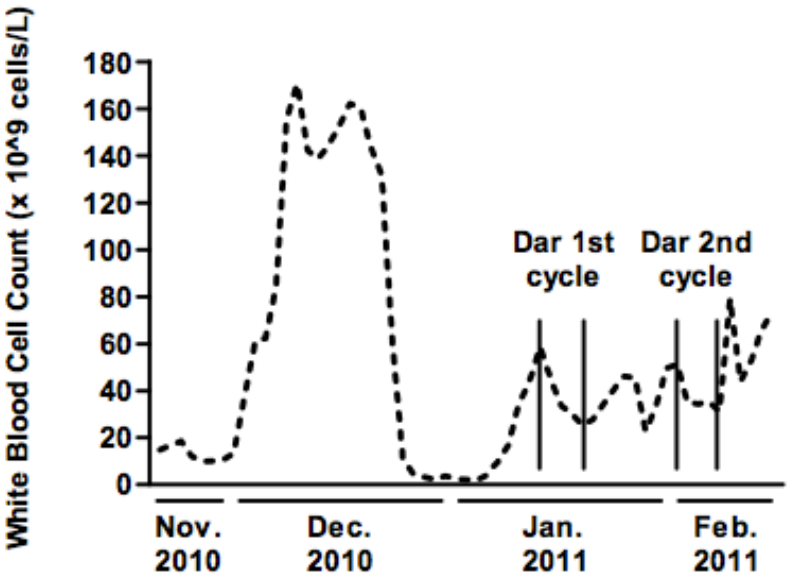


**Figure 4.3:** White blood cell counts were measured every time the patient was seen at our institution. The beginning and end of cycles of darinaparsin treatment are demarcated with vertical lines. Note that the x-axis is not to scale.

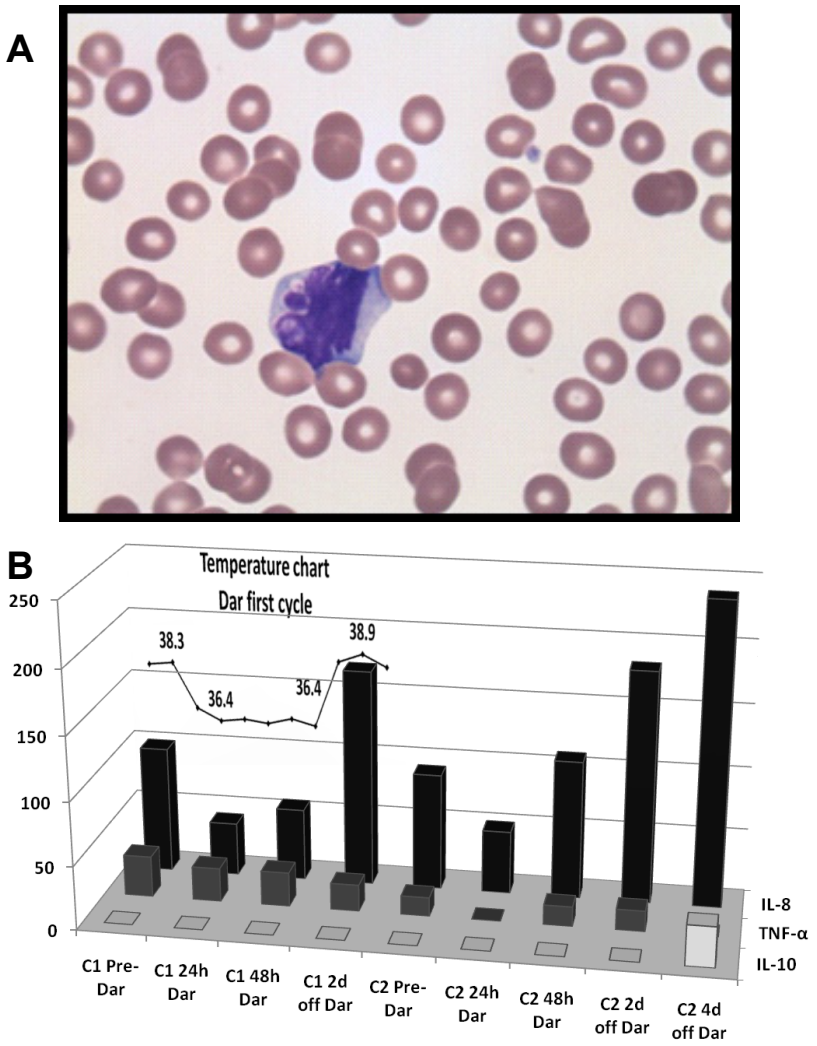


**Figure 4.4: (A)** Micrograph of peripheral blood smear stained with Wright's Giemsa stain while the patient was on darinaparsin treatment. Nuclear blebbing suggests cells are dying by apoptosis. **(B)** While the patient was in hospital, her temperature was monitored daily (measured in degrees Celsius). The temperature curve has been overlaid graphs showing expression of circulating cytokines in plasma, measured by a multiplex immunoassay kit. Only 3 out of the 11 cytokines measured by the kit were detected at levels above the assay's limit of detection. IL-8 = interleukin 8, IL-10 = interleukin 10, TNF-$\alpha$ = tumor necrosis factor-alpha. Samples taken prior to starting treatment with darinaparsin are labeled "Pre" while time points during and after darinaparsin treatment are labeled with cycle number (C1 = cycle 1, h = hours and d = days) and time on or off darinaparsin treatment. The patient was allowed to go home 3 days after completing her first course of darinaparsin.

**Table 2: Pearson correlations**

| Date | IL-8 Conc. (pg/mL) | Temp. (Celcius) | WBC counts + 1 day |
|---|---|---|---|
| 11 Jan 2011 | 99.36 | 38.3 | 45.1 |
| 12 Jan 2011 | 41.69 | 36.8 | 33.5 |
| 13 Jan 2011 | 56.53 | 36.4 | 30.3 |
| 18 Jan 2011 | 170.4 | 38.6 | 46.1 |

| | |
|---|---|
| **Pearson IL-8 vs Temp. Correlation Co-eff:** | **0.883715871** |
| **Pearson IL-8 vs WBC+1day Correlation Co-eff:** | **0.854039474** |
| **Pearson Temp. vs WBC+1day Correlation Co-eff:** | **0.998008274** |

**Table 4.2:** Calculation of Pearson correlation coefficients for the relation of temperature, white blood cell counts and interleukin 8 (IL-8) plasma concentration.

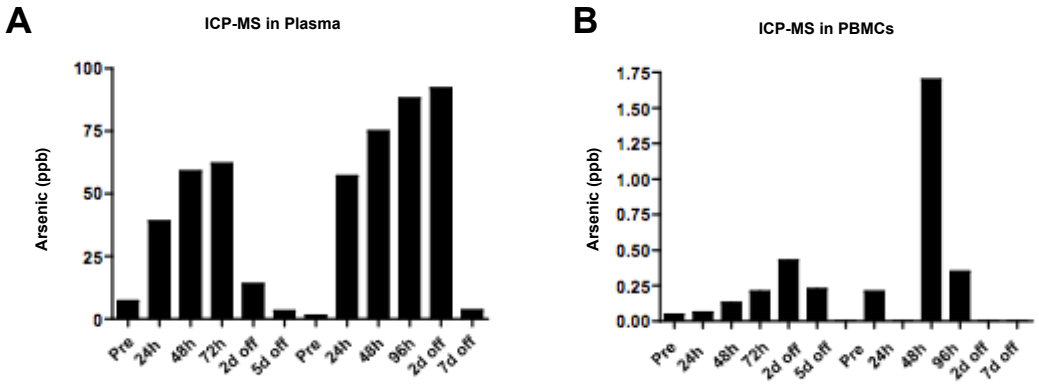


**Figure 4.5:** Elemental arsenic levels were measured in patient plasma **(A)** and peripheral blood mononuclear cells (PBMCs) **(B)** by inductively coupled plasma mass spectrometry. The highest plasma level of arsenic measured with this dosing schedule was approximately 90 parts per billion (ppb). Given arsenic's molar mass of 75 g/mol, this is equal to a plasma concentration of 1.2 μM, which corresponds well with the doses used for *ex vivo* experiments in figure 1C and 1F. Samples taken prior to starting treatment with darinaparsin are labeled "Pre" while time points during and after darinaparsin treatment are labeled with cycle number (C1 = cycle 1, h = hours and d = days) and time on or off darinaparsin treatment.

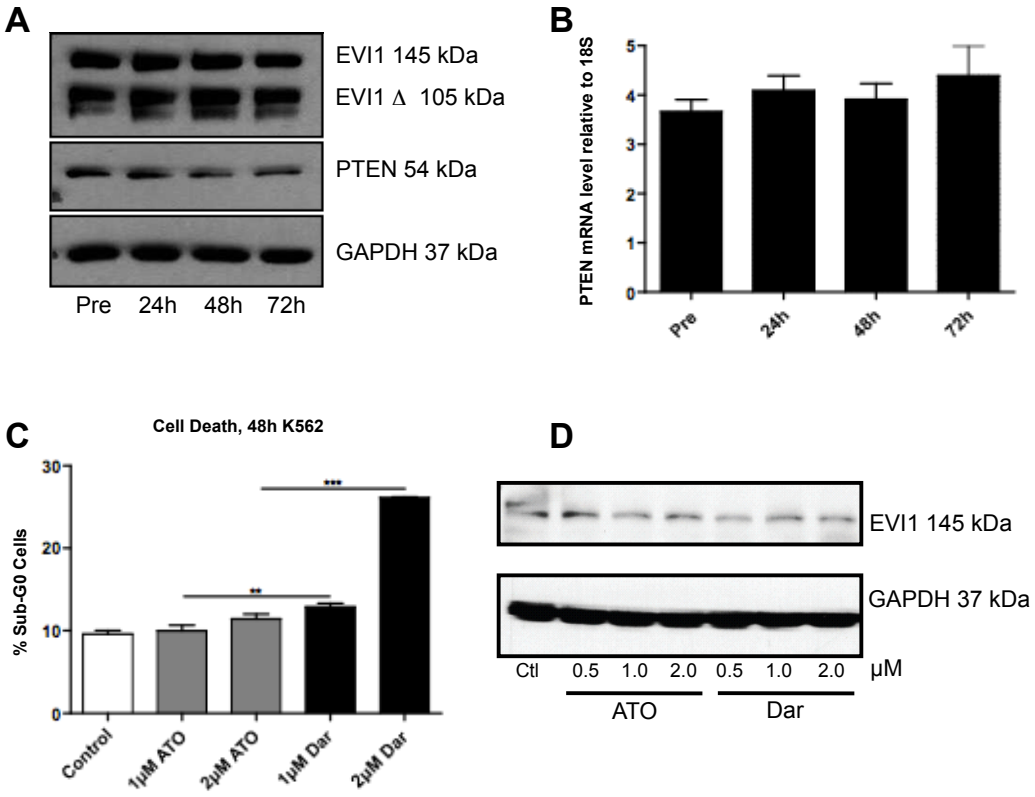


**Figure 4.6: (A)** Western blot of full-length ecotropic viral integration site 1 (EVI1), a truncated form of EVI1 (EVI1 Δ) and PTEN expression in peripheral blood mononuclear cells at the time points indicated. No fusion of EVI1 and MDS1 was detected in these cells. GAPDH is included as a loading control. **(B)** Levels of PTEN mRNA measured by qPCR. Expression levels are shown as PTEN ΔΔct/GAPDH ΔΔct. Error bars indicate SEM. No statistically significant differences in mRNA levels were found. **(C)** K562 chronic myeloid leukemia cells were treated for 48 hours with the indicated doses of arsenic trioxide (ATO) and darinaparsin (Dar) to assess sensitivity to arsenicals. Cell death was measured as the percentage of cells with sub-$G_0$ DNA content. Error bars indicate SEM. **(D)** Western blot of EVI1 in K562 cells treated for 24 hours with the indicated doses of arsenic trioxide (ATO) and darinaparsin (Dar). GAPDH is included as a loading control.

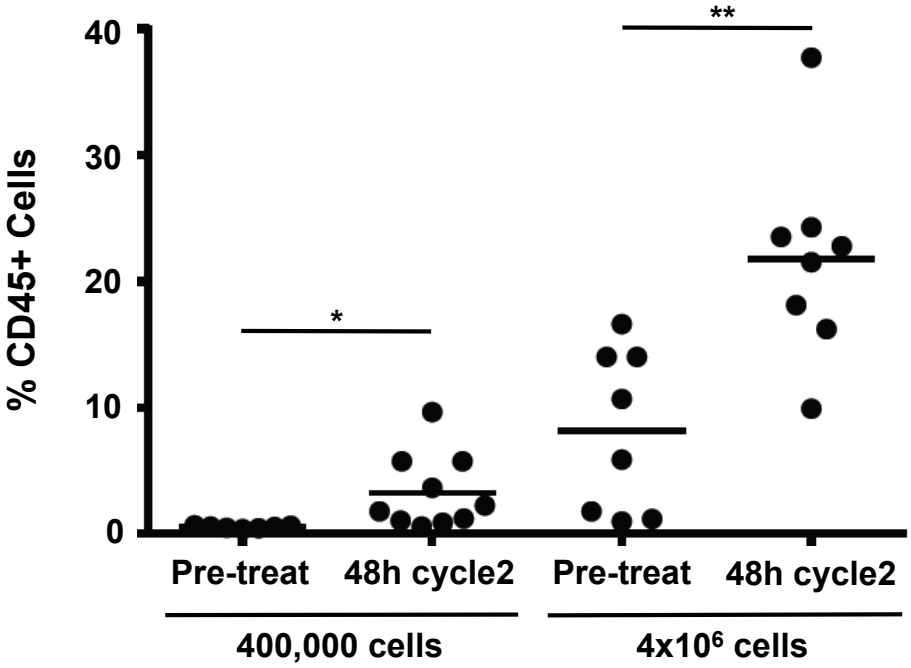


**Figure 4.7:** Percentage of engraftment in NOD/SCID/IL2Rγc mice for the indicated cells. Each symbol represents a single animal analyzed 12 weeks after transplantation, mean engraftment is indicated by horizontal bars. The percentage of human CD45 in the BM was determined via flow cytometry.

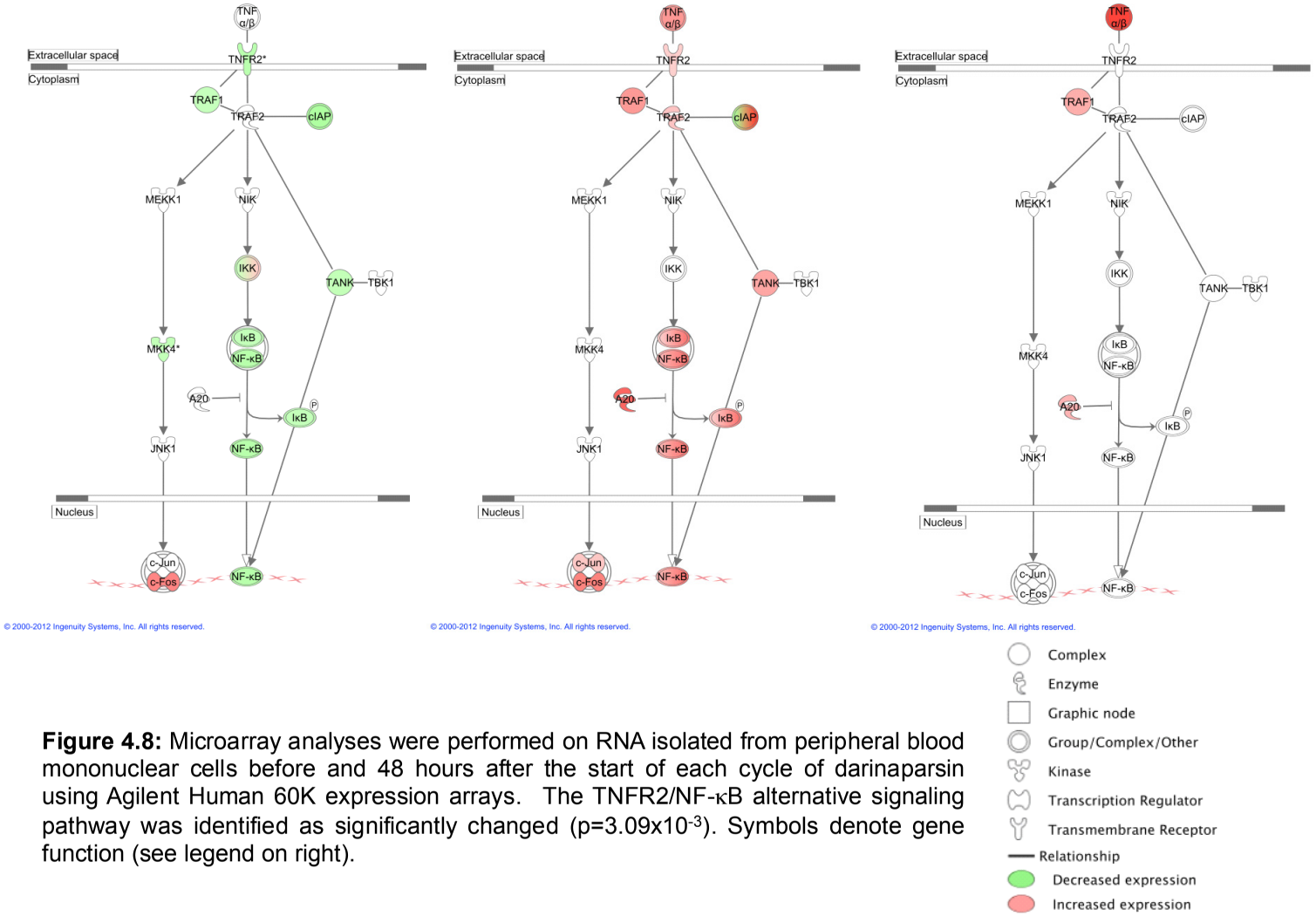


**Figure 4.8:** Microarray analyses were performed on RNA isolated from peripheral blood mononuclear cells before and 48 hours after the start of each cycle of darinaparsin using Agilent Human 60K expression arrays. The TNFR2/NF-κB alternative signaling pathway was identified as significantly changed ($p=3.09x10^{-3}$). Symbols denote gene function (see legend on right).

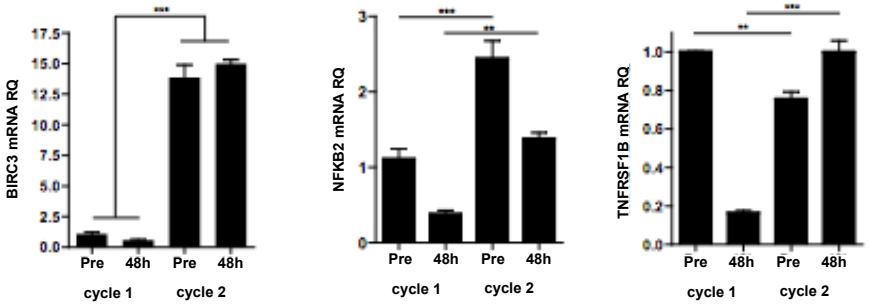


**Figure 4.9:** Validation of expression of selected genes from the alternative NF-κB pathway (BIRC3, NFKB2 and TNFRSF1B) reveals good agreement with results from microarray analysis. Expression levels are shown as NF-κB pathway ΔΔct/GAPDH ΔΔct. Error bars indicate SEM. BIRC3 = baculoviral IAP repeat containing 3, NFKB2 = nuclear factor of kappa light polypeptide gene enhancer in B-cells 2, TNFRSF1B = tumor necrosis factor receptor superfamily, member 1B.

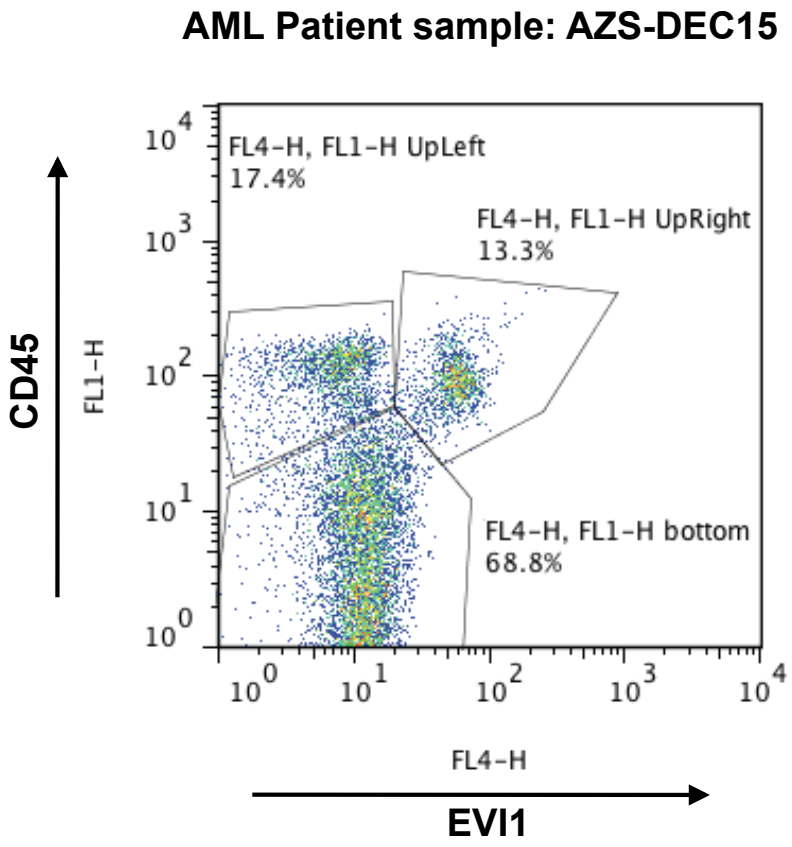


**Figure 4.10:** Assessment of EVI1 status in a primary AML sample. The upper right population contains the EVI1-positive blood cells.

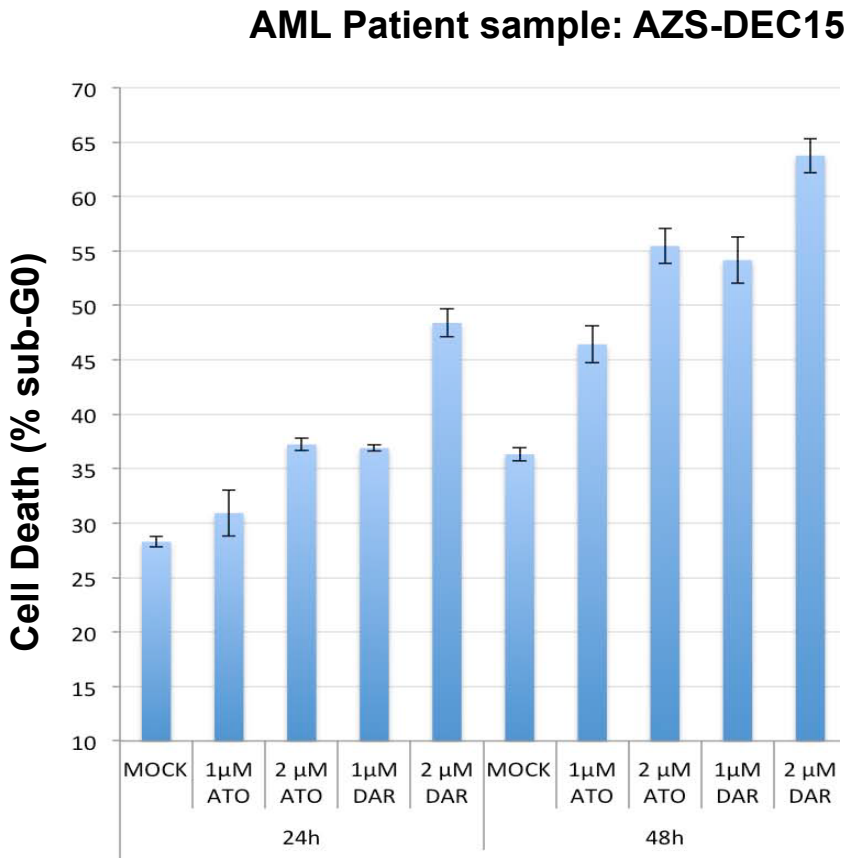


**Figure 4.11:** *Ex vivo* investigation of sensitivity to arsenicals. Cell death is assessed by propidium iodide stain.

# Chapter 5

## Concluding remarks

A few overarching thoughts and conclusions transcend the work presented in each of the preceding chapters. These will be discussed here.

**5.1 Translational research as a spectrum:** One of the main points, which I hope that the collected work presented in this thesis makes, is that translational research can be viewed as a spectrum rather than two opposite poles of research (the bench and the clinic, respectively) (figure 5.1). Almost none of the projects described in this thesis can be satisfactorily investigated from a purely "bench science" point of view, just as almost none can be completely illuminated using only the tools available in the clinic. As such, each project incorporates different elements from bench and clinical science to varying degrees, thus giving rise to the idea of a spectrum. Working in the area near each pole offers different advantages and disadvantages: For example, bench science offers a high degree of freedom of experimental design, excellent control over the experimental settings, as well as the opportunity for (almost) unlimited repetition. The "cost" associated with bench science is that it is performed in a model of the system in which it is finally hoped to work. As such, one cannot be certain that results will be reliably translated to human beings. At the other end of the spectrum, clinical science offers a chance to test hypotheses under the exact conditions that a

treatment will be given. However, this comes at the disadvantage of high background variability, limited freedom of experimental conditions (patient safety comes before scientific curiosity) and high economic cost.

As I hope to have demonstrated in chapters two, three and four, information gained at one point of the spectrum can lead to hypotheses which "translate" the project along in either direction of the spectrum. For example, preclinical work described in chapter two led to the design of a clinical trial, described in chapter three. However, we knew that we would have to incorporate tumor biopsies in the trial design in order to properly investigate the ideas we gleaned from the preclinical work. When the clinical trial is done, we will likely want to go back and test hypotheses based on these results in preclinical models again. However, we may also have found a predictor of response, which we will want to test in a new clinical trial. As such, the flow of knowledge does not just move from one pole to the other and back again but rather ebbs and flows back and forth. The idea of translational research as a spectrum is not novel[191] and it may seem like a trivial point but I think it has at least one practical consequence: In order to be able to translate a project from one stage of the spectrum to another, collaboration with a number of colleagues is often necessary (more on this below). If there were only two poles involved, one might expect that translation from the bench to the clinic would be a simple matter of a basic scientist contacting his/her colleague in the clinic and translation would happen. In my (admittedly limited) experience, this situation very rarely

happens. Instead, it seems that translational research is best facilitated when a basic researcher with some experience with clinical science talks to a clinician with some basic science training. My interpretation of this is that bridging the gap between the bench and the clinic is a serious challenge, whether it be due to language and/or cultural differences, and that successful translation requires people who are familiar with both sides/speak both languages. As such, representing translational research as two poles may be an oversimplification that neglects some of the steps associated with successful translation.

**5.2 It takes a village to do translational research:** As hinted at above and as evidenced by the extensive list of contributors in the preface of this thesis, translational research is rarely a solitary endeavor. The projects described in this thesis have required the collaboration of a great number of experts from various fields. As with any effort that draws upon the expertise of many different people in different places, coordinating everything in an efficient manner has, at times, been a challenge. However, I have been greatly impressed with the interest and willingness to participate with which our cries for help have been met.

**5.3 Collaboration breeds collaboration:** One interesting corollary of the many collaborations that have been necessary in order to put together the projects described here has been the generation of a number of new projects, all stemming from the clinical trial and the biomaterials that are accumulated through it. The measurement of metabolomics data

spearheaded by Leandro Cerchietti is one such effort. This project encompasses many aims but one, which is directly derived from the QCROC-02 trial, is an effort to investigate changes in metabolites in response to HDACi treatment. Lists of HDACi dependent metabolites will then be correlated with response to treatment in order to pinpoint enzymatic activities, which are modulated by HDACi treatment in patients who respond well to treatment. Another offshoot from the QCROC-02 trial is a project to investigate the genomic changes that occur as DLBCL patients relapse on R-CHOP treatment. The genomes of *de novo* DLBCL have been described in the literature, however, the QCROC-02 trial will provide us with a number of relapsed DLBCL tumor genomes. It will be interesting to compare these with either previously published *de novo* genomes or, better yet, with material from their own diagnostic biopsy from before they became resistant.

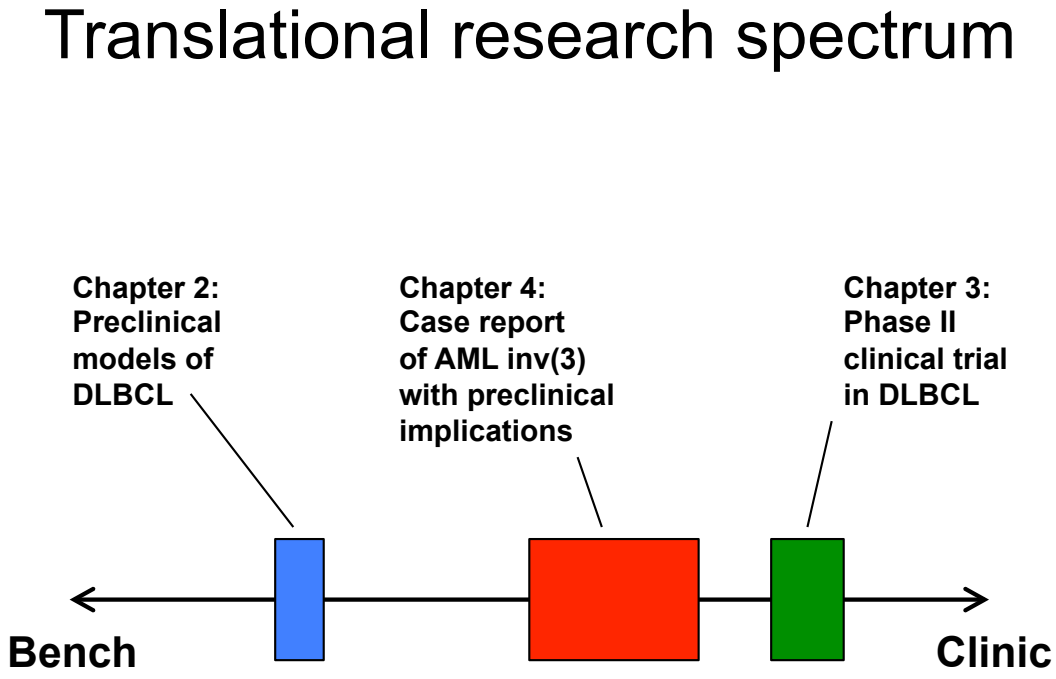


**Figure 5.1:** Translational research as a spectrum. The research described in each of the preceding chapters is not limited to either of the two poles of research but rather covers varying degrees of the "bench-to-clinic" spectrum.

# Bibliography


**1.** Jemal A, Siegel R, Xu J, Ward E. Cancer statistics, 2010. *CA: a cancer journal for clinicians.* Sep-Oct 2010;60(5):277-300.

**2.** Canadian Cancer Statistics 2012. Toronto, ON: Canadian Cancer Society; 2012.

**3.** Meric-Bernstam F, Mills GB. Overcoming implementation challenges of personalized cancer therapy. *Nature reviews. Clinical oncology.* Sep 2012;9(9):542-548.

**4.** National Institutes of Health Institutional Clinical and Translational Science Award (U54). 2007; http://grants.nih.gov/grants/guide/rfa-files/RFA-RM-07-007.html. Accessed October 10, 2012.

**5.** Hanahan D, Weinberg RA. The hallmarks of cancer. *Cell.* Jan 7 2000;100(1):57-70.

**6.** Hanahan D, Weinberg RA. Hallmarks of cancer: the next generation. *Cell.* Mar 4 2011;144(5):646-674.

**7.** Parsons DW, Jones S, Zhang X, et al. An integrated genomic analysis of human glioblastoma multiforme. *Science (New York, N.Y.).* Sep 26 2008;321(5897):1807-1812.

**8.** Jones S, Zhang X, Parsons DW, et al. Core signaling pathways in human pancreatic cancers revealed by global genomic analyses. *Science (New York, N.Y.).* Sep 26 2008;321(5897):1801-1806.

**9.** Sjoblom T, Jones S, Wood LD, et al. The consensus coding sequences of human breast and colorectal cancers. *Science (New York, N.Y.).* Oct 13 2006;314(5797):268-274.

**10.** Mardis ER, Ding L, Dooling DJ, et al. Recurring mutations found by sequencing an acute myeloid leukemia genome. *The New England journal of medicine.* Sep 10 2009;361(11):1058-1066.

**11.** Integrated genomic analyses of ovarian carcinoma. *Nature.* Jun 30 2011;474(7353):609-615.

**12.** Campbell PJ, Pleasance ED, Stephens PJ, et al. Subclonal phylogenetic structures in cancer revealed by ultra-deep sequencing. *Proceedings of the National Academy of Sciences of the United States of America.* Sep 2 2008;105(35):13081-13086.

**13.** Mullighan CG, Phillips LA, Su X, et al. Genomic analysis of the clonal origins of relapsed acute lymphoblastic leukemia. *Science (New York, N.Y.).* Nov 28 2008;322(5906):1377-1380.

**14.** Shah NP, Nicoll JM, Nagar B, et al. Multiple BCR-ABL kinase domain mutations confer polyclonal resistance to the tyrosine kinase inhibitor imatinib (STI571) in chronic phase and blast crisis chronic myeloid leukemia. *Cancer cell.* Aug 2002;2(2):117-125.

**15.** Navin N, Kendall J, Troge J, et al. Tumour evolution inferred by single-cell sequencing. *Nature.* Apr 7 2011;472(7341):90-94.
**16.** Gerlinger M, Rowan AJ, Horswell S, et al. Intratumor heterogeneity and branched evolution revealed by multiregion sequencing. *The New England journal of medicine.* Mar 8 2012;366(10):883-892.
**17.** Swanton C. Intratumor heterogeneity: evolution through space and time. *Cancer research.* Oct 1 2012;72(19):4875-4882.
**18.** Biomarkers and surrogate endpoints: preferred definitions and conceptual framework. *Clinical pharmacology and therapeutics.* Mar 2001;69(3):89-95.
**19.** Swerdlow SH, Campo, E., Harris, N.L., Jaffe, E.S., Pileri, S.A., Stein, H., Thiele, J., Vardiman, J.W. *WHO Classification of Tumours of Haematopoietic and Lymphoid Tissues, Fourth Edition.* Vol 2: World Health Organization; 2008.
**20.** Alizadeh AA, Eisen MB, Davis RE, et al. Distinct types of diffuse large B-cell lymphoma identified by gene expression profiling. *Nature.* Feb 3 2000;403(6769):503-511.
**21.** Klein U, Tu Y, Stolovitzky GA, et al. Transcriptional analysis of the B cell germinal center reaction. *Proceedings of the National Academy of Sciences of the United States of America.* Mar 4 2003;100(5):2639-2644.
**22.** Allen CD, Okada T, Cyster JG. Germinal-center organization and cellular dynamics. *Immunity.* Aug 2007;27(2):190-202.
**23.** Jacob J, Kelsoe G, Rajewsky K, Weiss U. Intraclonal generation of antibody mutants in germinal centres. *Nature.* Dec 5 1991;354(6352):389-392.
**24.** Berek C, Berger A, Apel M. Maturation of the immune response in germinal centers. *Cell.* Dec 20 1991;67(6):1121-1129.
**25.** Klein U, Dalla-Favera R. Germinal centres: role in B-cell physiology and malignancy. *Nature reviews. Immunology.* Jan 2008;8(1):22-33.
**26.** Liu YJ, Arpin C, de Bouteiller O, et al. Sequential triggering of apoptosis, somatic mutation and isotype switch during germinal center development. *Seminars in immunology.* Jun 1996;8(3):169-177.
**27.** Muramatsu M, Kinoshita K, Fagarasan S, Yamada S, Shinkai Y, Honjo T. Class switch recombination and hypermutation require activation-induced cytidine deaminase (AID), a potential RNA editing enzyme. *Cell.* Sep 1 2000;102(5):553-563.
**28.** Pasqualucci L, Neumeister P, Goossens T, et al. Hypermutation of multiple proto-oncogenes in B-cell diffuse large-cell lymphomas. *Nature.* Jul 19 2001;412(6844):341-346.
**29.** Lenz G, Nagel I, Siebert R, et al. Aberrant immunoglobulin class switch recombination and switch translocations in activated B cell-like diffuse large B cell lymphoma. *The Journal of experimental medicine.* Mar 19 2007;204(3):633-643.
**30.** Tunyaplin C, Shaffer AL, Angelin-Duclos CD, Yu X, Staudt LM, Calame KL. Direct repression of prdm1 by Bcl-6 inhibits plasmacytic

differentiation. *Journal of immunology (Baltimore, Md. : 1950).* Jul 15 2004;173(2):1158-1165.

**31.** Lenz G, Staudt LM. Aggressive lymphomas. *The New England journal of medicine.* Apr 15 2010;362(15):1417-1429.

**32.** Schneider C, Pasqualucci L, Dalla-Favera R. Molecular pathogenesis of diffuse large B-cell lymphoma. *Seminars in diagnostic pathology.* May 2011;28(2):167-177.

**33.** Mey U, Hitz F, Lohri A, et al. Diagnosis and treatment of diffuse large B-cell lymphoma. *Swiss medical weekly.* 2012;142:0.

**34.** Coiffier B, Lepage E, Briere J, et al. CHOP chemotherapy plus rituximab compared with CHOP alone in elderly patients with diffuse large-B-cell lymphoma. *The New England journal of medicine.* Jan 24 2002;346(4):235-242.

**35.** Pfreundschuh M, Trumper L, Osterborg A, et al. CHOP-like chemotherapy plus rituximab versus CHOP-like chemotherapy alone in young patients with good-prognosis diffuse large-B-cell lymphoma: a randomised controlled trial by the MabThera International Trial (MInT) Group. *The lancet oncology.* May 2006;7(5):379-391.

**36.** Barrans S, Crouch S, Smith A, et al. Rearrangement of MYC is associated with poor prognosis in patients with diffuse large B-cell lymphoma treated in the era of rituximab. *Journal of clinical oncology : official journal of the American Society of Clinical Oncology.* Jul 10 2010;28(20):3360-3365.

**37.** Mounier N, Gisselbrecht C. Stem cell transplantation for diffuse large B-cell lymphoma patients in the rituximab era. *Current opinion in oncology.* Mar 2011;23(2):209-213.

**38.** Ohno H, Fukuhara S. Significance of rearrangement of the BCL6 gene in B-cell lymphoid neoplasms. *Leukemia & lymphoma.* Sep 1997;27(1-2):53-63.

**39.** Basso K, Saito M, Sumazin P, et al. Integrated biochemical and computational approach identifies BCL6 direct target genes controlling multiple pathways in normal germinal center B cells. *Blood.* Feb 4 2010;115(5):975-984.

**40.** Lipford E, Wright JJ, Urba W, et al. Refinement of lymphoma cytogenetics by the chromosome 18q21 major breakpoint region. *Blood.* Dec 1987;70(6):1816-1823.

**41.** Savage KJ, Johnson NA, Ben-Neriah S, et al. MYC gene rearrangements are associated with a poor prognosis in diffuse large B-cell lymphoma patients treated with R-CHOP chemotherapy. *Blood.* Oct 22 2009;114(17):3533-3537.

**42.** Monti S, Savage KJ, Kutok JL, et al. Molecular profiling of diffuse large B-cell lymphoma identifies robust subtypes including one characterized by host inflammatory response. *Blood.* Mar 1 2005;105(5):1851-1861.

**43.** Lenz G, Wright G, Dave SS, et al. Stromal gene signatures in large-B-cell lymphomas. *The New England journal of medicine.* Nov 27 2008;359(22):2313-2323.
**44.** Rimsza LM, Wright G, Schwartz M, et al. Accurate classification of diffuse large B-cell lymphoma into germinal center and activated B-cell subtypes using a nuclease protection assay on formalin-fixed, paraffin-embedded tissues. *Clinical cancer research : an official journal of the American Association for Cancer Research.* Jun 1 2011;17(11):3727-3732.
**45.** Davis RE, Ngo VN, Lenz G, et al. Chronic active B-cell-receptor signalling in diffuse large B-cell lymphoma. *Nature.* Jan 7 2010;463(7277):88-92.
**46.** Lenz G, Davis RE, Ngo VN, et al. Oncogenic CARD11 mutations in human diffuse large B cell lymphoma. *Science (New York, N.Y.).* Mar 21 2008;319(5870):1676-1679.
**47.** Compagno M, Lim WK, Grunn A, et al. Mutations of multiple genes cause deregulation of NF-kappaB in diffuse large B-cell lymphoma. *Nature.* Jun 4 2009;459(7247):717-721.
**48.** Honma K, Tsuzuki S, Nakagawa M, et al. TNFAIP3/A20 functions as a novel tumor suppressor gene in several subtypes of non-Hodgkin lymphomas. *Blood.* Sep 17 2009;114(12):2467-2475.
**49.** Mandelbaum J, Bhagat G, Tang H, et al. BLIMP1 is a tumor suppressor gene frequently disrupted in activated B cell-like diffuse large B cell lymphoma. *Cancer cell.* Dec 14 2010;18(6):568-579.
**50.** Ngo VN, Young RM, Schmitz R, et al. Oncogenically active MYD88 mutations in human lymphoma. *Nature.* Feb 3 2011;470(7332):115-119.
**51.** Davis RE, Brown KD, Siebenlist U, Staudt LM. Constitutive nuclear factor kappaB activity is required for survival of activated B cell-like diffuse large B cell lymphoma cells. *The Journal of experimental medicine.* Dec 17 2001;194(12):1861-1874.
**52.** Lam LT, Davis RE, Pierce J, et al. Small molecule inhibitors of IkappaB kinase are selectively toxic for subgroups of diffuse large B-cell lymphoma defined by gene expression profiling. *Clinical cancer research : an official journal of the American Association for Cancer Research.* Jan 1 2005;11(1):28-40.
**53.** Dunleavy K, Pittaluga S, Czuczman MS, et al. Differential efficacy of bortezomib plus chemotherapy within molecular subtypes of diffuse large B-cell lymphoma. *Blood.* Jun 11 2009;113(24):6069-6076.
**54.** Iqbal J, Greiner TC, Patel K, et al. Distinctive patterns of BCL6 molecular alterations and their functional consequences in different subgroups of diffuse large B-cell lymphoma. *Leukemia.* Nov 2007;21(11):2332-2343.
**55.** Tam W, Gomez M, Chadburn A, Lee JW, Chan WC, Knowles DM. Mutational analysis of PRDM1 indicates a tumor-suppressor role in

diffuse large B-cell lymphomas. *Blood.* May 15 2006;107(10):4090-4100.

**56.** Pasqualucci L, Compagno M, Houldsworth J, et al. Inactivation of the PRDM1/BLIMP1 gene in diffuse large B cell lymphoma. *The Journal of experimental medicine.* Feb 20 2006;203(2):311-317.

**57.** Calado DP, Zhang B, Srinivasan L, et al. Constitutive canonical NF-kappaB activation cooperates with disruption of BLIMP1 in the pathogenesis of activated B cell-like diffuse large cell lymphoma. *Cancer cell.* Dec 14 2010;18(6):580-589.

**58.** Seifert M, Kuppers R. Molecular footprints of a germinal center derivation of human IgM+(IgD+)CD27+ B cells and the dynamics of memory B cell generation. *The Journal of experimental medicine.* Nov 23 2009;206(12):2659-2669.

**59.** Cattoretti G, Buttner M, Shaknovich R, Kremmer E, Alobeid B, Niedobitek G. Nuclear and cytoplasmic AID in extrafollicular and germinal center B cells. *Blood.* May 15 2006;107(10):3967-3975.

**60.** Rosenwald A, Wright G, Chan WC, et al. The use of molecular profiling to predict survival after chemotherapy for diffuse large-B-cell lymphoma. *The New England journal of medicine.* Jun 20 2002;346(25):1937-1947.

**61.** Lossos IS, Alizadeh AA, Eisen MB, et al. Ongoing immunoglobulin somatic mutation in germinal center B cell-like but not in activated B cell-like diffuse large cell lymphomas. *Proceedings of the National Academy of Sciences of the United States of America.* Aug 29 2000;97(18):10209-10213.

**62.** Saito M, Novak U, Piovan E, et al. BCL6 suppression of BCL2 via Miz1 and its disruption in diffuse large B cell lymphoma. *Proceedings of the National Academy of Sciences of the United States of America.* Jul 7 2009;106(27):11294-11299.

**63.** Pasqualucci L, Migliazza A, Basso K, Houldsworth J, Chaganti RS, Dalla-Favera R. Mutations of the BCL6 proto-oncogene disrupt its negative autoregulation in diffuse large B-cell lymphoma. *Blood.* Apr 15 2003;101(8):2914-2923.

**64.** Lenz G, Wright GW, Emre NC, et al. Molecular subtypes of diffuse large B-cell lymphoma arise by distinct genetic pathways. *Proceedings of the National Academy of Sciences of the United States of America.* Sep 9 2008;105(36):13520-13525.

**65.** Pasqualucci L, Dominguez-Sola D, Chiarenza A, et al. Inactivating mutations of acetyltransferase genes in B-cell lymphoma. *Nature.* Mar 10 2011;471(7337):189-195.

**66.** Morin RD, Mendez-Lago M, Mungall AJ, et al. Frequent mutation of histone-modifying genes in non-Hodgkin lymphoma. *Nature.* Aug 18 2011;476(7360):298-303.

**67.** Morin RD, Johnson NA, Severson TM, et al. Somatic mutations altering EZH2 (Tyr641) in follicular and diffuse large B-cell lymphomas of germinal-center origin. *Nature genetics.* Feb 2010;42(2):181-185.

**68.** Pasqualucci L, Trifonov V, Fabbri G, et al. Analysis of the coding genome of diffuse large B-cell lymphoma. *Nature genetics.* Sep 2011;43(9):830-837.
**69.** McCabe MT, Graves AP, Ganji G, et al. Mutation of A677 in histone methyltransferase EZH2 in human B-cell lymphoma promotes hypertrimethylation of histone H3 on lysine 27 (H3K27). *Proceedings of the National Academy of Sciences of the United States of America.* Feb 21 2012;109(8):2989-2994.
**70.** Sneeringer CJ, Scott MP, Kuntz KW, et al. Coordinated activities of wild-type plus mutant EZH2 drive tumor-associated hypertrimethylation of lysine 27 on histone H3 (H3K27) in human B-cell lymphomas. *Proceedings of the National Academy of Sciences of the United States of America.* Dec 7 2010;107(49):20980-20985.
**71.** Yap DB, Chu J, Berg T, et al. Somatic mutations at EZH2 Y641 act dominantly through a mechanism of selectively altered PRC2 catalytic activity, to increase H3K27 trimethylation. *Blood.* Feb 24 2011;117(8):2451-2459.
**72.** Wigle TJ, Knutson SK, Jin L, et al. The Y641C mutation of EZH2 alters substrate specificity for histone H3 lysine 27 methylation states. *FEBS letters.* Oct 3 2011;585(19):3011-3014.
**73.** Ryan RJ, Nitta M, Borger D, et al. EZH2 codon 641 mutations are common in BCL2-rearranged germinal center B cell lymphomas. *PloS one.* 2011;6(12):e28585.
**74.** Knutson SK, Wigle TJ, Warholic NM, et al. A selective inhibitor of EZH2 blocks H3K27 methylation and kills mutant lymphoma cells. *Nature chemical biology.* Nov 2012;8(11):890-896.
**75.** McCabe MT, Ott HM, Ganji G, et al. EZH2 inhibition as a therapeutic strategy for lymphoma with EZH2-activating mutations. *Nature.* Dec 6 2012;492(7427):108-112.
**76.** Baylin SB, Jones PA. A decade of exploring the cancer epigenome - biological and translational implications. *Nature reviews. Cancer.* Oct 2011;11(10):726-734.
**77.** Berdasco M, Esteller M. Aberrant epigenetic landscape in cancer: how cellular identity goes awry. *Developmental cell.* Nov 16 2010;19(5):698-711.
**78.** Rideout WM, 3rd, Coetzee GA, Olumi AF, Jones PA. 5-Methylcytosine as an endogenous mutagen in the human LDL receptor and p53 genes. *Science (New York, N.Y.).* Sep 14 1990;249(4974):1288-1290.
**79.** Jones PA, Baylin SB. The fundamental role of epigenetic events in cancer. *Nature reviews. Genetics.* Jun 2002;3(6):415-428.
**80.** van Haaften G, Dalgliesh GL, Davies H, et al. Somatic mutations of the histone H3K27 demethylase gene UTX in human cancer. *Nature genetics.* May 2009;41(5):521-523.
**81.** Kanai Y, Ushijima S, Nakanishi Y, Sakamoto M, Hirohashi S. Mutation of the DNA methyltransferase (DNMT) 1 gene in human colorectal cancers. *Cancer letters.* Mar 20 2003;192(1):75-82.

**82.** Singh RR, Bains A, Patel KP, et al. Detection of high-frequency and novel DNMT3A mutations in acute myeloid leukemia by high-resolution melting curve analysis. *The Journal of molecular diagnostics : JMD.* Jul 2012;14(4):336-345.
**83.** Pasini D, Malatesta M, Jung HR, et al. Characterization of an antagonistic switch between histone H3 lysine 27 methylation and acetylation in the transcriptional regulation of Polycomb group target genes. *Nucleic acids research.* Aug 2010;38(15):4958-4969.
**84.** Han A, He J, Wu Y, Liu JO, Chen L. Mechanism of recruitment of class II histone deacetylases by myocyte enhancer factor-2. *Journal of molecular biology.* Jan 7 2005;345(1):91-102.
**85.** Allfrey VG, Mirsky AE. Evidence for the complete DNA-dependence of RNA synthesis in isolated thymus nuclei. *Proceedings of the National Academy of Sciences of the United States of America.* Sep 15 1962;48:1590-1596.
**86.** Pogo BG, Allfrey VG, Mirsky AE. RNA synthesis and histone acetylation during the course of gene activation in lymphocytes. *Proceedings of the National Academy of Sciences of the United States of America.* Apr 1966;55(4):805-812.
**87.** Vidali G, Gershey EL, Allfrey VG. Chemical studies of histone acetylation. The distribution of epsilon-N-acetyllysine in calf thymus histones. *The Journal of biological chemistry.* Dec 25 1968;243(24):6361-6366.
**88.** Spotswood HT, Turner BM. An increasingly complex code. *The Journal of clinical investigation.* Sep 2002;110(5):577-582.
**89.** Jenuwein T, Allis CD. Translating the histone code. *Science (New York, N.Y.).* Aug 10 2001;293(5532):1074-1080.
**90.** Brownell JE, Zhou J, Ranalli T, et al. Tetrahymena histone acetyltransferase A: a homolog to yeast Gcn5p linking histone acetylation to gene activation. *Cell.* Mar 22 1996;84(6):843-851.
**91.** Taunton J, Hassig CA, Schreiber SL. A mammalian histone deacetylase related to the yeast transcriptional regulator Rpd3p. *Science (New York, N.Y.).* Apr 19 1996;272(5260):408-411.
**92.** Martin M, Kettmann R, Dequiedt F. Class IIa histone deacetylases: conducting development and differentiation. *The International journal of developmental biology.* 2009;53(2-3):291-301.
**93.** Nakagawa M, Oda Y, Eguchi T, et al. Expression profile of class I histone deacetylases in human cancer tissues. *Oncology reports.* Oct 2007;18(4):769-774.
**94.** Choudhary C, Kumar C, Gnad F, et al. Lysine acetylation targets protein complexes and co-regulates major cellular functions. *Science (New York, N.Y.).* Aug 14 2009;325(5942):834-840.
**95.** Bereshchenko OR, Gu W, Dalla-Favera R. Acetylation inactivates the transcriptional repressor BCL6. *Nature genetics.* Dec 2002;32(4):606-613.

**96.** Faiola F, Liu X, Lo S, et al. Dual regulation of c-Myc by p300 via acetylation-dependent control of Myc protein turnover and coactivation of Myc-induced transcription. *Molecular and cellular biology.* Dec 2005;25(23):10220-10234.

**97.** Patel JH, Du Y, Ard PG, et al. The c-MYC oncoprotein is a substrate of the acetyltransferases hGCN5/PCAF and TIP60. *Molecular and cellular biology.* Dec 2004;24(24):10826-10834.

**98.** Vervoorts J, Luscher-Firzlaff JM, Rottmann S, et al. Stimulation of c-MYC transcriptional activity and acetylation by recruitment of the cofactor CBP. *EMBO reports.* May 2003;4(5):484-490.

**99.** Lanzillotta A, Sarnico I, Ingrassia R, et al. The acetylation of RelA in Lys310 dictates the NF-kappaB-dependent response in post-ischemic injury. *Cell death & disease.* 2010;1:e96.

**100.** Kiernan R, Bres V, Ng RW, et al. Post-activation turn-off of NF-kappa B-dependent transcription is regulated by acetylation of p65. *The Journal of biological chemistry.* Jan 24 2003;278(4):2758-2766.

**101.** Finnin MS, Donigian JR, Cohen A, et al. Structures of a histone deacetylase homologue bound to the TSA and SAHA inhibitors. *Nature.* Sep 9 1999;401(6749):188-193.

**102.** Glaser KB, Staver MJ, Waring JF, Stender J, Ulrich RG, Davidsen SK. Gene expression profiling of multiple histone deacetylase (HDAC) inhibitors: defining a common gene set produced by HDAC inhibition in T24 and MDA carcinoma cell lines. *Molecular cancer therapeutics.* Feb 2003;2(2):151-163.

**103.** Peart MJ, Smyth GK, van Laar RK, et al. Identification and functional significance of genes regulated by structurally different histone deacetylase inhibitors. *Proceedings of the National Academy of Sciences of the United States of America.* Mar 8 2005;102(10):3697-3702.

**104.** McBain JA, Eastman A, Nobel CS, Mueller GC. Apoptotic death in adenocarcinoma cell lines induced by butyrate and other histone deacetylase inhibitors. *Biochemical pharmacology.* May 9 1997;53(9):1357-1368.

**105.** Bernhard D, Ausserlechner MJ, Tonko M, et al. Apoptosis induced by the histone deacetylase inhibitor sodium butyrate in human leukemic lymphoblasts. *FASEB journal : official publication of the Federation of American Societies for Experimental Biology.* Nov 1999;13(14):1991-2001.

**106.** Dupere-Richer D, Kinal M, Menasche V, et al. Vorinostat-induced autophagy switches from a death-promoting to a cytoprotective signal to drive acquired resistance. *Cell death & disease.* 2013;4:e486.

**107.** Gammoh N, Lam D, Puente C, Ganley I, Marks PA, Jiang X. Role of autophagy in histone deacetylase inhibitor-induced apoptotic and nonapoptotic cell death. *Proceedings of the National Academy of Sciences of the United States of America.* Apr 24 2012;109(17):6561-6565.

**108.** Petruccelli LA, Dupere-Richer D, Pettersson F, Retrouvey H, Skoulikas S, Miller WH, Jr. Vorinostat induces reactive oxygen species and DNA damage in acute myeloid leukemia cells. *PloS one.* 2011;6(6):e20987.
**109.** Pettazzoni P, Pizzimenti S, Toaldo C, et al. Induction of cell cycle arrest and DNA damage by the HDAC inhibitor panobinostat (LBH589) and the lipid peroxidation end product 4-hydroxynonenal in prostate cancer cells. *Free radical biology & medicine.* Jan 15 2011;50(2):313-322.
**110.** Prystowsky MB, Adomako A, Smith RV, et al. The histone deacetylase inhibitor LBH589 inhibits expression of mitotic genes causing G2/M arrest and cell death in head and neck squamous cell carcinoma cell lines. *The Journal of pathology.* Aug 2009;218(4):467-477.
**111.** Gilbert J, Baker SD, Bowling MK, et al. A phase I dose escalation and bioavailability study of oral sodium phenylbutyrate in patients with refractory solid tumor malignancies. *Clinical cancer research : an official journal of the American Association for Cancer Research.* Aug 2001;7(8):2292-2300.
**112.** Piekarz RL, Robey R, Sandor V, et al. Inhibitor of histone deacetylation, depsipeptide (FR901228), in the treatment of peripheral and cutaneous T-cell lymphoma: a case report. *Blood.* Nov 1 2001;98(9):2865-2868.
**113.** Duvic M, Talpur R, Ni X, et al. Phase 2 trial of oral vorinostat (suberoylanilide hydroxamic acid, SAHA) for refractory cutaneous T-cell lymphoma (CTCL). *Blood.* Jan 1 2007;109(1):31-39.
**114.** Olsen EA, Kim YH, Kuzel TM, et al. Phase IIb multicenter trial of vorinostat in patients with persistent, progressive, or treatment refractory cutaneous T-cell lymphoma. *Journal of clinical oncology : official journal of the American Society of Clinical Oncology.* Jul 20 2007;25(21):3109-3115.
**115.** Whittaker SJ, Demierre MF, Kim EJ, et al. Final results from a multicenter, international, pivotal study of romidepsin in refractory cutaneous T-cell lymphoma. *Journal of clinical oncology : official journal of the American Society of Clinical Oncology.* Oct 10 2010;28(29):4485-4491.
**116.** Piekarz RL, Frye R, Turner M, et al. Phase II multi-institutional trial of the histone deacetylase inhibitor romidepsin as monotherapy for patients with cutaneous T-cell lymphoma. *Journal of clinical oncology : official journal of the American Society of Clinical Oncology.* Nov 10 2009;27(32):5410-5417.
**117.** Crump M, Coiffier B, Jacobsen ED, et al. Phase II trial of oral vorinostat (suberoylanilide hydroxamic acid) in relapsed diffuse large-B-cell lymphoma. *Annals of oncology : official journal of the European Society for Medical Oncology / ESMO.* May 2008;19(5):964-969.
**118.** O'Connor OA, Heaney ML, Schwartz L, et al. Clinical experience with intravenous and oral formulations of the novel histone deacetylase inhibitor suberoylanilide hydroxamic acid in patients with advanced

hematologic malignancies. *Journal of clinical oncology : official journal of the American Society of Clinical Oncology.* Jan 1 2006;24(1):166-173.

**119.** Crump M, Andreadis C, Assouline S, et al. Treatment of relapsed or refractory non-hodgkin lymphoma with the oral isotype-selective histone deacetylase inhibitor MGCD0103: Interim results from a phase II study. *ASCO Meeting Abstracts.* August 18, 2008 2008;26(15_suppl):8528.

**120.** Giles F, Fischer T, Cortes J, et al. A phase I study of intravenous LBH589, a novel cinnamic hydroxamic acid analogue histone deacetylase inhibitor, in patients with refractory hematologic malignancies. *Clinical cancer research : an official journal of the American Association for Cancer Research.* Aug 1 2006;12(15):4628-4635.

**121.** Fukutomi A, Hatake K, Matsui K, et al. A phase I study of oral panobinostat (LBH589) in Japanese patients with advanced solid tumors. *Investigational new drugs.* Jun 2012;30(3):1096-1106.

**122.** Ghobrial IM, Campigotto F, Murphy TJ, et al. Results of a phase 2 trial of the single-agent histone deacetylase inhibitor panobinostat in patients with relapsed/refractory Waldenstrom macroglobulinemia. *Blood.* Feb 21 2013;121(8):1296-1303.

**123.** Loken MR, Shah VO, Dattilio KL, Civin CI. Flow cytometric analysis of human bone marrow. II. Normal B lymphocyte development. *Blood.* Nov 1987;70(5):1316-1324.

**124.** Stashenko P, Nadler LM, Hardy R, Schlossman SF. Expression of cell surface markers after human B lymphocyte activation. *Proceedings of the National Academy of Sciences of the United States of America.* Jun 1981;78(6):3848-3852.

**125.** Maloney DG, Grillo-Lopez AJ, White CA, et al. IDEC-C2B8 (Rituximab) anti-CD20 monoclonal antibody therapy in patients with relapsed low-grade non-Hodgkin's lymphoma. *Blood.* Sep 15 1997;90(6):2188-2195.

**126.** Dall'Ozzo S, Tartas S, Paintaud G, et al. Rituximab-dependent cytotoxicity by natural killer cells: influence of FCGR3A polymorphism on the concentration-effect relationship. *Cancer research.* Jul 1 2004;64(13):4664-4669.

**127.** Lefebvre ML, Krause SW, Salcedo M, Nardin A. Ex vivo-activated human macrophages kill chronic lymphocytic leukemia cells in the presence of rituximab: mechanism of antibody-dependent cellular cytotoxicity and impact of human serum. *Journal of immunotherapy (Hagerstown, Md. : 1997).* Jul-Aug 2006;29(4):388-397.

**128.** Hernandez-Ilizaliturri FJ, Jupudy V, Ostberg J, et al. Neutrophils contribute to the biological antitumor activity of rituximab in a non-Hodgkin's lymphoma severe combined immunodeficiency mouse model. *Clinical cancer research : an official journal of the American Association for Cancer Research.* Dec 1 2003;9(16 Pt 1):5866-5873.

**129.** Koene HR, Kleijer M, Algra J, Roos D, von dem Borne AE, de Haas M. Fc gammaRIIIa-158V/F polymorphism influences the binding of IgG by natural killer cell Fc gammaRIIIa, independently of the Fc gammaRIIIa-48L/R/H phenotype. *Blood.* Aug 1 1997;90(3):1109-1114.

**130.** Cartron G, Dacheux L, Salles G, et al. Therapeutic activity of humanized anti-CD20 monoclonal antibody and polymorphism in IgG Fc receptor FcgammaRIIIa gene. *Blood.* Feb 1 2002;99(3):754-758.

**131.** Weng WK, Levy R. Two immunoglobulin G fragment C receptor polymorphisms independently predict response to rituximab in patients with follicular lymphoma. *Journal of clinical oncology : official journal of the American Society of Clinical Oncology.* Nov 1 2003;21(21):3940-3947.

**132.** Treon SP, Hansen M, Branagan AR, et al. Polymorphisms in FcgammaRIIIA (CD16) receptor expression are associated with clinical response to rituximab in Waldenstrom's macroglobulinemia. *Journal of clinical oncology : official journal of the American Society of Clinical Oncology.* Jan 20 2005;23(3):474-481.

**133.** Treon SP, Mitsiades C, Mitsiades N, et al. Tumor cell expression of CD59 is associated with resistance to CD20 serotherapy in patients with B-cell malignancies. *Journal of immunotherapy (Hagerstown, Md. : 1997).* May-Jun 2001;24(3):263-271.

**134.** Rubenstein JL, Fridlyand J, Abrey L, et al. Phase I study of intraventricular administration of rituximab in patients with recurrent CNS and intraocular lymphoma. *Journal of clinical oncology : official journal of the American Society of Clinical Oncology.* Apr 10 2007;25(11):1350-1356.

**135.** Kheirallah S, Caron P, Gross E, et al. Rituximab inhibits B-cell receptor signaling. *Blood.* Feb 4 2010;115(5):985-994.

**136.** Semac I, Palomba C, Kulangara K, et al. Anti-CD20 therapeutic antibody rituximab modifies the functional organization of rafts/microdomains of B lymphoma cells. *Cancer research.* Jan 15 2003;63(2):534-540.

**137.** Vega MI, Huerta-Yepaz S, Garban H, Jazirehi A, Emmanouilides C, Bonavida B. Rituximab inhibits p38 MAPK activity in 2F7 B NHL and decreases IL-10 transcription: pivotal role of p38 MAPK in drug resistance. *Oncogene.* Apr 29 2004;23(20):3530-3540.

**138.** Shi W, Han X, Yao J, Yang J, Shi Y. Combined effect of histone deacetylase inhibitor suberoylanilide hydroxamic acid and anti-CD20 monoclonal antibody rituximab on mantle cell lymphoma cells apoptosis. *Leukemia research.* Jun 2012;36(6):749-755.

**139.** Zhao WL, Wang L, Liu YH, et al. Combined effects of histone deacetylase inhibitor and rituximab on non-Hodgkin's B-lymphoma cells apoptosis. *Experimental hematology.* Dec 2007;35(12):1801-1811.

**140.** Jazirehi AR, Gan XH, De Vos S, Emmanouilides C, Bonavida B. Rituximab (anti-CD20) selectively modifies Bcl-xL and apoptosis protease activating factor-1 (Apaf-1) expression and sensitizes human non-Hodgkin's lymphoma B cell lines to paclitaxel-induced apoptosis. *Molecular cancer therapeutics.* Nov 2003;2(11):1183-1193.

**141.** Alas S, Emmanouilides C, Bonavida B. Inhibition of interleukin 10 by rituximab results in down-regulation of bcl-2 and sensitization of B-cell non-Hodgkin's lymphoma to apoptosis. *Clinical cancer research : an official journal of the American Association for Cancer Research.* Mar 2001;7(3):709-723.

**142.** Vega MI, Jazirehi AR, Huerta-Yepez S, Bonavida B. Rituximab-induced inhibition of YY1 and Bcl-xL expression in Ramos non-Hodgkin's lymphoma cell line via inhibition of NF-kappa B activity: role of YY1 and Bcl-xL in Fas resistance and chemoresistance, respectively. *Journal of immunology (Baltimore, Md. : 1950).* Aug 15 2005;175(4):2174-2183.

**143.** Jazirehi AR, Huerta-Yepez S, Cheng G, Bonavida B. Rituximab (chimeric anti-CD20 monoclonal antibody) inhibits the constitutive nuclear factor-{kappa}B signaling pathway in non-Hodgkin's lymphoma B-cell lines: role in sensitization to chemotherapeutic drug-induced apoptosis. *Cancer research.* Jan 1 2005;65(1):264-276.

**144.** Jazirehi AR, Vega MI, Chatterjee D, Goodglick L, Bonavida B. Inhibition of the Raf-MEK1/2-ERK1/2 signaling pathway, Bcl-xL down-regulation, and chemosensitization of non-Hodgkin's lymphoma B cells by Rituximab. *Cancer research.* Oct 1 2004;64(19):7117-7126.

**145.** Suzuki E, Umezawa K, Bonavida B. Rituximab inhibits the constitutively activated PI3K-Akt pathway in B-NHL cell lines: involvement in chemosensitization to drug-induced apoptosis. *Oncogene.* Sep 13 2007;26(42):6184-6193.

**146.** Hiraga J, Tomita A, Sugimoto T, et al. Down-regulation of CD20 expression in B-cell lymphoma cells after treatment with rituximab-containing combination chemotherapies: its prevalence and clinical significance. *Blood.* May 14 2009;113(20):4885-4893.

**147.** Tomita A, Hiraga J, Kiyoi H, et al. Epigenetic regulation of CD20 protein expression in a novel B-cell lymphoma cell line, RRBL1, established from a patient treated repeatedly with rituximab-containing chemotherapy. *International journal of hematology.* Jul 2007;86(1):49-57.

**148.** Lugthart S, Groschel S, Beverloo HB, et al. Clinical, molecular, and prognostic significance of WHO type inv(3)(q21q26.2)/t(3;3)(q21;q26.2) and various other 3q abnormalities in acute myeloid leukemia. *Journal of clinical oncology : official journal of the American Society of Clinical Oncology.* Aug 20 2010;28(24):3890-3898.

**149.** Buonamici S, Chakraborty S, Senyuk V, Nucifora G. The role of EVI1 in normal and leukemic cells. *Blood cells, molecules & diseases.* Sep-Oct 2003;31(2):206-212.
**150.** Lugthart S, Figueroa ME, Bindels E, et al. Aberrant DNA hypermethylation signature in acute myeloid leukemia directed by EVI1. *Blood.* Jan 6 2011;117(1):234-241.
**151.** Waxman S, Anderson KC. History of the Development of Arsenic Derivatives in Cancer Therapy. *The oncologist.* April 1, 2001 2001;6(suppl 2):3-10.
**152.** Lo-Coco F, Avvisati G, Vignetti M, et al. Retinoic Acid and Arsenic Trioxide for Acute Promyelocytic Leukemia. *New England Journal of Medicine.* 2013;369(2):111-121.
**153.** Mann KK, Wallner B, Lossos IS, Miller WH, Jr. Darinaparsin: a novel organic arsenical with promising anticancer activity. *Expert opinion on investigational drugs.* Nov 2009;18(11):1727-1734.
**154.** Matulis SM, Morales AA, Yehiayan L, et al. Darinaparsin induces a unique cellular response and is active in an arsenic trioxide-resistant myeloma cell line. *Molecular cancer therapeutics.* May 2009;8(5):1197-1206.
**155.** Diaz Z, Mann KK, Marcoux S, et al. A novel arsenical has antitumor activity toward As2O3-resistant and MRP1/ABCC1-overexpressing cell lines. *Leukemia (08876924).* 2008;22(10):1853-1863.
**156.** Shackelford D, Kenific C, Blusztajn A, Waxman S, Ren R. Targeted degradation of the AML1/MDS1/EVI1 oncoprotein by arsenic trioxide. *Cancer research.* Dec 1 2006;66(23):11360-11369.
**157.** Raza A, Buonamici S, Lisak L, et al. Arsenic trioxide and thalidomide combination produces multi-lineage hematological responses in myelodysplastic syndromes patients, particularly in those with high pre-therapy EVI1 expression. *Leukemia research.* Aug 2004;28(8):791-803.
**158.** Shimizu R, Kikuchi J, Wada T, Ozawa K, Kano Y, Furukawa Y. HDAC inhibitors augment cytotoxic activity of rituximab by upregulating CD20 expression on lymphoma cells. *Leukemia.* Oct 2010;24(10):1760-1768.
**159.** Chou T-C, Talalay P. Analysis of combined drug effects: a new look at a very old problem. *Trends in pharmacological sciences.* 1983;4:450-454.
**160.** Chou TC, Talalay P. Quantitative analysis of dose-effect relationships: the combined effects of multiple drugs or enzyme inhibitors. *Advances in enzyme regulation.* 1984;22:27-55.
**161.** Fu K, Weisenburger DD, Choi WWL, et al. Addition of Rituximab to Standard Chemotherapy Improves the Survival of Both the Germinal Center B-Cell–Like and Non–Germinal Center B-Cell–Like Subtypes of Diffuse Large B-Cell Lymphoma. *Journal of Clinical Oncology.* October 1, 2008 2008;26(28):4587-4594.
**162.** Gutierrez-Garcia G, Cardesa-Salzmann T, Climent F, et al. Gene-expression profiling and not immunophenotypic algorithms predicts

prognosis in patients with diffuse large B-cell lymphoma treated with immunochemotherapy. *Blood.* May 5 2011;117(18):4836-4843.

**163.** Cuenda A, Rouse J, Doza YN, et al. SB 203580 is a specific inhibitor of a MAP kinase homologue which is stimulated by cellular stresses and interleukin-1. *FEBS letters.* May 8 1995;364(2):229-233.

**164.** Eyers PA, Craxton M, Morrice N, Cohen P, Goedert M. Conversion of SB 203580-insensitive MAP kinase family members to drug-sensitive forms by a single amino-acid substitution. *Chemistry & biology.* Jun 1998;5(6):321-328.

**165.** Gum RJ, McLaughlin MM, Kumar S, et al. Acquisition of sensitivity of stress-activated protein kinases to the p38 inhibitor, SB 203580, by alteration of one or more amino acids within the ATP binding pocket. *The Journal of biological chemistry.* Jun 19 1998;273(25):15605-15610.

**166.** Andresen L, Jensen H, Pedersen MT, Hansen KA, Skov S. Molecular regulation of MHC class I chain-related protein A expression after HDAC-inhibitor treatment of Jurkat T cells. *Journal of immunology (Baltimore, Md. : 1950).* Dec 15 2007;179(12):8235-8242.

**167.** Ihlefeld K, Claas RF, Koch A, Pfeilschifter JM, Meyer Zu Heringdorf D. Evidence for a link between histone deacetylation and Ca(2)+ homoeostasis in sphingosine-1-phosphate lyase-deficient fibroblasts. *The Biochemical journal.* Nov 1 2012;447(3):457-464.

**168.** McKinsey TA, Zhang CL, Lu J, Olson EN. Signal-dependent nuclear export of a histone deacetylase regulates muscle differentiation. *Nature.* Nov 2 2000;408(6808):106-111.

**169.** Hofmeister JK, Cooney D, Coggeshall KM. Clustered CD20 induced apoptosis: src-family kinase, the proximal regulator of tyrosine phosphorylation, calcium influx, and caspase 3-dependent apoptosis. *Blood cells, molecules & diseases.* Apr 2000;26(2):133-143.

**170.** Janas E, Priest R, Wilde JI, White JH, Malhotra R. Rituxan (anti-CD20 antibody)-induced translocation of CD20 into lipid rafts is crucial for calcium influx and apoptosis. *Clinical and experimental immunology.* Mar 2005;139(3):439-446.

**171.** Shan D, Ledbetter JA, Press OW. Signaling events involved in anti-CD20-induced apoptosis of malignant human B cells. *Cancer immunology, immunotherapy : CII.* Mar 2000;48(12):673-683.

**172.** Glasel JA. Validity of nucleic acid purities monitored by 260nm/280nm absorbance ratios. *BioTechniques.* Jan 1995;18(1):62-63.

**173.** Schroeder A, Mueller O, Stocker S, et al. The RIN: an RNA integrity number for assigning integrity values to RNA measurements. *BMC molecular biology.* 2006;7:3.

**174.** Asmar F, Christensen J, Johansen JV, et al. TET2 mutations in Diffuse Large B-Cell Lymphoma: The Role of TET2 in the Regulation of Methylation Patterns at TET2 Target Genes. *ASH Annual Meeting Abstracts.* November 18, 2011 2011;118(21):1364-.

**175.** Ichikawa A, Kinoshita T, Watanabe T, et al. Mutations of the p53 gene as a prognostic factor in aggressive B-cell lymphoma. *The New England journal of medicine.* Aug 21 1997;337(8):529-534.
**176.** Lohr JG, Stojanov P, Lawrence MS, et al. Discovery and prioritization of somatic mutations in diffuse large B-cell lymphoma (DLBCL) by whole-exome sequencing. *Proceedings of the National Academy of Sciences of the United States of America.* Mar 6 2012;109(10):3879-3884.
**177.** Scholl V, Stefanoff CG, Hassan R, Spector N, Renault IZ. Mutations within the 5' region of FAS/CD95 gene in nodal diffuse large B-cell lymphoma. *Leukemia & lymphoma.* May 2007;48(5):957-963.
**178.** El-Osta H, Hong D, Wheler J, et al. Outcomes of research biopsies in phase I clinical trials: the MD anderson cancer center experience. *The oncologist.* 2011;16(9):1292-1298.
**179.** Gomez-Roca CA, Lacroix L, Massard C, et al. Sequential research-related biopsies in phase I trials: acceptance, feasibility and safety. *Annals of oncology : official journal of the European Society for Medical Oncology / ESMO.* May 2012;23(5):1301-1306.
**180.** Olson EM, Lin NU, Krop IE, Winer EP. The ethical use of mandatory research biopsies. *Nature reviews. Clinical oncology.* Oct 2011;8(10):620-625.
**181.** Nielsen TH, Johnson N, Garnier N, et al. Monitoring Response and Resistance to the Novel Arsenical Darinaparsin in an AML Patient. *Frontiers in pharmacology.* 2013;4:9.
**182.** Yuasa H, Oike Y, Iwama A, et al. Oncogenic transcription factor Evi1 regulates hematopoietic stem cell proliferation through GATA-2 expression. *The EMBO journal.* Jun 1 2005;24(11):1976-1987.
**183.** Hardin JA, Sherr DH, DeMaria M, Lopez PA. A simple fluorescence method for surface antigen phenotyping of lymphocytes undergoing DNA fragmentation. *Journal of immunological methods.* Sep 18 1992;154(1):99-107.
**184.** Tsimberidou AM, Camacho LH, Verstovsek S, et al. A phase I clinical trial of darinaparsin in patients with refractory solid tumors. *Clinical cancer research : an official journal of the American Association for Cancer Research.* Jul 15 2009;15(14):4769-4776.
**185.** Kornblau SM, McCue D, Singh N, Chen W, Estrov Z, Coombes KR. Recurrent expression signatures of cytokines and chemokines are present and are independently prognostic in acute myelogenous leukemia and myelodysplasia. *Blood.* Nov 18 2010;116(20):4251-4261.
**186.** Waugh DJ, Wilson C. The interleukin-8 pathway in cancer. *Clinical cancer research : an official journal of the American Association for Cancer Research.* Nov 1 2008;14(21):6735-6741.
**187.** Yoshimi A, Goyama S, Watanabe-Okochi N, et al. Evi1 represses PTEN expression and activates PI3K/AKT/mTOR via interactions with polycomb proteins. *Blood.* Mar 31 2011;117(13):3617-3628.

**188.** Barjesteh van Waalwijk van Doorn-Khosrovani S, Erpelinck C, van Putten WL, et al. High EVI1 expression predicts poor survival in acute myeloid leukemia: a study of 319 de novo AML patients. *Blood.* Feb 1 2003;101(3):837-845.
**189.** Gröschel S, Schlenk RF, Engelmann J, et al. Deregulated Expression of EVI1 Defines a Poor Prognostic Subset of MLL-Rearranged Acute Myeloid Leukemias: A Study of the German-Austrian Acute Myeloid Leukemia Study Group and the Dutch-Belgian-Swiss HOVON/SAKK Cooperative Group. *Journal of Clinical Oncology.* January 1, 2013 2013;31(1):95-103.
**190.** Lugthart S, van Drunen E, van Norden Y, et al. High EVI1 levels predict adverse outcome in acute myeloid leukemia: prevalence of EVI1 overexpression and chromosome 3q26 abnormalities underestimated. *Blood.* Apr 15 2008;111(8):4329-4337.
**191.** Horig H, Marincola E, Marincola FM. Obstacles and opportunities in translational research. *Nature medicine.* Jul 2005;11(7):705-708.

# Appendix: Biopsy and Blood Processing Protocols

## LYMPH NODE CORE NEEDLE BIOPSY RECEPTION AND PROCESSING

### 1. PURPOSE

This SOP defines the processing, handling and storage of lymph node core needle biopsies for Q-CROC02.

### 2. APPLICABLE TO

This SOP is to be read and applied by all personnel involved in the Q-CROC02 study.

### 3. SUPPLIES

Trypan blue
Falcon 5 ml Polystyrene Round-Bottom Tubes
Qiagen Allprep DNA/RNA mini kit
β-mercaptoethanol
RNase free water
100% ethanol
Dounce homogenizer
EasySep human B cell enrichment kit without CD43 depletion (StemCell Technologies)
EasySep magnet (StemCell Technologies)
EasySep magnet (StemCell Technologies)
Phosphate buffered saline
Fetal bovine serum
PE mouse anti-human CD19
PE mouse $IgG_1$ Kappa Isotype control
1% paraformaldehyde in PBS
FACS wash buffer (500 mL PBS supplemented with 25 mL FBS and 0.325 g sodium azide)
Resuspension medium (PBS with 2% FBS)
1 ml syringe with 26G3/8 gauge needle
Data sheet and pen
Biohazard and sharps waste containers

### 4. PRECAUTIONS

Gloves must be worn at all times when handling specimens. This includes

disposal of contaminated tubes and clean up of any spills. Tubes, plates and sharps must be properly disposed of in biohazard containers, in accordance with institutional requirements. Human tissue is considered a biohazard and should be handled using universal precautions according to local Health and Safety rules.

## 5. WORKING PROCEDURES

**PATIENT SAMPLES SHOULD BE PROCESSED AS SOON AS THEY ARRIVE IN THE LAB.**

Enrichment of human B-cells:

- Record the biopsy processing start time in the datasheet or case report form (CRF). Note that the Dounce homogenizer must be UV-irradiated for at least 15 minutes prior to starting isolation protocol.
- Open the vial of RPMI with three needle core biopsies inside. Obtain a single-cell suspension of the tissue cores by cutting with scalpels followed by gentle homogenization using a Dounce homogenizer.
- Transfer cell suspension to a 5 ml Falcon tube and count the cells using trypan blue (see below). Unlikely to get enough cells to use the recommended concentration of 5 x $10^7$ cells/ml but lower concentration seems to work well (around 1 x $10^7$ cells/ml).
- Add EasySep Negative Selection Human B Cell Enrichment Cocktail Without CD43 Depletion at 50 µl/5 x $10^7$ cells. Mix well and incubate at room temp for 10 mins.
- Mix EasySep Magnetic Nanoparticles to ensure that they are in a uniform suspension by vigorously pipetting up and down more than 5 times. Vortexing is not recommended. Add the nanoparticles at 50 µl/5 x $10^7$ cells. Mix well and incubate at room temperature for 10 minutes.
- Bring the cell suspension up to a total volume of 2.5 ml by adding recommended medium (PBS with 2% FBS). Mix the cells in the tube by gently pipetting up and down 2-3 times. Place the tube (without cap) into the magnet. Set aside for five minutes.
- Pick up the EasySep Magnet, and in one continuous motion invert the magnet and tube, pouring off the desired fraction into a new 12 x 75 mm polystyrene tube. The magnetically labeled unwanted cells will remain bound inside the original tube, held by the magnetic field of the magnet. Leave the magnet and the tube in inverted position for 2-3 seconds, then return to upright position. Do not shake or blot off any drops that may remain hanging from the mouth of the tube. The negatively selected, enriched cells in the new tube are now ready for use or for a second round of separation.

Counting leukocytes using trypan blue.

- Trypan blue is diluted 1:5 with PBS before use.
- Mix 10 ul cells with 30 ul diluted trypan blue. Count using hemocytometer. Count at least four large squares.
- Two-hundred thousand cells will be used for CD19 stain, the remainder (preferably > 1,000,000 cells) will be used for RNA/DNA isolation.
- In the event of an insufficient number of cells (< 1,000,000 cells), priority should be given to RNA/DNA isolation.

CD19 stain to ascertain purity of B cell isolate:

- Pipet 100000 cells for isotype control and 100000 cells for CD19 stain into FACS tubes. Spin for 5 mins at 1500 rpm (RT). Invert to discard supernatant.
- Add approximately 1 ml FACS wash buffer, spin for 5 mins at 1500 rpm (RT). Invert.
- In the approximately 50-100 μl of FACS wash buffer remaining in the tube, add 2 μl of either isotype control Ab or CD19 Ab. Incubate in dark at $4^{o}$C for 20 – 30 mins.
- Add approximately 1ml FACS wash buffer. Spin for 5 mins at 1500 rpm (RT). Invert.
- Fix with 1% paraformaldehyde in PBS (350 μl per sample). Store at $4^{o}$C in dark until analysis.

DNA/RNA Isolation

- Prepare QiagenAllprep DNA/RNA kit. Add β-mercaptoethanol (β-ME) to Buffer RLT Plus before use. Add 10 µl β-ME per 1 ml Buffer RLT Plus (for each sample, up to 5 x $10^6$ cells, 350 µl Buffer RLT Plus (plus 3.5 µl β-ME) is needed). Buffer RPE, Buffer AW1, and Buffer AW2 are each supplied as a concentrate. Before using for the first time, add the appropriate volume of ethanol (96–100%), as indicated on the bottle, to obtain a working solution.
- Perform all steps of the procedure at room temperature.
- Cells grown in suspension (do not use more than 1 x $10^7$ cells): Determine the number of cells. Pellet the appropriate number of cells by centrifuging for 5 min at 300 x g(approximately 2500 rpm in table-top centrifuge) in a centrifuge tube. Carefully remove all supernatant by aspiration.
- Disrupt the cells by adding Buffer RLT Plus. For pelleted cells, loosen the cell pellet thoroughly by flicking the tube. Add the appropriate volume of Buffer RLT Plus (5 x $10^6$ cells or less, use 350 µl Buffer RLT Plus, more than 5 x $10^6$ cells, use 600 µl Buffer RLT Plus). Vortex or pipet to mix.
- Homogenize the lysate by passing the lysate at least 5 times through a 26G3/8 needle fitted to an RNase-free syringe.
- Transfer the homogenized lysate to an AllPrep DNA spin column placed in a 2 ml collection tube (supplied). Close the lid gently, and centrifuge for 30 s at ≥8000 x g (≥10,000 rpm).
- Place the AllPrep DNA spin column in a new 2 ml collection tube, and store at room temperature (15–25ºC) or at 4ºC for later DNA purification. Use the flow-through for RNA purification. Note: Do not store the AllPrep DNA spin column at room temperature or at 4ºC for long periods. Do not freeze the column.

Total RNA purification:

- Add 1 volume (usually 350 µl or 600 µl) of 70% ethanol to the flowthrough from step 5, and mix well by pipetting. Do not centrifuge.
- Transfer up to 700 µl of the sample, including any precipitate that may have formed, to an RNeasy spin column placed in a 2 ml collection tube. Close the lid gently, and centrifuge for 15 s at ≥8000 x g (≥10,000 rpm). Discard the flow-through.
- Add 700 µl Buffer RW1 to the RNeasy spin column. Close the lid gently, and centrifuge for 15 s at ≥8000 x g (≥10,000 rpm) to wash the spin column membrane. Discard the flow-through. Reuse the collection tube in the next step.
- Add 500 µl Buffer RPE to the RNeasy spin column. Close the lid gently, and centrifuge for 15 s at ≥8000 x g (≥10,000 rpm) to wash the spin column membrane. Discard the flow-through. Reuse the collection tube in the next step.

- Add 500 µl Buffer RPE to the RNeasy spin column. Close the lid gently, and centrifuge for 2 min at ≥8000 x g (≥10,000 rpm) to wash the spin column membrane.
- Place the RNeasy spin column in a new 2 ml collection tube (supplied), and discard the old collection tube with the flowthrough. Centrifuge at full speed for 1 min.
- Place the RNeasy spin column in a new 1.5 ml collection tube. Add 30 µl RNase-free water directly to the spin column membrane. Close the lid gently, and centrifuge for 1 min at ≥8000 x g (≥10,000 rpm) to elute the RNA.
- To optimize RNA concentration, aspirate the 30 ul flow through and apply to the column a second time. Close the lid gently and centrifuge for 1 min at ≥8000 x g (≥10,000 rpm) to elute the RNA.
- Measure concentration and ratio 260/280 and note this on freezer box chart.
- Store at -80ºC in "LBH trial/Q-CROC2" box.

Genomic DNA purification:

- Add 500 µl Buffer AW1 to the AllPrep DNA spin column from step 5. Close the lid gently, and centrifuge for 15 s at ≥8000 x g (10,000 rpm) to wash the spin column membrane. Discard the flowthrough. Reuse the spin column in the next step.
- Add 500 µl Buffer AW2 to the AllPrep DNA spin column. Close the lid gently, and centrifuge for 2 min at full speed to wash the spin column membrane.
- Place the AllPrep DNA spin column in a new 1.5 ml collection tube. Add 50 µl Buffer EB (pre-heated to 70ºC) directly to the spin column membrane and close the lid. Incubate at room temperature (15–25ºC) for 1 min, and then centrifuge for 1 min at ≥8000 x g (10,000 rpm) to elute the DNA.
- Repeat the last step, adding 50 ul Buffer EB to the same column to elute further DNA.
- Measure concentration and ratio 260/280 and note this on freezer box chart.
- Store at -80ºC in "LBH trial/Q-CROC2" box.

**Any deviation to this procedure should be carefully recorded on the datasheet or CRF.**

# HEPARIN BLOOD RECEPTION AND PROCESSING

## 1. PURPOSE

This SOP defines how to standardize the processing, handling and storage of whole blood samples collected in heparin tubes.

## 2. APPLICABLE TO

This SOP is to be read and applied by all personnel involved in all Q-CROC's projects where heparin blood needs to be processed.

## 3. SUPPLIES

Trypan blue
Qiagen Allprep DNA/RNA mini kit
β-mercaptoethanol
RNase free water
100% ethanol
Phosphate buffered saline
Fetal bovine serum
Ficoll-Paque PLUS
HBSS
Protein lysis buffer (50 mM Tris-HCl (pH 8.0), 150 mM NaCl and 1% Triton X-100) supplemented with aprotinin, leupeptin, PMSF, $NaVO_4$ and phosphatase inhibitors.
15 ml Falcon polystyrene tubes
1 ml syringe with 26G3/8 gauge needle
Data sheet and pen
Biohazard and sharps waste containers

## 4. PRECAUTIONS

Gloves must be worn at all times when handling specimens. This includes during removal of the rubber stopper from the blood tubes, disposal of contaminated tubes, and clean up of any spills. Tubes must be properly disposed of in biohazard containers, in accordance with institutional requirements. Blood material is considered a biohazard and should be handled using universal precautions according to local Health and Safety rules.

## 5. WORKING PROCEDURES

**PATIENT SAMPLES SHOULD BE PROCESSED AS SOON AS THEY**

**ARRIVE IN THE LAB.**

Ficoll isolation of leukocytes:

- Record the blood processing start time in the datasheet or case report form (CRF).
- Transfer the whole blood to a Falcon polystyrene tubes to a maximum of 10mL.
- Place tubes into a centrifuge; ensure it is balanced, and spin at approximately 1200 rpm for 10 minutes. CENTRIFUGE MUST BE AT ROOM TEMPERATURE.
- Remove the tubes carefully from the centrifuge to avoid disturbing the cells.
- Remove 1500µL aliquots of plasma (top layer) using a pipette and place the aliquots into eppendorf tubes
- Immediately bring the eppendorf tubes to the -80°C freezer and place them into an appropriately labeled storage box. If samples are to be added to a new box, enter all the information on the label, place it on the box and then place the cryovials in the box. Immediately bring the box to the -80$^{o}$C freezer.

- Dilute the remaining cell pellet in HBSS up to total volume of 10 ml.
- Put 4 ml Ficoll in 15 ml vial. Slowly layer the diluted cells onto the Ficoll.
- Spin for 30 mins at 2200 rpm (RT) with the brake off the centrifuge.
- Remove the buffy coat (middle white layer) and place immediately in 10 ml HBSS in a 15 ml tube.
- Spin for 10 mins at 1200 rpm (RT).
- Discard supernatant and resuspend pellet in 10 ml HBSS again.
- Spin for 10 mins at 1200 rpm (RT).
- Resuspend cells in 2 ml resuspension buffer (RPMI media with 10% FBS or PBS with 2% FBS).

Counting leukocytes using trypan blue:

- Trypan blue is diluted 1:5 with PBS before use.

- Mix 10 ul cells with 30 ul diluted trypan blue. Count using hemocytometer. Count at least four large squares.

- For samples where more than 3 million cells are isolated, the sample is split in half and one half of the cells are used for RNA/DNA isolation while the other half is be used for whole cell extracts. In the event that fewer than 3 million PBMCs are isolated, all cells will be used for isolation of DNA/RNA.

DNA/RNA Isolation:

- Prepare QiagenAllprep DNA/RNA kit. Add β-mercaptoethanol (β-ME) to Buffer RLT Plus before use. Add 10 µl β-ME per 1 ml Buffer RLT Plus (for each sample, up to 5 x $10^6$ cells, 350 µl Buffer RLT Plus (plus 3.5 µl β-ME) is needed). Buffer RPE, Buffer AW1, and Buffer AW2 are each supplied as a concentrate. Before using for the first time, add the appropriate volume of ethanol (96–100%), as indicated on the bottle, to obtain a working solution.
- Perform all steps of the procedure at room temperature.
- Cells grown in suspension (do not use more than 1 x $10^7$ cells): Determine the number of cells. Pellet the appropriate number of cells by centrifuging for 5 min at 300 x g (approximately 2500 rpm in table-top centrifuge) in a centrifuge tube. Carefully remove all supernatant by aspiration.
- Disrupt the cells by adding Buffer RLT Plus. For pelleted cells, loosen the cell pellet thoroughly by flicking the tube. Add the appropriate volume of Buffer RLT Plus (5 x $10^6$ cells or less, use 350 µl Buffer RLT Plus, more than 5 x $10^6$ cells, use 600 µl Buffer RLT Plus). Vortex or pipet to mix.
- Homogenize the lysate by passing the lysate at least 5 times through a 26G3/8 needle fitted to an RNase-free syringe.
- Transfer the homogenized lysate to an AllPrep DNA spin column placed in a 2 ml collection tube (supplied). Close the lid gently, and centrifuge for 30 s at ≥8000 x g (≥10,000 rpm).
- Place the AllPrep DNA spin column in a new 2 ml collection tube, and store at room temperature (15–25ºC) or at 4ºC for later DNA purification. Use the flow-through for RNA purification. Note: Do not store the AllPrep DNA spin column at room temperature or at 4ºC for long periods. Do not freeze the column.

<u>Total RNA purification:</u>

- Add 1 volume (usually 350 µl or 600 µl) of 70% ethanol to the flowthrough from step 5, and mix well by pipetting. Do not centrifuge.
- Transfer up to 700 µl of the sample, including any precipitate that may have formed, to an RNeasy spin column placed in a 2 ml collection tube. Close the lid gently, and centrifuge for 15 s at ≥8000 x g (≥10,000 rpm). Discard the flow-through.
- Add 700 µl Buffer RW1 to the RNeasy spin column. Close the lid gently, and centrifuge for 15 s at ≥8000 x g (≥10,000 rpm) to wash the spin column membrane. Discard the flow-through. Reuse the collection tube in the next step.
- Add 500 µl Buffer RPE to the RNeasy spin column. Close the lid gently, and centrifuge for 15 s at ≥8000 x g (≥10,000 rpm) to wash the spin column membrane. Discard the flow-through. Reuse the collection tube in the next step.

- Add 500 µl Buffer RPE to the RNeasy spin column. Close the lid gently, and centrifuge for 2 min at ≥8000 x g (≥10,000 rpm) to wash the spin column membrane.
- Place the RNeasy spin column in a new 2 ml collection tube (supplied), and discard the old collection tube with the flowthrough. Centrifuge at full speed for 1 min.
- Place the RNeasy spin column in a new 1.5 ml collection tube. Add 30–50 µl RNase-free water directly to the spin column membrane. Close the lid gently, and centrifuge for 1 min at ≥8000 x g (≥10,000 rpm) to elute the RNA.
- To optimize RNA concentration, aspirate the 30 ul flow through and apply to the column a second time. Close the lid gently and centrifuge for 1 min at ≥8000 x g (≥10,000 rpm) to elute the RNA.
- Measure concentration and ratio 260/280 and note this on freezer box chart.
- Store at -80ºC in "LBH trial/Q-CROC2" box.

Genomic DNA purification:

- Add 500 µl Buffer AW1 to the AllPrep DNA spin column from step 5. Close the lid gently, and centrifuge for 15 s at ≥8000 x g (10,000 rpm) to wash the spin column membrane. Discard the flowthrough. Reuse the spin column in the next step.
- Add 500 µl Buffer AW2 to the AllPrep DNA spin column. Close the lid gently, and centrifuge for 2 min at full speed to wash the spin column membrane.
- Place the AllPrep DNA spin column in a new 1.5 ml collection tube. Add 50 µl Buffer EB (pre-heated to 70ºC) directly to the spin column membrane and close the lid. Incubate at room temperature (15–25ºC) for 1 min, and then centrifuge for 1 min at ≥8000 x g (10,000 rpm) to elute the DNA.
- Repeat the last step, adding 50 ul Buffer EB to the same column to elute DNA again.
- Measure concentration and ratio 260/280 and note this on freezer box chart.
- Store at -80ºC in "LBH trial/Q-CROC2" box.

Whole cell extract:

- Prepare 1 ml of protein lysis buffer by adding 2 µl PMSF, 1 µl aprotinin, 1 µl leupeptin, 1 µl $NaVO_4$ and 100 µl phosphatase inhibitors on ice.
- Spin down ⅓ of the total cells isolated with the negative selection kit in an Eppendorf tube; 1500 rpm for 5 mins at 4$^{o}$C. Discard supernatant.
- Add 100 – 500 µl protein lysis buffer depending on pellet size.
- Leave at 4$^{o}$C on orbitron in cold room for 30 mins.
- Spin down 13,000 rpm for 15 mins at 4$^{o}$C.

- Transfer supernatant to new Eppendorf tube. Store at - 80$^{o}$C in ”LBH trial/Q-CROC2 box”.

**Any deviation to this procedure should be carefully recorded on the datasheet or CRF.**